Georgia Tech | NASA **USLI**
UNIVERSITY STUDENT LAUNCH INITIATIVE
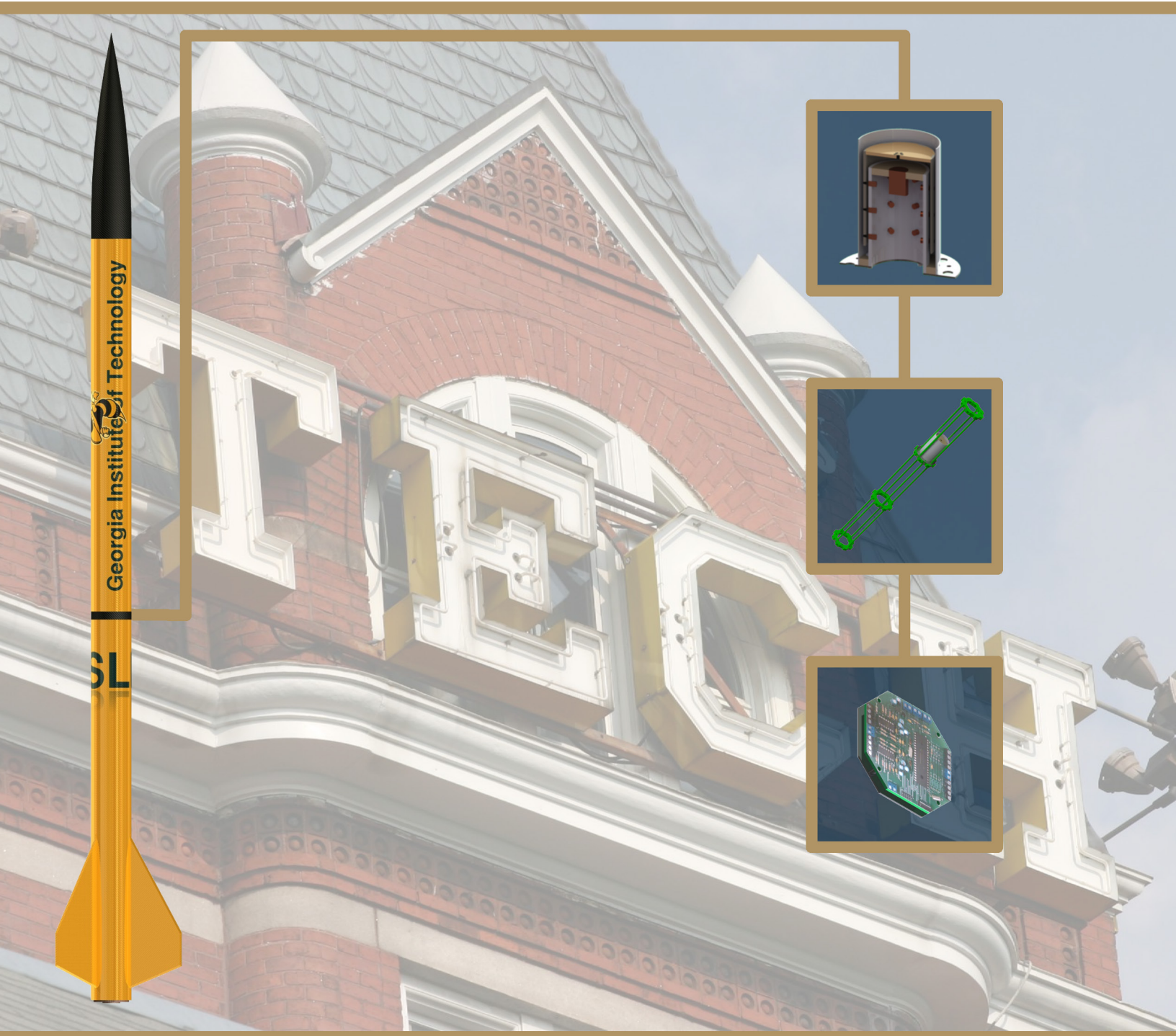
Project A.P.E.S

Active Platform Electromagnetic Stabilization

Flight Readiness Review

March 2012

Table of Contents

List of Figures

List of Tables

1. Team Summary

Team Summary	
School Name	Georgia Institute of Technology
Team Name	Mile High Yellow Jackets
Project Title	Active Platform Electromagnetic Stabilization (A.P.E.S.)
Launch vehicle Name	Vespula
Project Lead	Richard
Safety Officer	Matt
Team Advisors	Dr. Eric Feron, Dr. Marilyn Wolf
NAR Section	Primary: Southern Area Rocketry (SoAR) #571
	Secondary: GA Tech Ramblin' Launch vehicle Club #701
NAR Contact	Primary: Matthew Vildzius
	Secondary: Jorge Blanco

2. Project A.P.E.S. Overview

2.1. *Mission Statement*

The mission of the Mile High Yellow Jackets is:

> To maintain a sustainable team dedicated to the gaining of knowledge through the designing, building, and launching of reusable launch vehicles with innovative payloads in accordance with the NASA University Student Launch Initiative Guidelines.

2.2. *Requirments Flow Down*

The requirements flow down is illustrated in Figure 1. As illustrated by the requirements flow down, the Mission Success Criteria flow down from the Mission Objectives of Project A.P.E.S. All system and sub-system level requirements flow down from the either of the Mission Objectives, Mission Success Criteria, or the USLI Handbook.
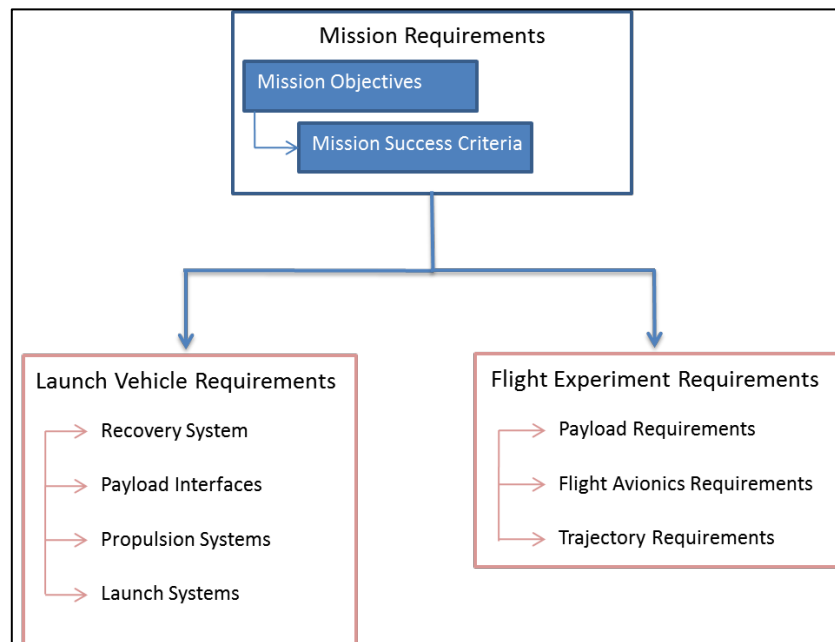
Figure 1. Flow down of requirements.

2.3. *Mission Objectives and Mission Success Criteria*

The Mission Objectives and Mission Success Criteria for Project A.P.E.S. are listed in Table 1.

Table 1. Project A.P.E.S. Mission Objectives & Mission Success Criteria.

MO	Mission Objectives			
MO-1	An altitude of 5,280 ft. above the ground is achieved.			
MO-2	Stabilize and isolate the A.P.E.S. platform from the induced vibrations of the Launch Vehicle.			
MO-3	Closed-loop control of the platform via real-time image processing.			
MO-4	Successful recovery of the launch vehicle resulting in no damage to the launch vehicle.			
MSC	**Mission Success Criteria**	**Source**	**Verification Method**	**Status**
MSC-1	Achieve an altitude of 5,280 ft., with a tolerance of +320 ft./-640 ft.	MO-1	Testing, Analysis	Completed
MSC-2	The Flight Experiment is successfully activated and data is collected.	MO-2, MO-3	Inspection, Analysis	Completed
MSC-2.1	*Minimum Mission Success*: Platform is stabilized and isolated during the coast phase of flight	MO-2	Testing	In Progress
MSC-2.2	*Minimum Mission Success*: Relative position and rotation data of the platform to the camera is collected during all phases of the experiment.	MO-2, MSC-2	Testing	In Progress
MSC-2.3	*Minimum Mission Success*: The flight experiment terminates at apogee.	MO-4, MSC-2	Inspection	In Progress
MSC-2.4	*Full Mission Success*: Platform is stabilized and isolated from environmental vibrations during the powered and un-powered portions of the flight.	MO-2, MSC-2	Testing	In Progress
MSC-2.5	*Full Mission Success*: Platform does not come into contact with any other components of the A.P.E.S. System.	MO-3, MSC-2.4	Testing	In Progress
MSC-3	The launch vehicle experiences no in-flight anomalies.	MO-4	Testing	In Progress
MSC-3.1	*Minimum Mission Success*: The launch vehicle is recovered with no damage.	MO-4, MSC-3	Testing	In Progress
MSC-4	*Minimum Mission Success:* The cost of the all the components, including the Launch Vehicle, Flight Experiment, Flight Avionics, and Motor, shall cost no more than $5,000.	USLI Handbook	Inspection, Analysis	Completed

2.4. *System Level Requirements*

The System requirements for Project A.P.E.S. are listed in Table 2.

Table 2. Project A.P.E.S. system requirements.

LV	Launch Vehicle	Source	Verification Method	Status	Verification Source
`LV-1	The Launch Vehicle shall carry a scientific or engineering payload.	USLI Handbook	Inspection	Completed	Section 4.4
LV-1.1	The maximum payload weight including any supporting avionics shall not exceed 15 lbs.	LV-1	Inspection	Completed	Table 21, Figure 4
LV-1.2	The Launch Vehicle shall have a maximum of four (4) independent or tethered sections	LV-1	Inspection	Completed	
LV-2	The Launch Vehicle shall carry the payload to an altitude of 5,280 ft. above the ground.	USLI Handbook, MSC-1, MO-1	Inspection, Testing	Completed	Figure 43
LV-2.1	The total impulse provided by the Launch Vehicle shall not exceed 5,120 N-s.	LV-2	Inspection	Completed	Figure 44
LV-2.2	The Launch Vehicle shall use a commercially available solid motor.	LV-2	Inspection	Completed	Figure 13
LV-2.3	The Launch Vehicle shall remain subsonic throughout the entire flight.	LV-2	Analysis	Completed	Figure 43
LV-3	The Launch Vehicle shall be safely recovered and be reusable.	USLI Handbook, MSC-3.1, MO-4	Testing, Inspection	Completed	Section 4.2
LV-3.1	The Launch Vehicle shall contain redundant altimeters.	LV-3, USLI Handbook	Inspection	Completed	Figure 7
LV-3.2	The Launch Vehicle shall carry one altimeter for recording of the official altitude used in the competition scoring.	LV-3, USLI Handbook	Inspection	Completed	Figure 8
LV-3.3	The recovery system shall be designed to be armed on the pad.	LV-3, USLI Handbook	Inspection	Completed	Figure 9
LV-3.4	The recovery system electronics shall be completely independent of the payload electronics.	LV-3, USLI Handbook	Inspection, Testing	Completed	Figure 7

LV	Launch Vehicle	Source	Verification Method	Status	Verification Source
LV-3.5	Each altimeter shall be armed by a dedicated arming switch.	LV-3, USLI Handbook	Inspection	Completed	Figure 9
LV-3.6	Each altimeter shall have a dedicated battery.	LV-3, USLI Handbook	Inspection	Completed	Figure 7
LV-3.7	Each arming switch shall be accessible from the exterior of the airframe.	LV-3, USLI Handbook	Inspection	Completed	Figure 9
LV-3.8	Each arming switch shall be capable of being locked in the "ON" position for launch.	LV-3, USLI Handbook	Testing	Completed	Figure 10
LV-3.9	Each arming switch shall be a maximum of six (6) feet above the base of the Launch Vehicle.	LV-3, USLI Handbook	Inspection	Completed	Figure 41
LV-3.10	The Launch Vehicle shall stage the deployment of its recovery devices	LV-3, USLI Handbook	Testing	Completed	Figure 2
LV-3.11	Removable shear pins shall be used for both the main and drogue parachute compartments	LV-3, USLI Handbook	Inspection	Completed	Section 4.2.3
LV-3.12	All sections shall be designed to recover within 2,500 ft. of the launch pad assuming 15 MPH winds.	LV-3, USLI Handbook	Analysis	Completed	Figure 46
LV-3.13	Each section of the Launch Vehicle shall have a maximum landing kinetic energy of 75 ft-lb$_f$.	LV-3, USLI Handbook	Analysis	Completed	Table 16
LV-3.14	The recovery system electronics shall be shielded from all onboard transmitting devices.	LV-3, USLI Handbook	Testing, Analysis	Completed	Table 27 , Section 9.3.1
LV-4	The Launch Vehicle shall be launched standardized launch equipment	USLI Handbook	Inspection	Completed	Section 7
LV-4.1	The Launch Vehicle shall not require any external circuitry or special ground support equipment to initiate the launch other than what is provided by the range.	LV-4, USLI Handbook	Inspection	Completed	Appendix II

LV		Launch Vehicle	Source	Verification Method	Status	Verification Source
	LV-4.2	The Launch Vehicle shall be launched from a standard firing system using a 10 second countdown.	LV-4, USLI Handbook	Inspection	Completed	Appendix II
	LV-4.3	The Launch Vehicle shall have a pad stay time on one (1) hour.	LV-4, USLI Handbook	Testing, Analysis	Completed	Figure 66
	LV-4.4	The Launch Vehicle shall be capable of being prepared for flight at the launch site within 2 hours from the time the waiver opens.	LV-4, USLI Handbook	Testing	Completed	Appendix II

FS		Flight Systems	Source	Verification Method	Status	Verification Source
	FS-1	The platform shall be stabilized and isolated during ascent.	MSC-2.4, MO-2	Testing	In Progress	
	FS-1.1	The platform shall not deviate more than 0.1 inches from the center of experiment cylinder.	FS-1	Analysis, Testing	In Progress	
	FS-1.2	The platform shall not come into contact with any components of the A.P.E.S. System.	FS-1, MSC-2.5	Testing	Designed	
	FS-1.3	The platform shall not rotate more than 1 rad per second for than 1/10 of a second with respect to the camera.	FS-1	Analysis, Testing	In Progress	
	FS-2	All elements of the A.P.E.S. Systems shall weigh no more than 15 lbs.	LV-1.1	Inspection	Completed	Table 21
	FS-2.1	The A.P.E.S. Flight Experiment shall not weigh more than 10 lbs.	FS-2	Inspection	Completed	Table 21
	FS-2.2	The A.P.E.S. supporting electronics shall not weigh more than 5 lbs.	FS-2	Inspection	Designed	
	FS-3	The A.P.E.S. experiment shall be terminated at apogee.	MSC-2.3	Testing	In Progress	
	FS-3.1	The platform shall be secured during descent and landing.	FS-3	Testing	In Progress	

FA	Flight Avionics	Source	Verification Method	Status	Verification Source
FA-1	All Flight Avionics shall have a burn-in time of no less than 20 hours	MSC-2.2, MO-4	Inspection	In Progress	
FA-2	The Flight Computer shall collect Launch Vehicle position data, environment conditions (e.g. acceleration), and data from the A.P.E.S. experiment.	MSC-2.5, MSC-2.4, MSC-2,MO-2	Testing	Designed	
FA-3	The A.P.E.S. computer shall be able to perform real-time image processing and control the A.P.E.S. experiment.	MO-3	Testing	In Progress	
FA-3.1	The A.P.E.S. computer shall secure the platform at apogee for descent and landing	FS-3.1	Testing	In Progress	
FA-4	The Flight Avionics shall operate on independent power supplies	MSC-2.5, MSC-2.4, MSC-2,MO-2	Inspection	In Progress	
FA-4.1	The power supplies shall allow for successful payload operation during the Launch Vehicle flight with up to 3 hours of wait time.	USLI Handbook	Analysis, Testing	Completed	Figure 66
FA-5	The Flight Avionics shall downlink telemetry necessary to a Ground Station for the recovery of the Launch Vehicle	USLI Handbook	Analysis, Testing	In Progress	
FA-5.1	The GPS coordinates of all independent Launch Vehicle sections shall be transmitted to the Ground Station	MO-4	Inspection	In Progress	
FA-6	The Recovery Avionics and Recovery System shall be separate from the Flight Avionics.	USLI Handbook	Inspection	Completed	Figure 7, Section 9.2

2.5. *Mission Profile*

Figure 2 graphically illustrates the Mission Profile of Project A.P.E.S.
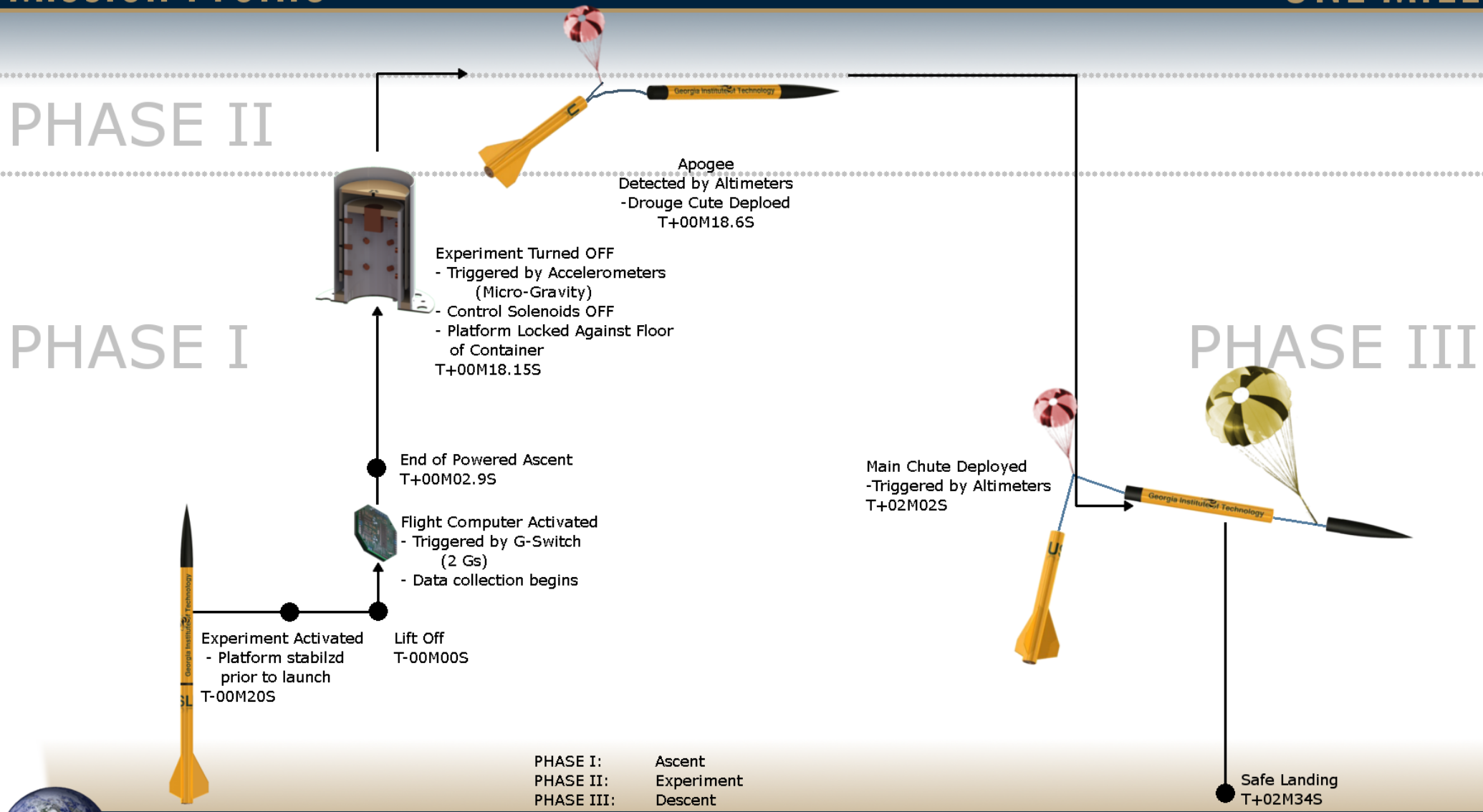
Figure 2. Project A.P.E.S. Mission Timeline

2.6. *Launch Vehicle Summary*

The *Vespula* launch vehicle features a modular design which allows for simplified integration of various payloads up to 10 lbs with a maximum launch weight of approximately 40 lbs utilizing an AeroTech L1390 motor. The A.P.E.S configuration, however, has a mass of approximately 32 lbs and uses an Aerotech L850. The structure of the launch vehicle features a rib-and-stringer design covered by a thin skin to minimize weight. The recovery system utilizes a 48" drogue parachute slowing the launch vehicle down to 50 feet per second (ft/s) from an apogee of approximately one mile above ground level (AGL) and a 120" main parachute to slow the launch vehicle down to 17 ft/s from 500 ft. AGL.

2.7. *Payload Summary*

The Mile High Yellow Jackets will design, build, test, and fly an electromagnetically levitated plate within their launch vehicle. This plate will be stabilized against the motion of the launch vehicle providing a vibration-free environment for a theoretical payload in an experiment known as A.P.E.S., or Active Platform Electromagnetic Stabilization. Flight Systems will utilize an ATmega 2560 for all data collection activities and the TI DM3730 DaVinci Multimedia Processor for the A.P.E.S. control law implementation.

3. Changes since CDR

3.1. *Changes to the Team*

No personnel changes to the Team since CDR

3.2. *Changes to the Launch Vehicle System*

- The main parachute diameter was reduced from 12 ft. to 10 ft.
- The new landing velocity under the 10 ft. diameter main parachute is 17 ft./s with a corresponding maximum landing kinetic energy of 62.2 ft.- lb_f .
- The ejection charge masses have been reduced from 3.6g and 4.5g to 3.0g and 4.0g respectively.
- L-brackets have been added to the recovery system bulkheads at epoxy joints for added strength.

3.3. Changes *to the Payload and Flight Systems Design*

- The success criterion for A.P.E.S. has been updated to increase specificity, relevance, and the inclusion of additional design parameters.
- The ground test platform for the one-dimensional (1-D) testing has been redesigned to better facilitate the development of the Flight Control Logic.
- The flight model for A.P.E.S. has been updated with sensors and lighting apparatus.
- Replaced the DRV104TI solenoid driver IC with the DRV103 IC allowing for two (2) times more current draw and simpler integrating characteristics.
- The A.P.E.S. Flight Computer – the BeagleBoard xM – runs a Xubuntu Linux distribution with a custom kernel.
- The main Flight Computer has been de-scoped from the custom circuit board to an Arduino Mega 2560 - which interfaces with our sensor array via a shield – due to manufacturing difficulties

3.4. *Changes to the Activity Plan*

- A rocket-themed Discovery Station is being integrated into the Discovery Station Program at the Smithsonian National Air and Space Museum, Udvar Hazy Center.
- The Mile High Yellow Jackets will be working with a local Civil Air Patrol squadron in teaching a Model Rocketry Program.

4. Launch Vehicle

4.1. *Overview*

The purpose of the launch vehicle is to carry a payload to one mile in altitude and safely return the vehicle to the surface of the Earth. Embracing innovative and out-of-the-box thinking, the Mile High Yellow Jackets have designed their launch vehicle *Vespula* the ability to carry a wide range of payloads, from scientific experiments to engineering flight demonstrations. The unique design of *Vespula* incorporates a standardized payload interface into the primary structure of the rocket allowing for higher structural efficiency, a lower structural mass fraction, and an increased payload carrying capacity.

The novel integrated structure coupled with the 5 inch airframe provides a unique platform to carry a wide range of payloads. As with any unique aerospace design, extensive ground testing will be performed to verify successful integration of the payload into the fully assembled launch vehicle. A subscale test flight occurred in December 2011 to test the launch vehicle's skin design and a full scale test was performed on March 10, 2012. The objective of the full scale test launch, from a vehicle perspective, was to verify the recovery system and the integrity of the overall structure during all phases of flight.

4.2. *Recovery System*

4.2.1. Overview

Vespula's recovery system will utilize a dual-deployment recovery system that uses a small drogue parachute to mitigate the effects of drift during the Launch Vehicle's descent back to the surface of the Earth and a larger main parachute to ensure a soft landing. OpenRocket vehicle analysis of the drogue chute indicates that the maximum descent rate will be 50 ft/s with deployment at apogee. Using the MATLAB code included in Appendix X: Recovery Testing Document

Appendix X, Figure 3 was produced to determine that main chute deployment will slow the launch vehicle to a maximum descent rate of 17 ft/s and will be deployed at 500 ft AGL altitude.
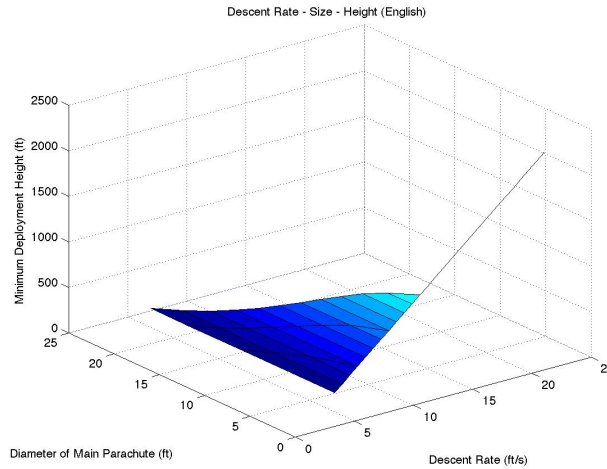
Figure 3: Main Chute Deployment altitude as a function of Descent Rate and Chute Size

The drogue chute is assumed to have a C_D of 1.2, and the main chute is assumed to have a C_D of 1.4. Figure 4 shows a section drawing of the launch vehicle and where the parachutes are contained**.**
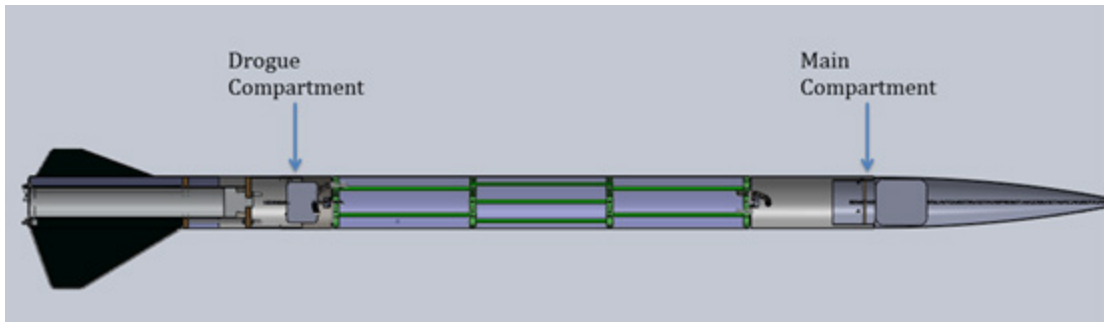
Figure 4: Section View of Launch vehicle

4.2.2. Parachute Dimensions

The main chute will be packed using the instructions in Appendix VII inside the nose cone – which has an outer diameter of 5.15", an inner diameter of 4.7", and a length of 25.5". A bulkhead connected to a 1" wide, 4 ft long nylon webbing is secured to the tip of the nose cone on one end. This structure will absorb the impulse of the ejection charge blast and prevent the chute from being stuck inside of the nose cone.

Figure 5: Detail view of the main parachute section

Nomex cloth will be used to prevent the shock cord and parachute from being damaged by the ejection charges. Nylon webbing, 1" wide and 30 ft long, will connect the main parachute to the rocket. The main chute is attached to the Nylon webbing such that the parachute and nose cone are separated by 20 ft of webbing. The rest of the rocket is 10 ft from the main chute and is attached using a 3/8" diameter steel cable as shown in Figure 5. Once ejected, the inertia of the nose cone will allow the main chute to be pulled free from storage.
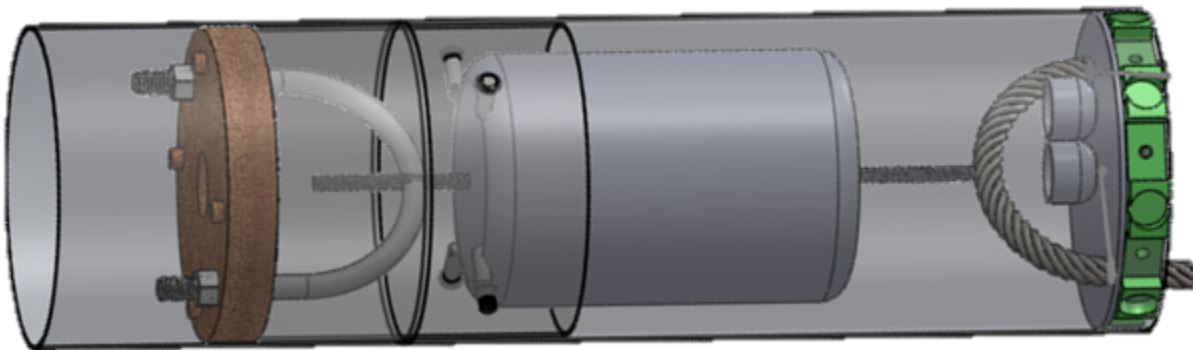
Figure 6: Detail view the of drogue parachute section

The drogue parachute will be housed in a cylindrical compartment attached to the thrust plate within the launch vehicle as illustrated by Figure 6. The drogue chute compartment has a 5.15 inch outer diameter and a height of 12". Another shock cord, made of 1-inch wide, 30 ft long nylon webbing, will connect the drogue parachute to the payload and booster sections of the launch vehicle. This allows for the entire rocket to remain a single unit during the recovery phase. There will be 20 ft of Nylon connecting the drogue chute to the booster section and 10 ft to the payload section. The drogue chute shock cord is attached to a U-Bolt on the reverse side of the thrust plate, and will be connected through a 3/8" diameter steel cable drilled into a G-10 Garolite bulkhead.

Table 3 outlines the dimensions and the weights of the parachutes.

Table 3: Parachute parameters

	Main Parachute	Drogue Parachute
Dimensions	10 ft diameter	4 ft diameter
Surface Area	78.54 ft^2	12.56 ft^2
Estimated C_D	1.4	1.2
Weight	2.0 lb	1.5 lb
Target Descent Rate	17 ft/s	50 ft/s

4.2.3. Ejection Charges

Black powder masses were calculated using Equation (1) with variables defined in Table 4.

$$W = \frac{\Delta PV}{RT} \tag{1}$$

Table 4: Ejection charge equation variables

Variable	Description	Units
W	Weight of the black powder in pound mass	$454 \cdot W_{gram}$
V	Volume of the container to be pressurized	in^3
ΔP	Pressure Differential	psi
R	Gas Combustion Constant for black powder	$\dfrac{22.16\,ft \cdot lb_f}{lb_m \cdot R}$
T	Gas Combustion Temperature	3307 °R

Volume, *V*, is set by the design, while the black powder determines the gas constant and temperature. Given the number and diameter of the shear pins, the necessary pressure and therefore ejection charge mass can be computed. A quarter-inch shear pin can take up to 35 pounds of shear force before it fails. The two compartments will be held together with 4 – 1/16" diameter Nylon shear pins each having a tensile yield strength of 12 ksi. Via Equation (2), a total force of 150 pounds per compartment is needed to achieve separation

$$F_{pin} = \frac{\sigma \pi d^2}{4}$$
(2)

Including 10 pounds of force per compartment for frictional resistance the corresponding amounts of black powder are summarized in Table 5.

Table 5: Ejection pressurization and black powder charge

	Main Parachute	Drogue Parachute
Total Pressurization	24.7 psia	23.7 psia
Pressure at Deployment Altitude	14.4 psia	12.1 psia
Differential Pressurization	10.3 psia	11.6 psia
Ejection Force	202.2 lbf	227.8 lbf
Amount of Black Powder	4.0 grams	3.0 grams
Factor of Safety	1.26	1.42

4.2.4. Altimeters

The StratoLogger collects flight data at a rate of twenty samples per second throughout the flight and stores the data for later transfer to a computer. The altimeter is capable of recording flights of up to 100,000 feet in altitude. Two altimeters will be used for redundancy, each with an independent power supply. The pin connections used are shown in Figure 7 and the system set up for each altimeter is shown in Figure 8.
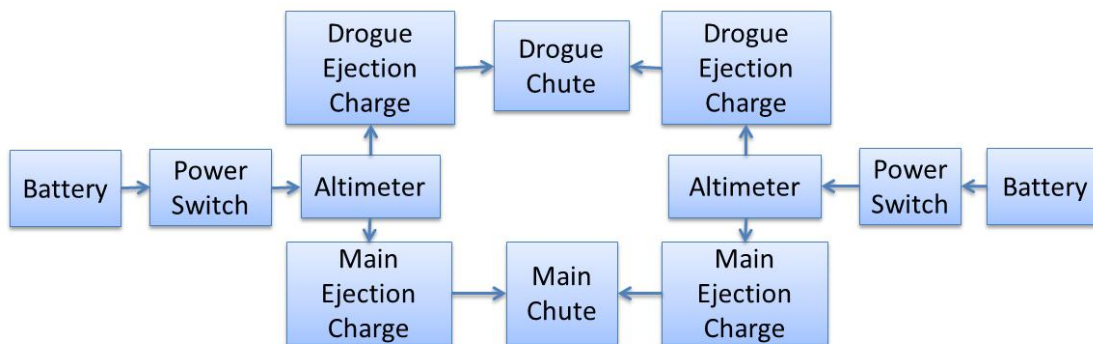
Figure 7: Electrical Schematic of Stratologger
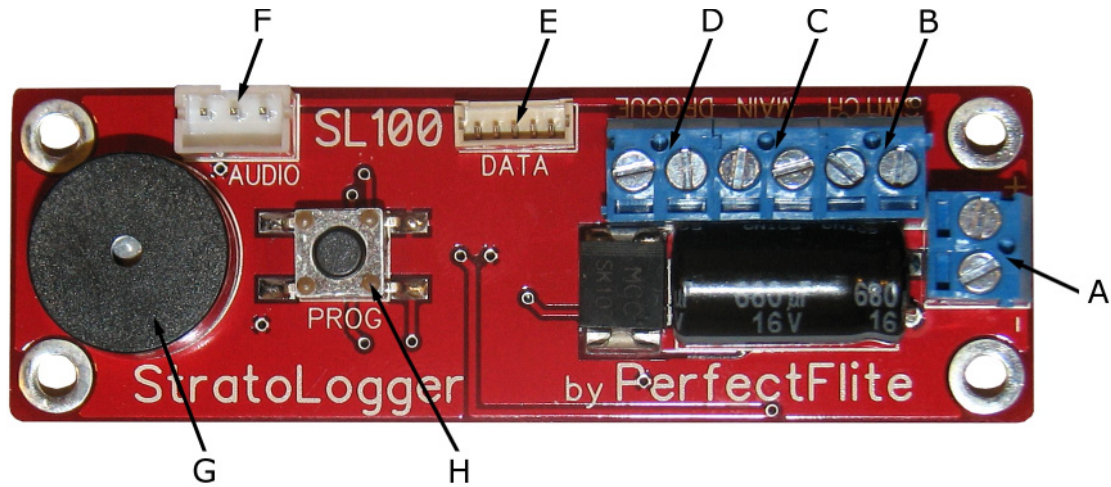
Port	Name	Description
A	Battery Port	Connect to a 9 V power source
B	Power Switch Port	Connect to a power switch
C	Main Chute Port	Connect to Main Chute E-matches
D	Drogue Chute Port	Connect to Drogue Chute E-matches
G	Beeper	Audibly reports settings, status, etc. via a sequence of beeps

Figure 8: Stratologger Configuration

4.2.5. Arming Switches

The Arming switch bracket houses the two redundant arming switches for the altimeters. The bracket is made out of ABS plastic and was made using a 3D printer. The bracket is mounted on the lower most rib of the payload section using the standard #8-32 bolt that is utilized by the rest of the structure and is illustrated in Figure 9.
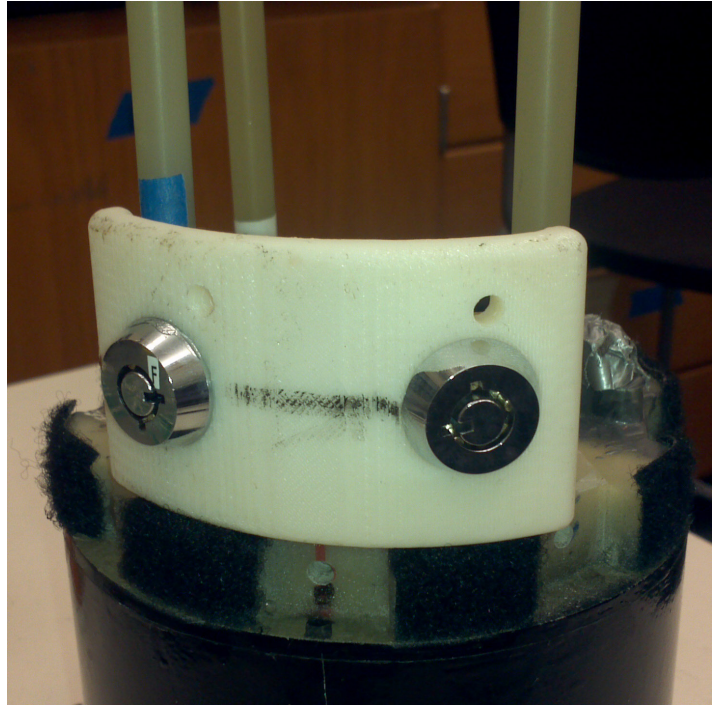
Figure 9: Arming Switch Bracket mounting in iMPS

When the switches are facing in towards each other, the rocket is unarmed. Otherwise, the rocket is armed. This is illustrated in Figure 10.
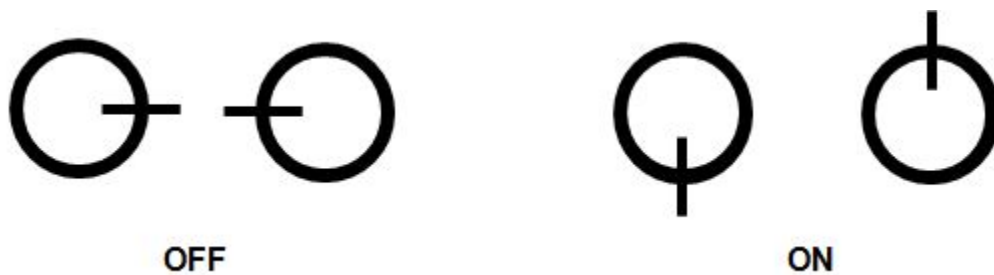
Figure 10: Arming Switch Positions

4.2.1. Manufacturing

Both the main and drogue parachutes are legacy hardware. The main and drogue parachute recovery casings consist of spun G10 Garolite. The bulkhead below the drogue parachute is made out of wood since it will also serve as the thrust plate. Four (4) shear pins will hold the

parachute recovery casings in launch configuration. The ejection blast will be directed away from the bulkheads via PVC end-caps to protect the casings from thermal shock. Additionally a NOMEX shield will be used to protect the chutes from thermal shock. Furthermore, the main coupler will be fixed to the compartment using mechanical fasteners. The top half of the compartment will then slide onto the coupler up to the inner wall of the compartment and will be held in place by shear pins. For more detailed manufacturing instructions, please see the Recovery Manufacturing and Fabrication Order (MFO) in Appendix IV.

4.2.2. Testing

Each compartment underwent testing for feasibility. These tests validated the estimated mass of black powder required in both the main and drogue compartments to achieve separation. Testing support equipment was used to prevent launch vehicle parts or debris from hitting bystanders during testing. A wooden track was used to keep the launch vehicle from being damaged due to friction from the terrain as well as protecting the field. The ejection charges were placed in PVC cups and were detonated by an e-match via a wired remote switch box at a distance of 15 feet from the test article.

For testing to be considered a success, it must meet all of the success criteria listed in Table 6 and the test is considered a failure if none of the criteria are met or if one of the failure modes occurs. The failure modes are shown in Table 7.

Table 6: Recovery testing success criteria

Success Criteria	Risk Level	Mitigation
Ejection charge ignites	Low	Keep Personnel a safe distance away
Shear pins break	Low	Keep Personnel a safe distance away
Launch vehicle moves half the distance of shock cord	Medium	Keep Personnel a safe distance away

Table 7: Recovery testing failure modes

Failure Criteria	Risk Level	Mitigation
The Garolite compartment or coupler shatters due to the charge	Medium	Keep Personnel a safe distance away
The shear pins don't shear, and the launch vehicle stays intact	Low	Keep Personnel a safe distance away
The NOMEX shield fails and the parachute is burned	Medium	Properly folding the parachute and shield
Ematches fail to ignite black powder	Low	Redundant ignition system

Both the drogue and main chute sections passed the feasibility tests. The drogue, as seen in Figure 11, managed to shear the pins and move the sections a safe distance using 3.0 grams of black powder.

Figure 11: Drogue Chute Test time $t = 0$ ***and time*** $t = +\frac{1}{30} sec$

The main chute, as seen in Figure 12, managed to shear the pins and move the sections a safe distance using 4.0 grams of black powder. The flight black powder amounts were then updated to match these validated values. For more detail of setup and test, see Recovery Test Document in Appendix X

Figure 12: Main Chute Test at time $t = 0$ and time $t = +\frac{1}{30} sec$

4.3. *Booster Section*

The booster system of *Vespula* uses traditional motors combined with a unique structure to yield a highly integrated design and thus minimizing the total weight of the launch vehicle. The primary components of the launch vehicle booster section are the launch vehicle motor and the Motor Retention System illustrated in Figure 13 and Figure 14 respectively.
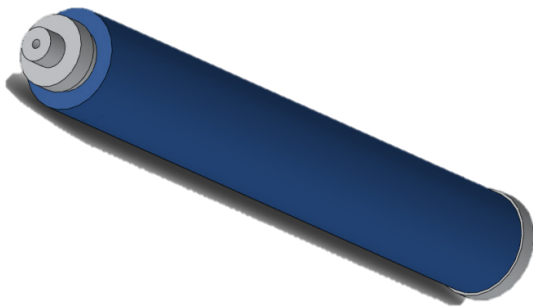
Figure 13: AeroTech 75/3840 Motor Casing
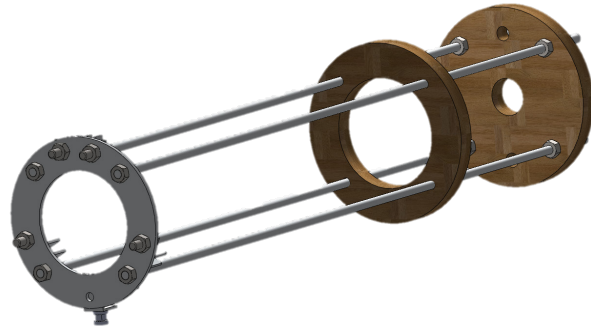
Figure 14: Motor Retention System

The Motor Retention System (MRS) can be broken down into several modular parts. The first part is the thrust plate located at the top of the MRS. The thrust plate provides the contact area necessary for the motor to provide thrust to the rest of the structure. The thrust plate is also part of the recovery system since it serves as a bulkhead with a U-bolt for attachment of the main parachute. Finally, the thrust plate will prevent the motor from penetrating the booster section and will provide torsional rigidity to the mounting rods running along the MRS. The current thrust plate is manufactured using marine grade plywood. The assembly of the thrust plate with the motor casing and mounting rod as shown in Figure 15 and the U-bolt attachment is shown in Figure 16.
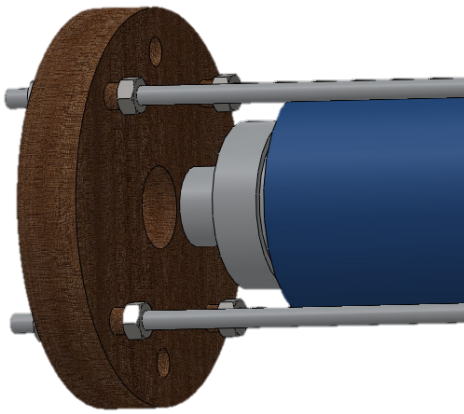
Figure 15: Thrust Plate Assembly
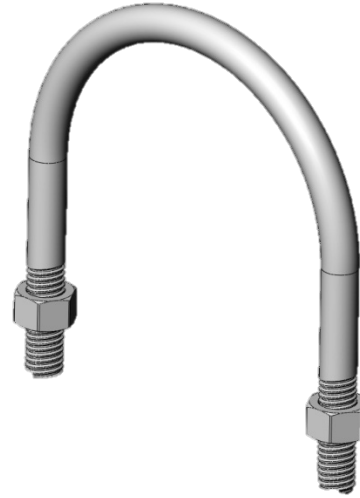
Figure 16: U-bolt Attachment

The major components of the MRS are the support plate at the rear of the booster section, the centering rings, and the cardboard motor tube. The main purpose of the support plate is to prevent the motor from falling out of the launch vehicle. Additionally, the rear retention plate will provide a base for L-brackets that will be bolted on. The L-brackets are designed to seat each fin and provide torsional support for the mounting rods. The assembled retention plate with L-brackets and the assembled retention plate with fin placement are shown in Figure 17 and Figure 18, respectively.
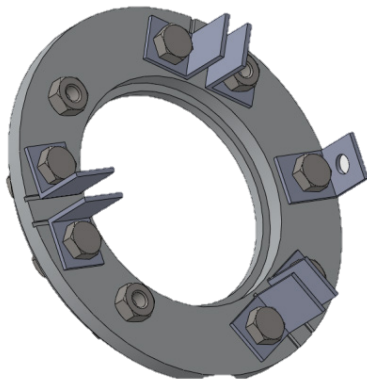
Figure 17: Assembled retention plate
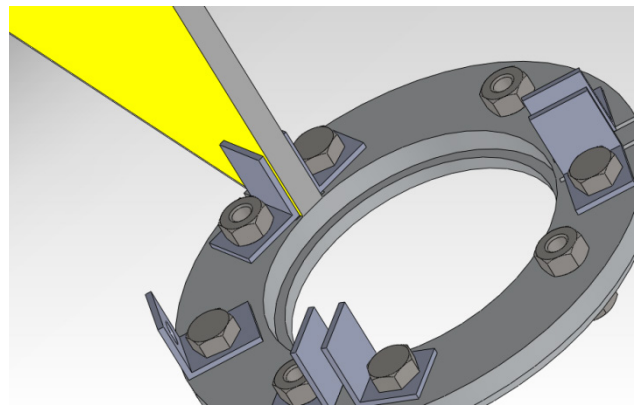
Figure 18: Fin Placement

The centering rings and the cardboard motor tube provide additional support to the fins and recovery section tubes. The motor retention and fin assembly are shown in Figure 19 and the total assembly including the recovery system is shown in Figure 20.
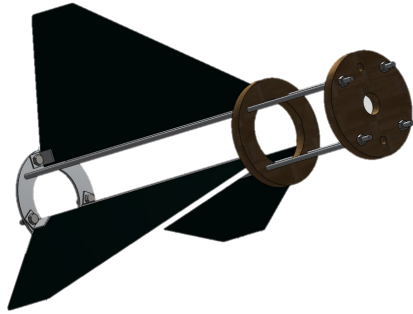
Figure 19: Motor retention and Fin Assembly
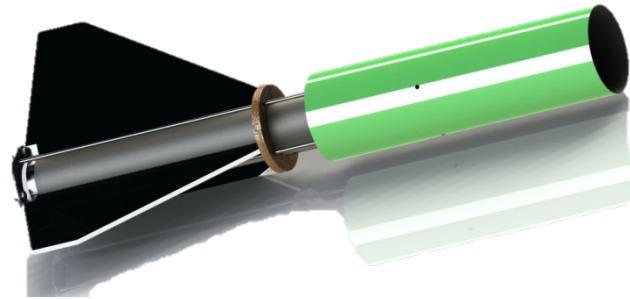
Figure 20: Booster Section with Recovery

4.3.1. Material Requirements

The majority of the booster section will be constructed from ½" BS1088 marine grade plywood and 1/8" think sheets of 6061-T6 aluminum. These materials will reduce the weight of the system while maintaining structural integrity. Epoxy will serve as an adhesive for attaching the fins to the L-brackets, centering ring, and motor tube.

4.3.2. Finite Element Analysis (FEA)

Finite Element Analysis (or FEA) is a method of finding approximate solutions to partial differential equations. This method is helpful in analyzing complex structures for design and development analysis. SolidWorks contains a design validation tool that carries out a basic FEA. This tool was used to structurally analyze the thrust plate and the booster section as a whole. The force applied during the analysis is 408 lb$_f$, which is the maximum thrust expected for an Aerotech L1390G-P. The first simulation contained only the thrust plate, shown in Figure 21 and Figure 22, which resulted in a maximum displacement of 0.00838 inches and an induced maximum stress of 404.6 psi. The next simulation was for the entire booster section, shown in Figure 23 and Figure 24. It is important to note that both figures have deformation scaled to a high level so that it appears as if the rods are buckling when they are not. To reduce complexity, the shape was generalized as a single part similar to the actual booster section which included the thrust plate, mounting rods, fin centering ring, and the two support plates. The material used for

the simulation was Aluminum 6061-T6. This simulation resulted in a maximum displacement of 0.00526 inches and an induced maximum stress of 483.3 psi. The results of the two simulations are summarized in Table 8 below. The loads have been determined from the expected max thrust of the L1390 motor.

Table 8: FEA results for the thrust plate and the assembly

Part	Material	Force Applied (lb_f)	Max. Displacement (inches)	Max. Stress (psi)	Factor of Safety
Thrust Plate	BS 1088	408	0.00838	404.6	3.3
Stringers	6061	408	0.00526	483.3	2.9
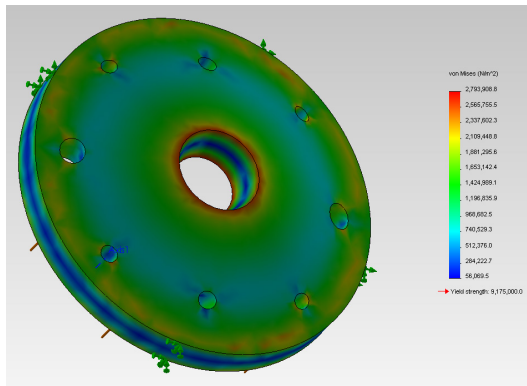
Figure 21: Thrust Plate Stresses (top-view)
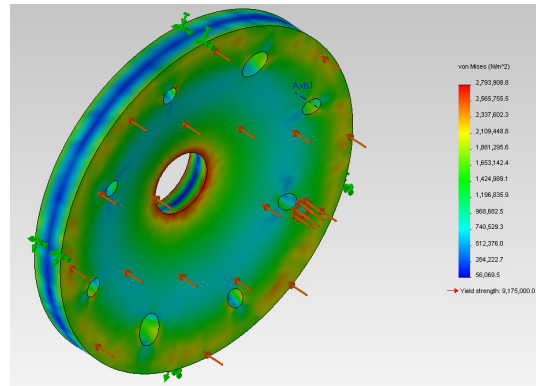
Figure 22: Thrust Plate Stress (bottom-view)
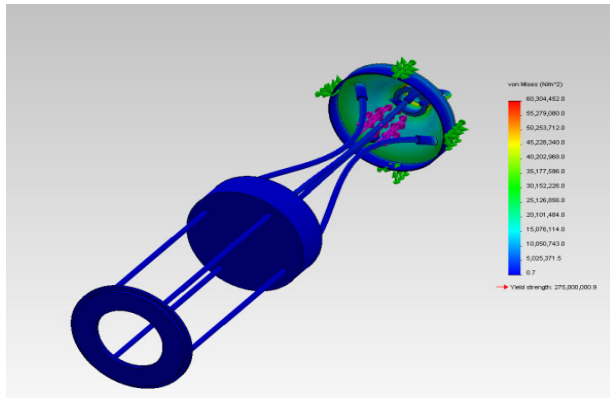
Figure 23: Booster section stresses
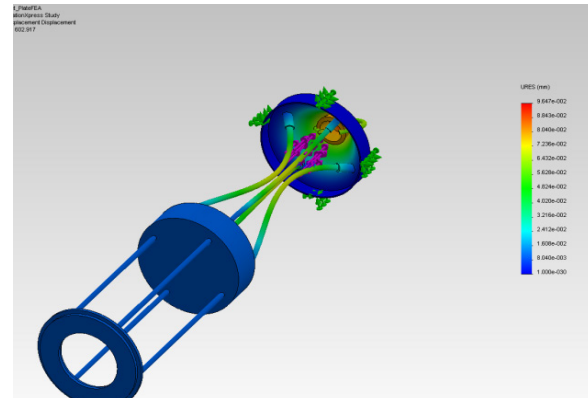
Figure 24: Booster section displacement

In order to verify structural integrity of the thrust plate during launch, static loading tests were performed. A 3-point bending test simulates the launch force loading where the central force simulates the rocket thrust acting upon the thrust plate. The supports are the recovery section tubes epoxied onto the thrust plate. An Instron loading machine and Vic-3D stress/strain analysis image capturing software was used[1]. Test safety was observed by wearing safety glasses and maintaining a safe distance from the test article throughout testing. The initial software reference and test configuration and are shown respectively in Figure 25 and Figure 26 below.
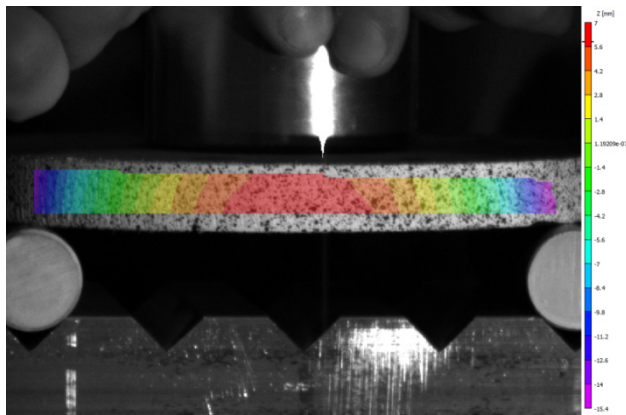
Figure 25: Vic-3D reference image
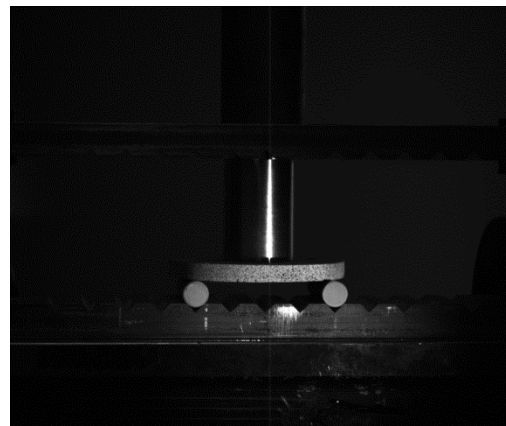
Figure 26: Initial Position for test

The loading in the test was conducted from 0 to 400 lbs and then 400 lbs to failure with 50 lbs increments. 400 lbs is the estimated thrust of the L-1390 motor. During testing, the thrust plate did not encounter signs of failure until 525 lbs. The test article was determined to have reached critical failure at 947 lbs. Figure 27 and Figure 28 show the test article at 400 lbs and during critical failure.

---

[1] Vic-3D is digital imaging correlation software that tracks surface deformation on a specimen element through the use of high-speed cameras.
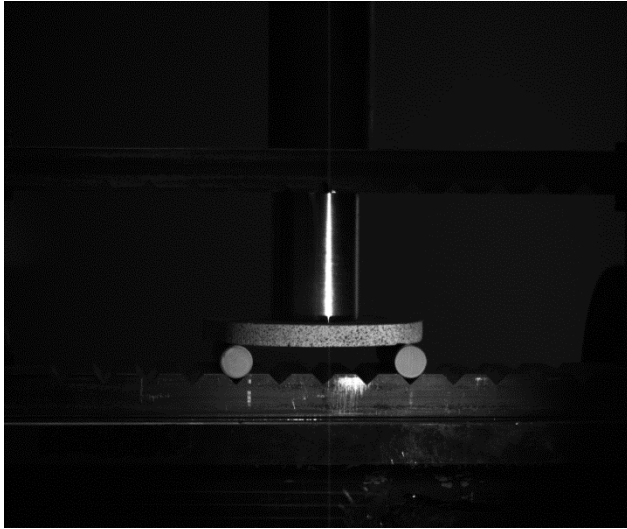
Figure 27: Test article at 400 lbs
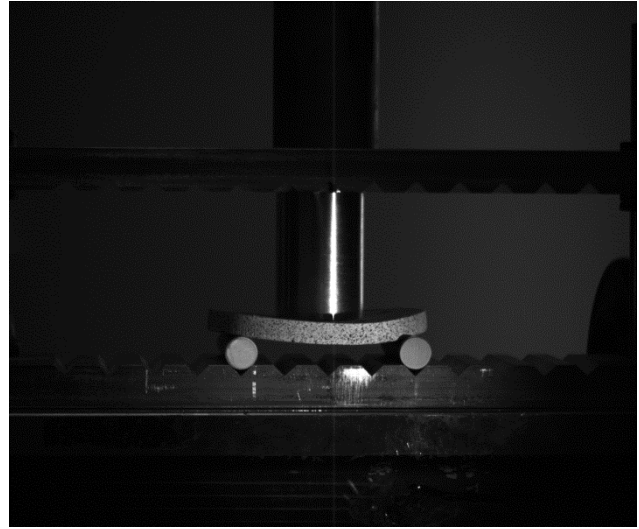
Figure 28: Test Article at critical failure (947 lbs)

Further analysis was done using the recorded data from a selected element of the test article using the Vic-3D software. Figure 29 shows the observed stresses in each point of a finite element in the test article with a loading of 403 lbs.

4.3.1. Manufacturing and Quality Assurance

Quality will be assured by utilizing proper manufacturing techniques that are appropriate for the materials and part designs. First, the thrust plate, rear support plate, and centering ring will be cut using a water jet. Next, the booster section will be assembled using epoxy and hex nuts on a threaded rod. For motor preparation, the rear retention plates will be removed by unscrewing the hex nuts. Afterwards, the motor propellant will be placed inside the motor casing and the rear retention plates will be reattached. For more detailed manufacturing instructions, please see the Booster Section Manufacturing and Fabrication Order (MFO) in Appendix V.

4.3.1. Fin Overview

Fins are used to keep the launch vehicle stable and the flight path straight by shifting the center of pressure aft of the center of gravity. The trailing edge of the fins is located forward of the end of the rocket body so that they are more protected from impact damage during landing. The dimensions of the fins are shown in Figure 30.
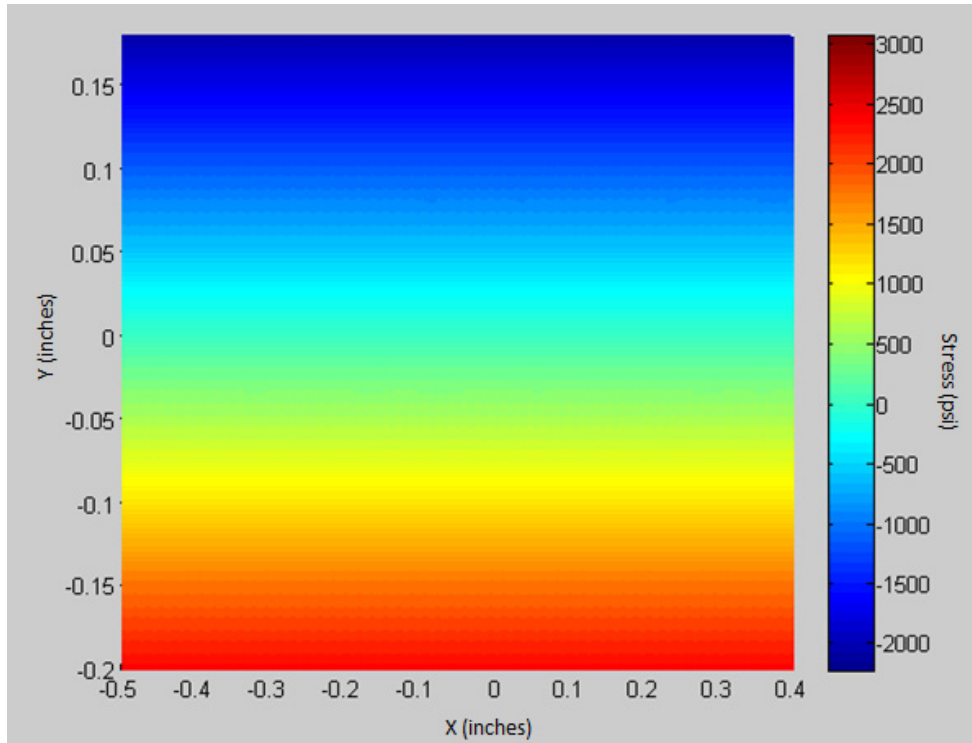
Figure 29: Axial stress field of Vic-3D analysis element with 403 lbs of loading
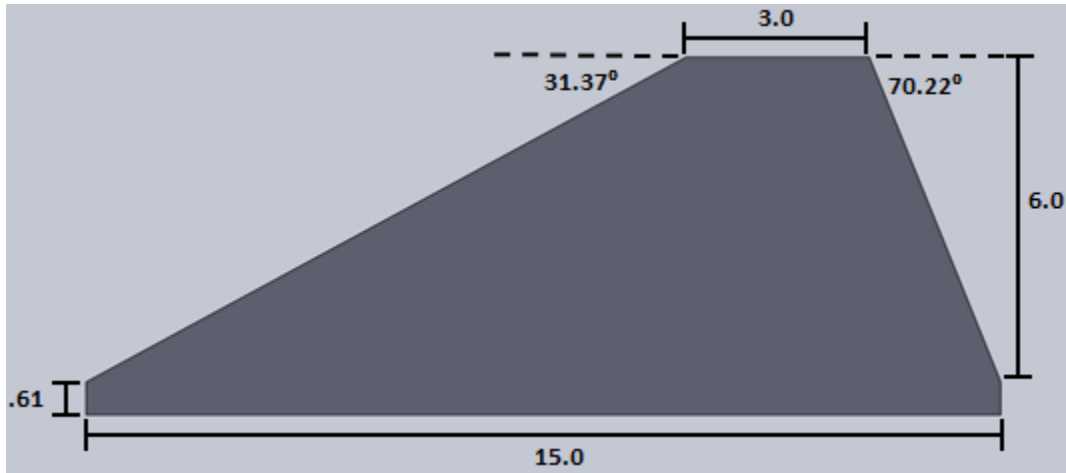
Figure 30: Fin Dimensions

The fins are made out of a composite honeycomb core with carbon fiber skins on both sides. This sandwich design provides strength to the fin structure while reducing weight. The leading edge will be constructed of plywood crafted in a rounded triangular shape and attached to the fin with epoxy. The fins will connect to the booster section of the launch vehicle through two L brackets on each side of the fin attaching it to the thrust plate. In addition epoxy fillets will run the length of the fin connecting it to the cardboard motor tube.

During flight, if the drag becomes too great the fins can detach from the launch vehicle structure due to the high moment acting at the interface between the fins and the structure of the launch vehicle. Another mode of failure is drag causing the leading edge to detach from the fin resulting in the carbon fiber honeycomb panel disintegrating during flight. Calculations of the max drag force per fin were performed utilizing Equation (3) and the moment was calculated as the product of force and the distance from the tip of the fin.

$$D = \frac{1}{2}\rho v^2 A C_D \qquad\qquad (3)$$

Further, the maximum velocity occurs at an altitude of 1,015 feet, which corresponds to a density of 0.07423 lb_m/ft^3. The results are summarized in Table 9 .

Table 9: Drag calculation values

Variable	Value
Density	0.07423 lbm/ft3
Velocity	613.88 ft/sec
Cross section area	0.0695 ft2
CD	0.295
Max drag force per fin	8.9 lbf
Moment	6.78 lbf –ft

4.3.1.1.   Fin Testing Article

The test rig used for these tests is designed to test the worst case scenario by applying the force at the maximum moment. The test rig is portable and the fin structure connects directly to the test rig with a qualification motor tube and fin unit as illustrated by Figure 31.

Figure 31: Fin static testing article

4.3.1.2.   Fin Static Loading Testing

The test was used to determine the capabilities of the test article while undergoing static loading. This is representative of the thrust during the boost phase of flight. The weight will be applied at the center of pressure until part failure and the test will be considered successful if a factor of safety of two (2) is achieved.

4.3.1.3.   Fin Test Results

The fin test article successfully withstood 28 lb$_f$, which corresponds to a factor of safety (F.S.) of three (3). There was no visible structural damage to the fins or the testing rig. Figure 32 shows an image of the test article at the max loading.

4.1. *iMPS – Integrated Modular Payload System*

4.1.1. Design and Analysis

A lightweight structure is essential to maximizing payload mass fraction. Most launch vehicles use a thick walled body tube as the structural member of the launch vehicle. Though simple, this design is inefficient in its use of material. The Mile High Yellow Jackets' launch vehicle will be unique amongst high power launch vehicles as it utilizes an internal structure consisting of ribs and stringers as illustrated by Figure 33. The ribs and stringers are fashioned out of G-10

fiberglass. The skin of the launch vehicle consists of a thin, flexible cellulose polymer composite.
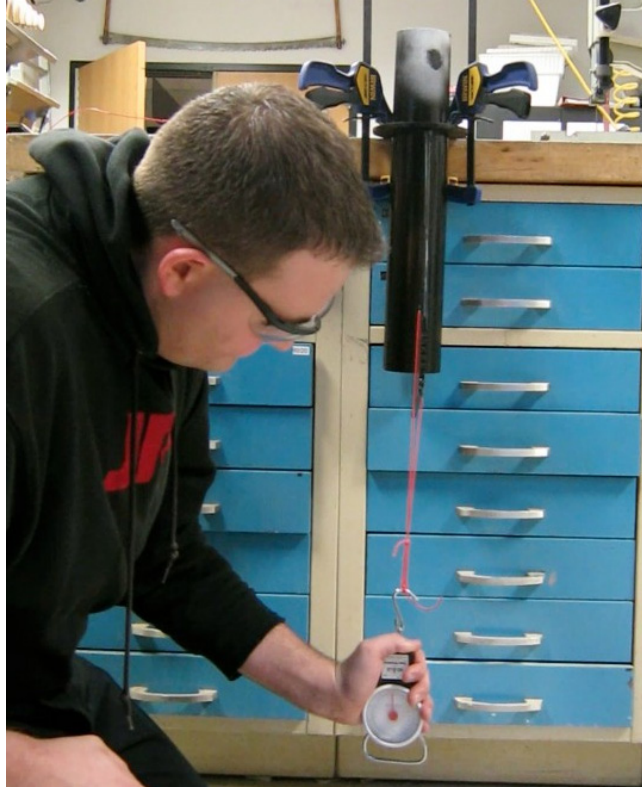
Figure 32: Fin Test Article at max loading
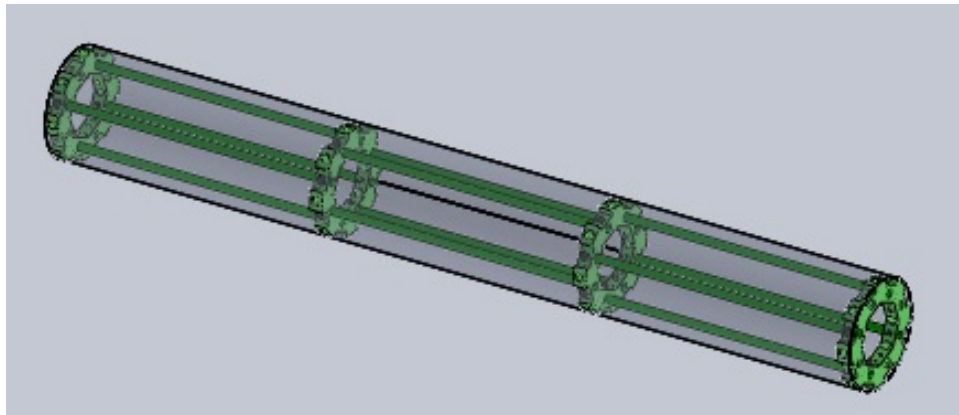
Figure 33: CAD model of the iMPS

To ensure the validity of the design, structural calculations were performed in order to ensure a factor of safety (F.S.) of at least 2.5 on the static loading for the structure. Consider a two dimensional view of the stringer in Figure 34. As a result of the hole, the loading path of the rod has changed significantly. That is, instead of the load being transferred through the entire cross-section of the rod, only a smaller cross-sectional area is carrying the load. The smallest cross-sectional area occurs along the diameter of the fastener hole. Thus, the point of failure will be about this hole due to increased stresses.
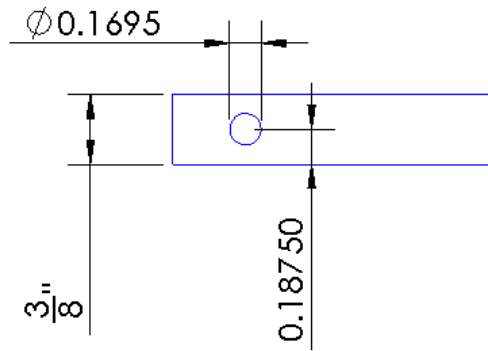
Figure 34: Dimensions for the stringer

Figure 35: Cross-sectional view of the rod with the fastener hole

The smallest cross-sectional area that will carry the load is 0.0537 in^2, shown in Figure 35. The stress concentration factor (SCF) for this geometry is 2.0, and was calculated utilizing Equation (4).

$$SCF = \frac{A_{rod}}{A_{min}}$$

(4)

This indicates that for a given load, the area around the hole will experience at least twice the amount of stress than compared to any other part. Therefore, for a maximum stress of 38 ksi, the maximum force that one rod can handle before breaking is 995.4 lb$_f$ as calculated utilizing Equation (5).

$$F_{max} = \frac{\sigma_{max}}{SCF} \qquad\qquad (5)$$

Since four stringers will be used and the max thrust from the motor is known, the factor of safety was calculated to be 9.75. The results are summarized in Table 10. The size of the stringers and ribs were determined by creating adequate fastener edge clearance. This is the cause of the high factor of safety.

Table 10: Values for factor of safety calculation

Condition	Values
Max thrust from motor	408 lb$_f$
A$_{rod}$	0.1104 in^2
A$_{min}$	0.0537 in^2
SCF	2.05
F.S.	9.75

In order to reduce structure mass, lightening holes have been added to the design of the ribs. These holes run radially about the structure and are the same diameter as the stringer holes. To ensure that these holes would not compromise the integrity of the structure, a FEA was run using ANSYS, shown in Figure 36. The maximum and minimum stresses were found to be 9,220 psi and 82 psi, respectively.

The analysis utilized a loading of 684 lbf, which occurs during parachute deployment and is the maximum loading that will act upon the ribs. Using the maximum loading and a yield stress of 43.5 ksi the factor of safety on the ribs is 4.7.
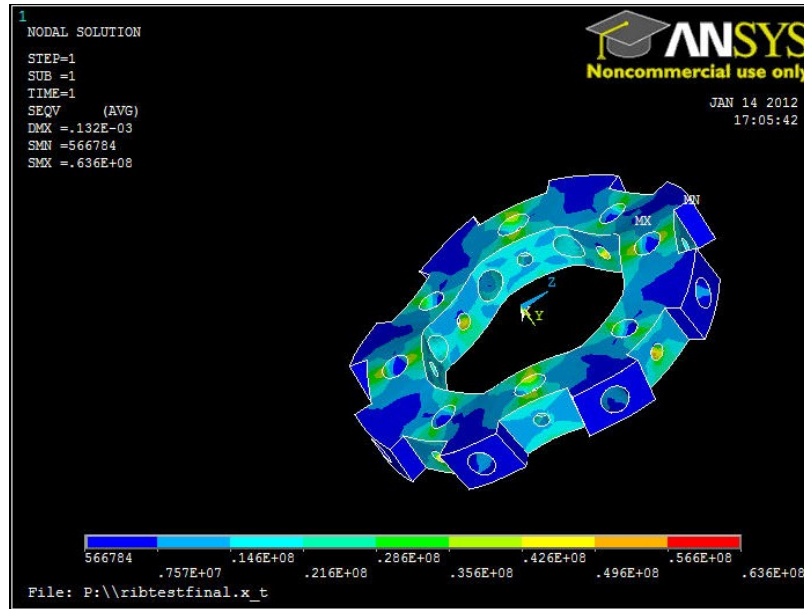
Figure 36: FEA of rib with lightening holes (note that units are in base SI)

4.1.2. Structure Fabrication and Manufacturing

Because fiberglass is a laminate composite, machining it can be difficult. To simplify manufacturing, the ribs were limited to being 2-D designs. This allows the ribs to be cut from a sheet using a water-jet. Starter holes are drilled in the plate in order to prevent delamination of the G-10 fiberglass when the water-jet pierces the material. The cutting jet can then be traversed from these starter holes to the part. The stringers are cut from lengths of 3/8 inch diameter G-10 rods. They are match drilled to the ribs to create a good fit with the fasteners. For more detailed manufacturing instructions, please see the iMPS Manufacturing and Fabrication Order (MFO) in Appendix VI.

A cellulose polymer composite covers the payload and booster sections of the rocket. A scaled outline of the skin was made using PowerPoint, printed on poster paper, and cut to size. Holes for the rail buttons, arming switches, and altimeters were then cut out. The layout can be seen in Figure 37.
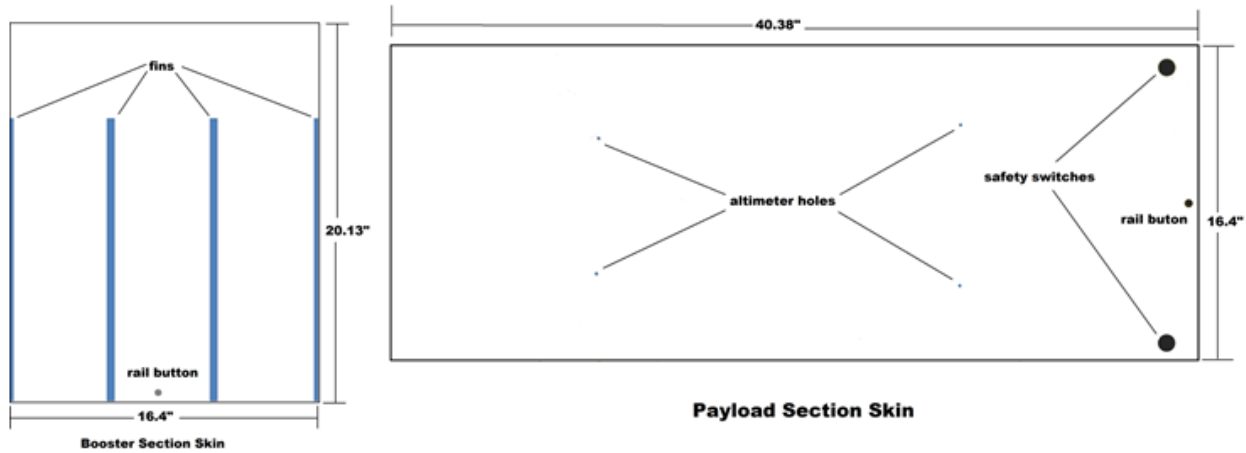
Figure 37. Vespula skin layout and dimensions.

The skin was then laminated and the borders were trimmed. Hook and loop fasteners are used to attach the skin to the rocket by adhering the hook side onto the ribs and centering rings with the loop part being adhered across the skin at the corresponding height. Before launch the seams were sealed with packing tape. This method was tested on the subscale rocket, *Korsakov*, to be discussed in Section 6.1

4.1.3. Structure Testing & Results

Testing was performed to ensure a F.S. of 3.0 on the impact energy during launch. The test rig used for these tests was designed to complete multiple types of test, such as static and dynamic structural loading. This was done to decrease test costs through the use of a multipurpose test device as shown in Figure 38. The testing device features a rail-mounted impact machine that can hold various amounts of mass and can be lifted to heights up to five feet for various sized test articles and/or impact energies.

Figure 38: Impact testing rig

Each test consisted of a known mass ,3.98 kilograms, being dropped from a known distance. The energy of the mass correlated to a design impulse (I) of 9.35 N-s. This value was determined from the calculated acceleration of the launch vehicle from the OpenRocket vehicle simulation. The height for the mass was derived using conservation of energy in Equation (6), where m_t is the drop mass.

Table 11 features the details of the test runs.

$$Height = \frac{1}{2g}\left(\frac{I}{m_t}\right)^2 \qquad (6)$$

Table 11: Impact test runs

Test Number	Impactor mass (kg)	Factor of Safety	Impact Energy (J)	Impactor Height (m)	Impactor Height (in)
1	3.98	1.0	5.23	0.064	11.08
2	3.98	1.5	7.85	0.096	16.62
3	3.98	2.0	10.47	0.128	22.16
4	3.98	2.5	13.08	0.160	27.70
5	3.98	3.0	15.70	0.192	33.24

The test article, which consisted of half of the iMPS structure illustrated in Figure 39, was inspected at various locations after each run, and passed the performance criteria, with only minor damage. The results are listed in Table 12.

Table 12: Testing results matrix, where X signifies damage, P signifies pass.

Fastener location	F.S. = 1.0	F.S. = 1.5	F.S. = 2.0	F.S. = 2.5	F.S. = 3.0
1	p	P	p	p	P
2	P	P	P	P	P
3	P	P	P	P	P
4	P	P	P	P	P
1A	P	P	P	P	X
2A	P	P	P	X	X
3A	P	P	P	X	X
4A	P	P	P	P	P
5	P	P	P	P	P
6	P	P	P	P	P
7	P	P	P	P	P
8	P	p	P	P	P

Figure 39: iMPS structure test article

The damage was very minor and featured discoloration from compression of the fiberglass at the faster locations in the stringers, but no fracturing occurred as seen in Figure 40.
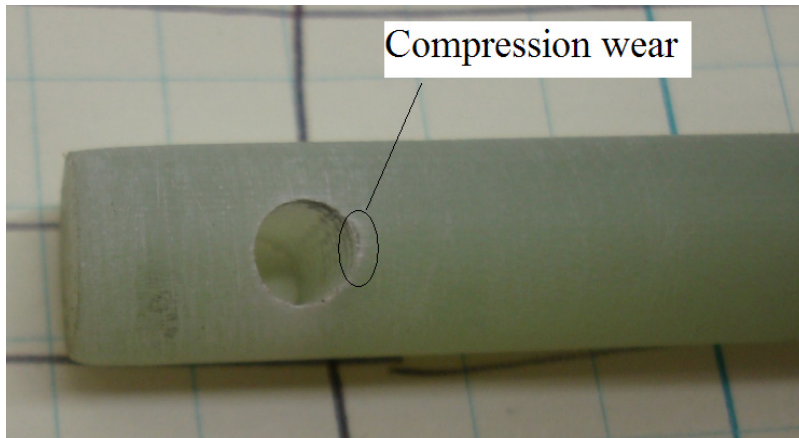
Figure 40: Evidence of minor compression damage occurring at F.S = 2.5

An internal review for this novel structural design was held and the team decided to continue with this option.

4.2. *Vespula Overall Dimension*

Figure 41 illustrates key dimensions of the *Vespula* launch vehicle.
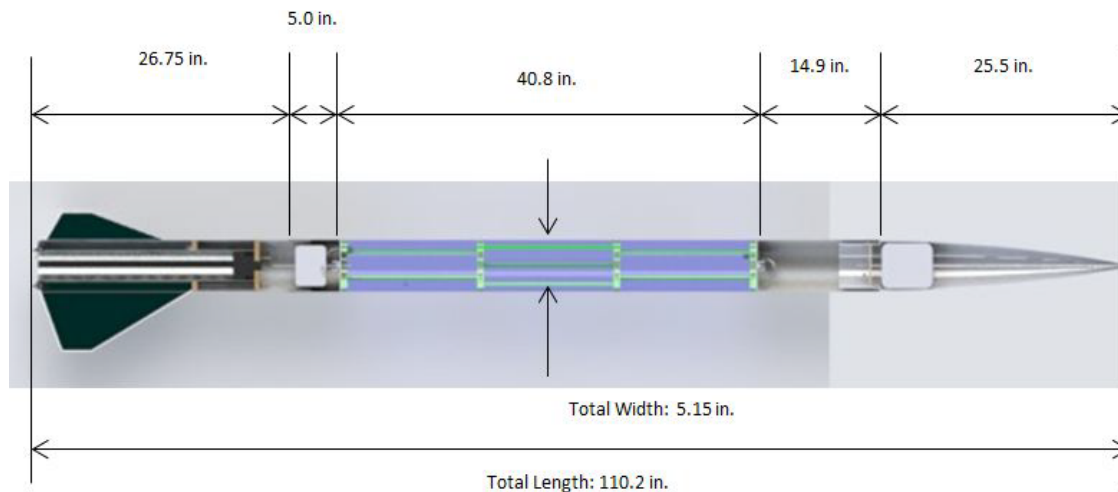
Figure 41: Dimensions for the Vespula Launch Vehicle

4.3. *Vespula Mass Breakdown*

The mass breakdown for each subsystem is summarized in Table 13 and Table 14. The system level mass breakdown and launch vehicle mass fractions are illustrated in Figure 42.

Table 13: iMPS component weight

Payload Section	Weight (lbs)	Quantity	Total Weight (lbs)
Tube for main chute (10")	0.78	1	0.78
Tube for drogue chute (6")	0.466	1	0.466
PVC Cup	0.1	4	0.4
G10 Fiberglass Ribs	0.4233	4	1.6932
Fiberglass rods	0.11	12	1.32
1" bolts	0.005	24	0.105816
Hook and Loop Fasteners	0.005	32	0.141088
Skin	0.1	1	0.1
Epoxy/Paint	0.13	1	0.13
Arming Switches & Bracket	0.28	1	0.28
Recovery Wiring harness	0.22	1	0.22
Altimeter	0.03	2	0.06
9V Battery	0.1	2	0.2
Total			5.90

Table 14: Booster Section Weight Budget

Booster Section	Weight (lbs)	Quantity	Total Weight (lbs)
Mounting Rod	0.15	4	0.6
Cardboard tube	0.06	1	0.06
U-bolt	0.5	1	0.5
Nuts	0.01	20	0.2
Skin	0.1	1	0.1
Fin	0.2	3	0.6
Rear Plate	0.28	1	0.28
Thrust Plate	0.17	1	0.17
Booster fiberglass tube (6")	0.47	1	0.47
Centering Ring	0.1	1	0.1
L-Brackets	0.01	25	0.25
Coupler	0.25	1	0.25
Epoxy/Paint	0.3	1	0.3
Total			**3.88**

Component	Weight (lbs)
Nose Cone	1.59
Drogue Chute & Shock Cords	1.43
Main Chute & Shock Cords	2.76
Avionics System/Payload	2.92
Payload & Recovery Structure	5.896104
Booster Structure	3.88
AeroTech L850	8.33
Ballast	5.0
Total	31.8

Launch Vehicle Mass Fraction

10%
28%
62%

- Payload
- Propulsion
- Inert Mass
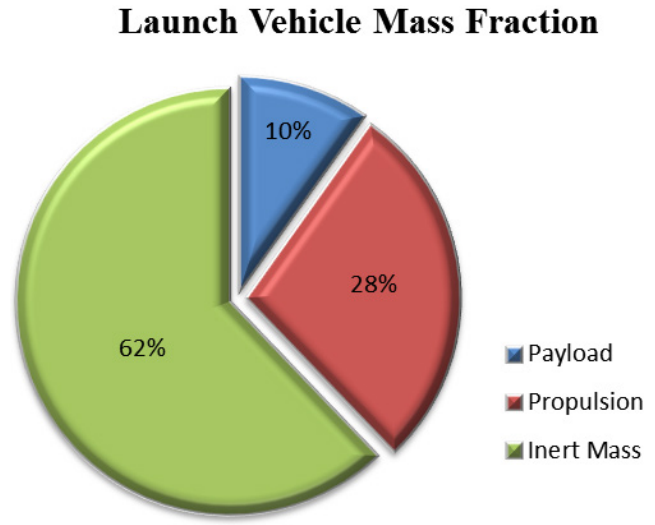
Figure 42. Vespula launch vehicle mass fraction.

5. Launch Vehicle Performance Predictions

Current mission performance predictions are based on a worst case scenario assuming a launch vehicle mass of approximately 32 pounds and an AeroTech L850 launch vehicle motor.

For the launch vehicle to fly along the predicted trajectory, the launch vehicle must leave the launch rail at a minimum velocity. For this launch vehicle configuration, the launch vehicle becomes stable, with a stability margin caliber of 1, at 57 ft/s, which occurs at 60 inches up the launch rail. Thus so long as our launch rail is a minimum of 97 inches, the launch vehicle will be stable when the rail buttons leave the guide rail. A launch rail length of 97 inches leaves 60 inches to reach stability plus allows for the necessary distance between rail buttons of 37 inches. The current launch pad is the Apogee "Gun Turret" Pad. The system consists of a rail and a base. Altogether the system costs roughly $500.00. The rail is a T-slot aluminum extrusion of approximately eight ft. in length and satisfies the minimum length required for the launch vehicle to reach an acceptable static stability margin. Depending on budgetary constraints, we may build our own launch pad to reduce cost.

All simulations utilized the highest gross launch weight on the chart and the corresponding motor selection. The assumptions for all simulations are listed in Table 15.

Table 15. Flight Simulation Conditions

Condition	Value
Windspeed	15 mph
Temperature	60.8^0 F
Latitude	34^0 N
Pressure	14.7 psi
Gross launch weight	31.8 lb
Motor	Aerotech L850

5.1. *Flight Simulation*

Figure 43 shows the flight profile of the launch vehicle utilizing flight simulation conditions from Table 15. Velocity, altitude, and acceleration were plotted as a function of time. Apogee occurs at approximately 18 seconds at an altitude of 5312 ft. At apogee, the ejection charge for the drogue chute will fire; slowing the decent rate to 50 ft/s. Deployment of the main chute will occur at 500 feet above ground level to further decelerate the launch vehicle to 17 ft/s. The entire flight duration is approximately 173 seconds.
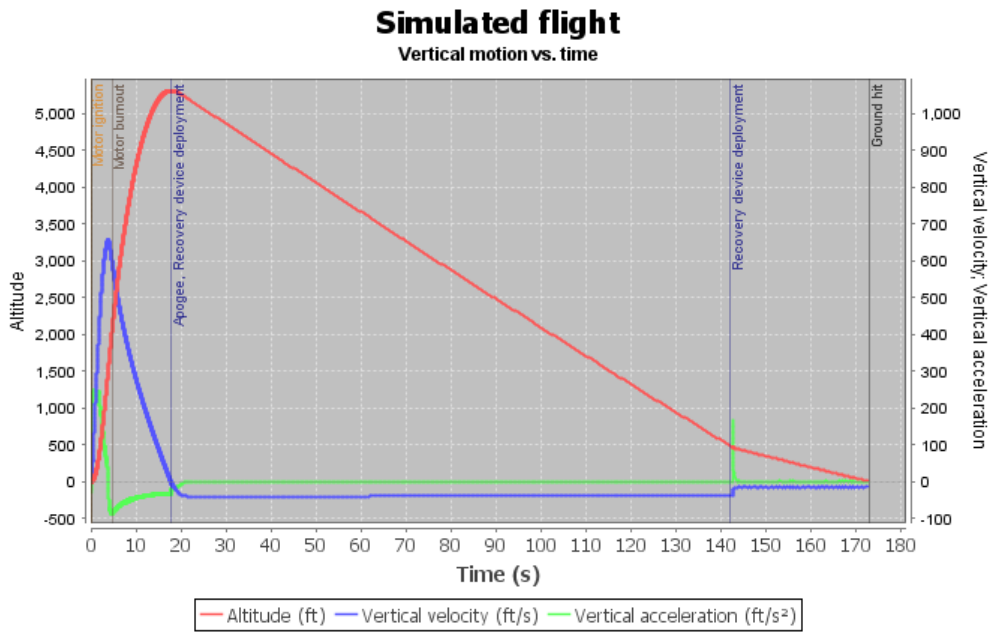
Figure 43: Flight profile with AeroTech L850 motor for a total takeoff weight of 31.5 pounds

5.2. *AeroTech L850 Simulated Thrust Curve*

The simulated thrust curve for Aerotech L850 is shown in Figure 44. It is the optimum projected motor for the launch vehicle to reach an altitude of 5,280 feet using the 75/3840 Aerotech motor case. The motor will follow this thrust curve closely, however it is important to keep in mind that the performance of the motor may vary slightly in actual flight.
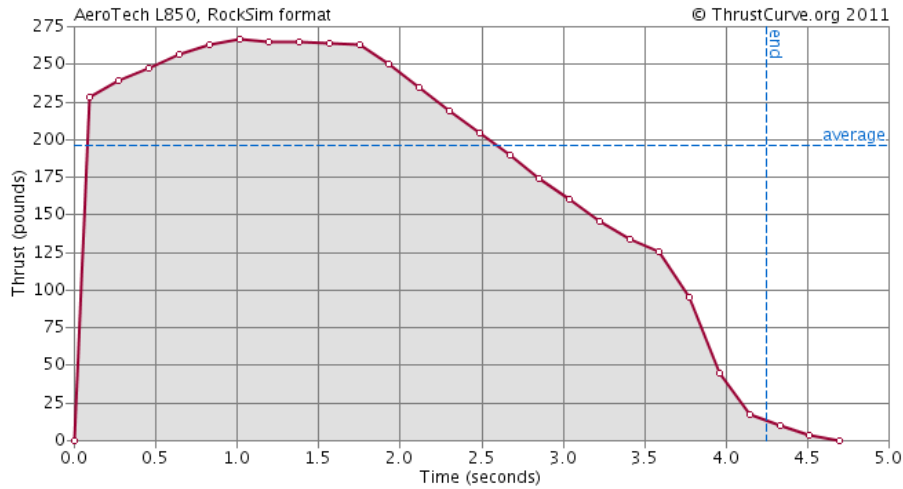
Figure 44: Thrust curve for Aerotech L850 motor

5.3. *Stability Margin*

In addition, a stability analysis was performed to ensure a safe flight profile as shown in Figure 45. The stability margin of our launch vehicle during most of the flight is four calibers, where one caliber is the maximum body diameter of the launch vehicle. This is higher than the general rule of thumb among model rocketeers that the C_P should be one to two calibers aft of the C_G. However, being over-stable is not bad; it simply means that the launch vehicle will have a greater tendency to weathercock if there is any wind at launch. To counter this, our launch rod will be at least 97 inches long to ensure stability when the rail buttons leave the guide rail as mentioned previously; additional length will be added to prevent weathercock.
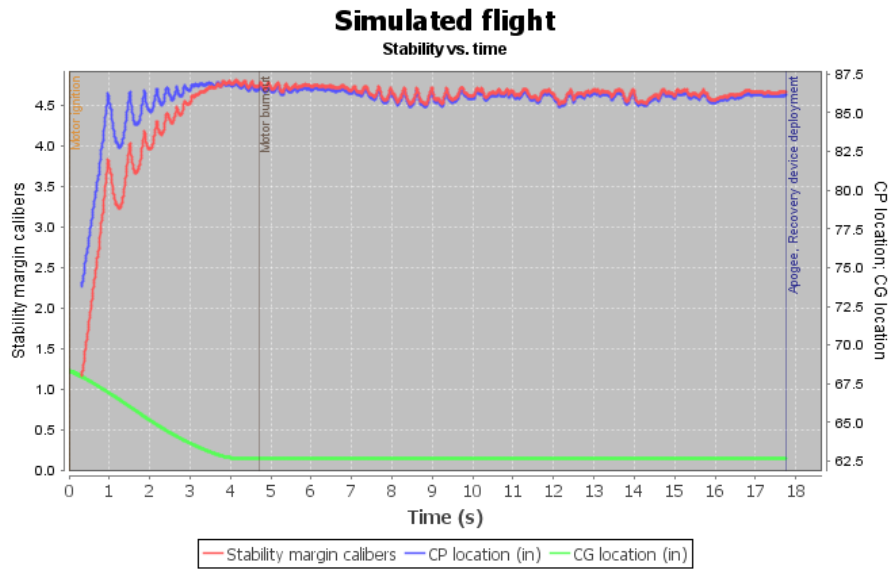
Figure 45: Stability margin calibers vs. Time

5.4. *Drift Profile Simulation*

The rocket must be recoverable within 2,500 ft. of the launch pad in a 15 mph head wind. The plot of lateral distance during the flight into a 15 mph headwind is shown in Figure 46. Here it is seen that the vehicle will land approximately 1,300 ft. from the launch pad.
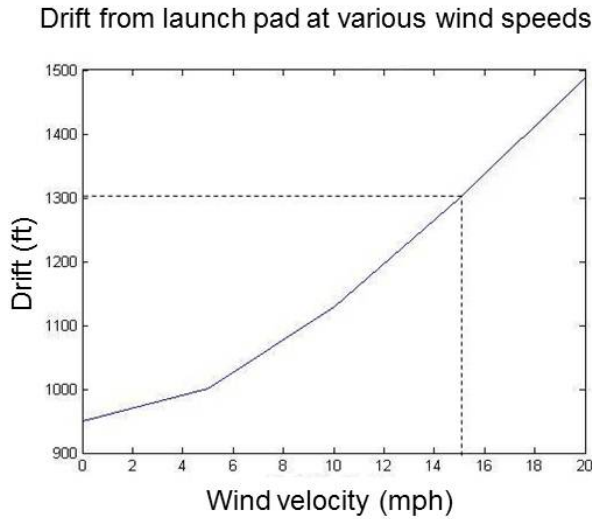
Figure 46: Drift from launch pad at various wind speeds

5.5. *Landing Kinetic Energy*

The kinetic energy (KE) at landing for each independent and tethered section of *Vespula* was calculated utilizing Equation (7) where m is the mass of each section and v is the velocity. The results are summarized in Table 16

$$KE = \frac{mv^2}{2}$$
(7)

Table 16: Kinetic energy upon landing for each section of Vespula

	Mass (lbs)	Velocity (ft/sec)	KE (ft-lb)	KE Margin (ft-lb)
Nose Cone	1.59	17	7.2	90.5 %
Booster Section	7.59	17	34.2	54.5 %
Payload Section	13.82	17	62.2	17.1 %

6. Launch Vehicle Testing

6.1. *Subscale Testing*

A subscale flight test was performed prior to CDR to determine the feasibility of specific aspects of our design. This testing primarily focused on the performance of our exterior skin which covers the booster and payload sections during flight. The basic design of our subscale launch vehicle, *Korsakov*, features a smaller diameter body tube, which is covered by a non-load bearing, thin-walled skin, as shown in Figure 47. Korsakov will utilize two 0.5 inch diameter launch lugs, with one placed on the top section and one on the bottom. The launch lugs will be two inches long and epoxied onto the sides. The thrust will transfer through the internal cardboard tube from the booster section to the nose cone. Due to the configuration of the launch vehicle, a dummy mass of 0.3 pounds was added beneath the nose cone to provide a stability margin of approximately 3.25 calibers for most of the flight as shown in Figure 48. The characteristics of Korsakov are summarized in Table 17.
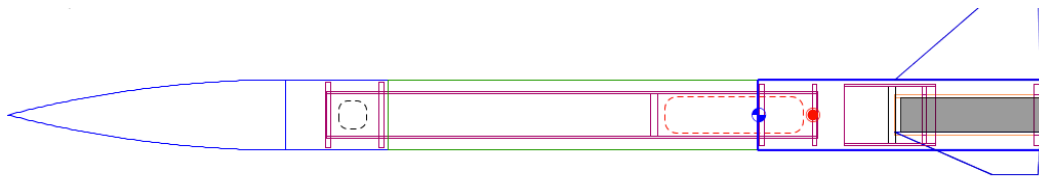
(a)

(b)

Figure 47: Korsakov (a) layout and (b) flight vehicle

Table 17: Characteristics of Korsakov vehicle

Condition	Value
Length	55.5 inches
Outer Diameter	3 inches
Motor	Aerotech H128
Max Mach Number	0.44
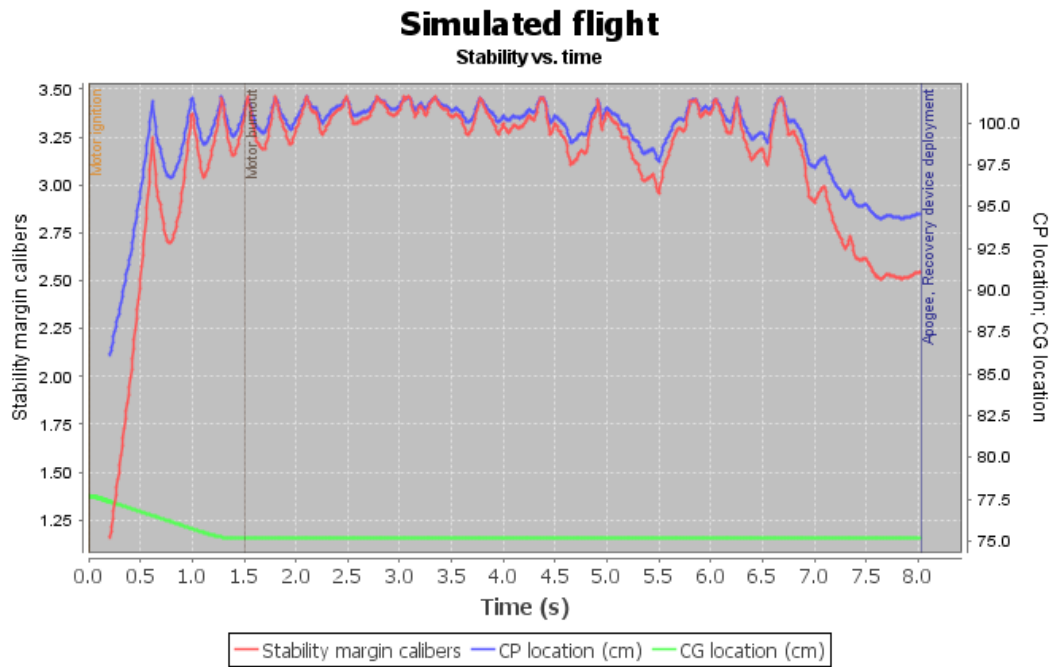
Figure 48: Stability profile for Korsakov vehicle.

Due to higher than expected winds aloft, Korsakov landed in a tree on private property and was unrecoverable. As a result, the actual loading on the skin from the onboard accelerometers could not be retrieved. However, upon visual inspection of the rocket, the skin remained intact throughout the flight and landing. In conclusion, the test was considered a success and the skin and hook and loop fasteners are rated for the flight characteristics predicted by the OpenRocket simulation as seen in Figure 49.

Table 18 shows all the materials required for building Korsakov with a total cost of $165.28 and the total weight was 3.4 lb$_f$.

Due to higher than expected winds aloft, Korsakov landed in a tree on private property and was unrecoverable. As a result, the actual loading on the skin from the onboard accelerometers could not be retrieved. However, upon visual inspection of the rocket, the skin remained intact throughout the flight and landing. In conclusion, the test was considered a success and the skin and hook and loop fasteners are rated for the flight characteristics predicted by the OpenRocket simulation as seen in Figure 49.

Table 18: Material and cost for Korsakov

Item	Use	Cost ($)
Motor reload kit	Launch vehicle motor	31.99
Airframe Tube 74/18 (Thin Wall 3" tube)	Main body	20.57
Airframe Tube 29/13	Inner body	8.790
Airframe Tube 56/18 (Estes BT-70 size)	Motor tube	11.52
Baltic Birch Plywood 6mm-1/4" x 24" x 30"	Fins	8.99
1/4" plywood	Centering rings	10.00
U-bolts	Recovery	2.000
Poster board	Skin	4.990
Hook and Loop fasteners	Skin fasteners	14.58
Parachute	Recovery	33.00
Nose cone	Aerodynamics	18.85
Total		**165.28**
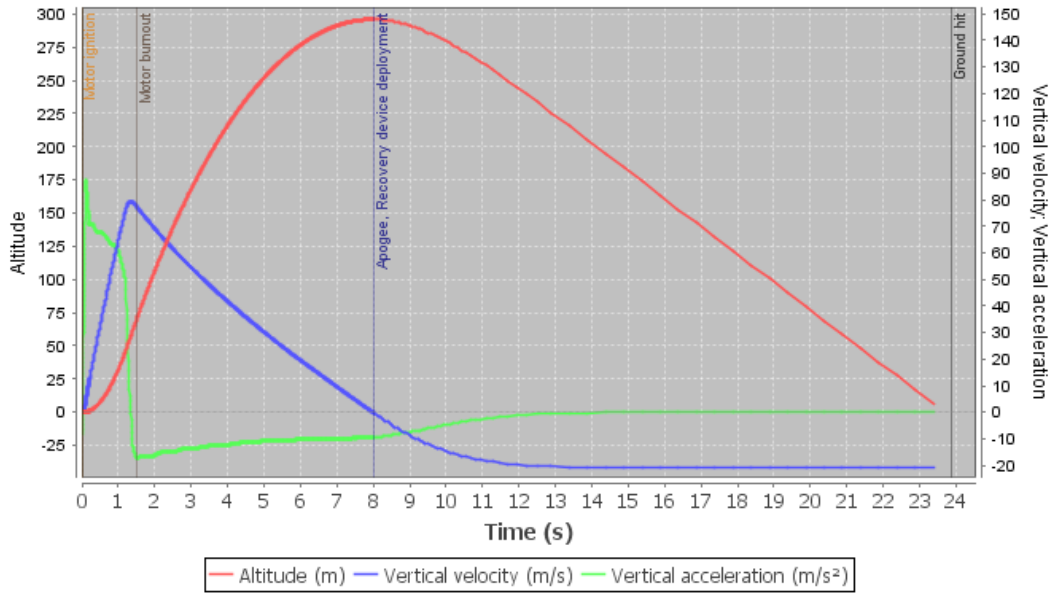
Figure 49: Korsakov Flight Profile as predicted by OpenRocket

As illustrated by Figure 50, with 25 MPH gusting winds, OpenRocket predicted a drift of 1,800 ft. In reality, Korsakov landed in the trees approximately 1,970 ft. from the launch pad as shown in Figure 51. This supports that OpenRocket's drift calculations are within approximately 10% of test data.
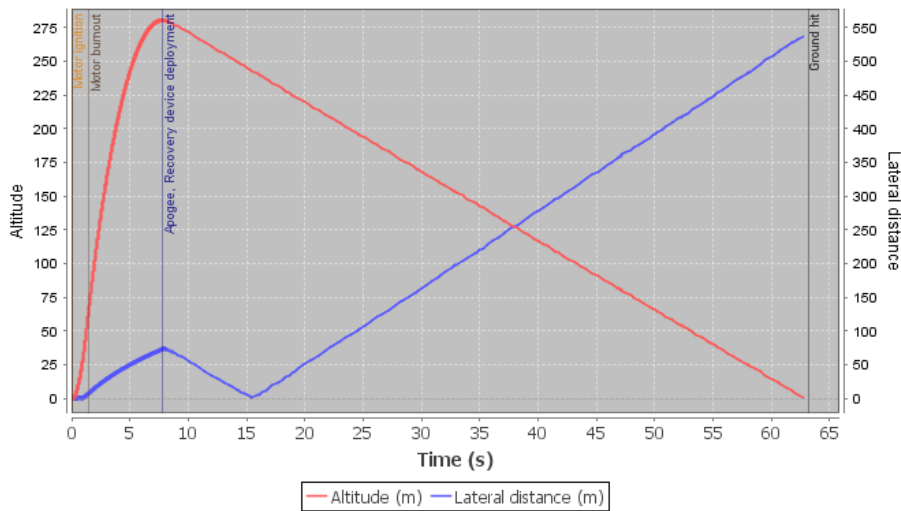
Figure 50: Korsakov Predicted Drift Profile

Figure 51: Korsakov Drift Distance

6.1. *Vespula Flight Test #1*

On 10 March 2012, in Manchester, TN, *Vespula* performed its first full scale test flight as shown in Figure 52. Because the manufacturer of the L850 that was ordered experienced delays in manufacturing a Ceseroni L990 was flown instead. With a 10 mph wind, the vehicle launched to an altitude of 4,910 ft. The comparison of the altimeter data to the predicated OpenRocket model is presented in Figure 53.

Figure 52: Vespula Flight Test #1
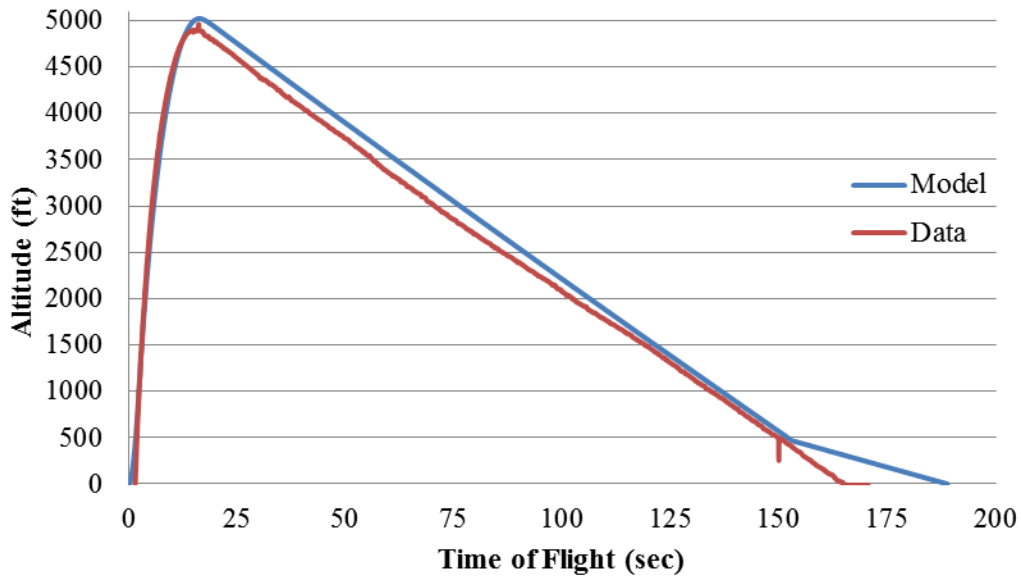
Figure 53: Comparison of Flight Data to Model for Flight Test #1

From this data, the rocket performed similarly to the predictions of the OpenRocket model. *Vespula* accelerated as predicted but didn't reach the predicted altitude of 5,022 ft, which could be caused by a higher than expected coefficient of drag for the flight vehicle. The drogue deployed as designed at apogee and followed the predicted slope of descent. However, at approximately 150 seconds into the flight, it can be seen that there was a flight anomaly. The main parachute did not deploy at the 500 ft altitude mark and the vehicle instead landed under drogue only.

During the post-flight investigation, it was discovered that an epoxy seal between the Garolite tube and the Garolite bulkhead failed as shown in Figure 54.

Figure 54: Photograph of Recovery Failure aftermath

The causes of this incident have been narrowed to an over-pressurization of the compartment due to improper chute packing. In order to mitigate this issue for future flights, more specific chute packing procedures have been written, a smaller main has been chosen, and L-brackets with mechanical fasteners will be added to fasten the recovery sections to the iMPS structure.

During landing there was minimal damage to the vehicle due to landing at drogue descent speed, approximately 50 ft/s. The only damage found was scratches in the paint on the nose cone and fins as well as approximately 1.5 in. long, tears in the iMPS skin as shown in Figure 54.

Figure 55: Photograph of Tears in iMPS skin

6.2. *Vespula Flight Test #2*

On 17 March 2012, in Palm Bay, FL, another launch was attempted with a repaired rocket. However, due to complications during assembly caused by an undermanned crew and unsatisfactory repairs, the launch was scrubbed. The second launch of Vespula is currently scheduled for 31 March 2012.

7. Launch System and Platform

As previously mentioned, the launch system that is showing the most promise is the Apogee "Gun Turret" Pad, as illustrated in Figure 56. The system consists of the rail and the base. Altogether the system costs $500.00. The rail is a T-Slot aluminum extrusion of approximately 8 feet in length and satisfies the requirements of the distance required for our launch vehicle to reach an acceptable static stability margin. The blast deflection pad is angled with the dimensions 9 x 9 x 0.25 inches, and is made of heavy-gauge steel. The rail and the deflection pad are attached to the head of the base, which can pivot horizontally for easy loading of launch vehicles. Three legs with leveling screws are attached to the base so that the launch angle can be adjusted to desired conditions, with all parts also being constructed from heavy-gauge steel. The entire system weighs approximately 30 pounds; and is collapsible for easy transportation.

Our launch vehicle will have two rail buttons attached in such a way that they do not interfere structurally with any other components. The rail buttons slide into the T-shaped aluminum extrusion and limit the launch vehicle's motion except in the desired launch direction. The first button will be attached to the thrust plate in the booster section, where there is a pre-existing attachment interface with minimal structural interference. The second button will be attached to the rear thrust retention plate. This ensures both buttons will be on the rail for enough time to reach an acceptable static stability margin upon launch.

The launch procedure checklist is presented in Appendix II.
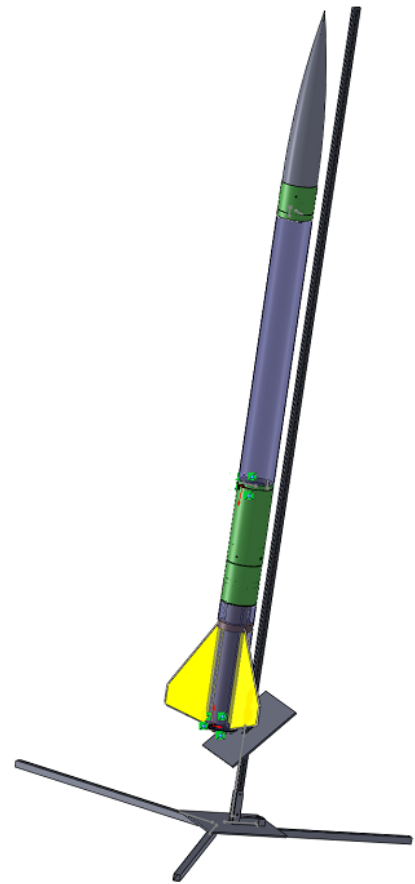
Figure 56. Gun Turret launch pad.

8. Payload

8.1. *Introduction to the Experiment and Payload Concept Features & Definition*

8.1.1. Motivations

Today, many entrepreneurs are beginning to build newer and more cost-effective launch vehicles. Every one of these launch vehicles must address a specific challenge in their design process: integration with the spacecraft payload. This integration presents difficulties in launch vehicle design because harmonic oscillations of the spacecraft mass could cause structural damage to either the launch vehicle or the spacecraft itself. To solve this dilemma, industry typically utilizes large mechanical springs – in addition to the placement of certain structural constraints on the payload spacecraft for use of a particular launch vehicle. Repeated deformation on vibration dampers and springs used in launch vehicles presents a further issue in providing reusability, as these parts must be intermittently replaced. Furthermore, modifications must be made to both payload and launch vehicle to tune the natural frequencies of both and prevent harmful oscillation. The net result of the present situation is an increase in overall structural mass, which combined with the necessary increase in fuel required and maintenance, dramatically increases the launch cost to the detriment of mission capability. The Mile High Yellow Jackets intend to provide a possible alternative solution in a demonstration of the ability of electromagnetic levitation to lower the necessary structural masses currently required to prevent harmonic oscillation, decreasing launch cost.

In addition to payload isolation, magnetically stabilized platforms can also be used to isolate both terrestrial and space-based optics and digital sensing devices from their housings ensure image stability and virtually eliminating image distortion that is commonly associated with long-duration exposures. For example, while the Hubble Space Telescope is in a micro-gravity environment, small perturbations due to thermal cycling may introduce unwanted distortion into images. Currently, these distortions are compensated for by training the optics and digital sensing devices real-time during the exposure in addition to post-processing of the collected image. However, the magnetic isolation techniques being pursued by the Mile High Yellow Jacket would isolate the optics or digital sensing devices– say, on a future space-based telescope collecting EM radiation of any spectrum – eliminating the need for this thermal characterization

and post-processing directly resulting in not only lower development costs but would also result in a shorter turn-around time for releasing the data for analysis.

8.1.2. Scientific Merit

The problem of magnetic force interactions from n-solenoids on a single sample is a non-trivial problem in electromagnetics. The difficulty in describing complex field relationships is similar to the difficulty in aerodynamics for describing complex fluid flows, and many of the computational techniques are similar. However, due to the nature of the complexity, the study of complex magnetic interactions must be a data-driven process, as in aerodynamics. The A.P.E.S. system will depend upon a theory-informed, data-driven model for control. This data will be generated through a series of ground test experiments that gradual increase the complexity of the problem. Final model testing on the ground will involve only permanent magnets and solenoids, simplifying the force interactions to compensate for complex geometry.

The A.P.E.S. project may be considered as a dual scientific-engineering payload. A period of scientific analysis is necessary, as stated above. However, the actual product flown in the launch vehicle will be flown for verification and validation purposes after the conclusion of ground testing; the flight will test the performance of the derived model, and engineering design, during the dynamics of the ascent phase. This process of scientific investigation followed by engineering development is not entirely unlike the development of experimental aircraft and spacecraft, where some scientific investigation may be needed before the engineering can proceed.

8.2. *A.P.E.S. Success Criteria and Requirements Definition*

The success criteria for the A.P.E.S. system are derived directly from the Project's Mission Objectives and Mission Success Criteria – which are listed in Table 1, Section 2.3Table 1. The requirements and verification methods for the A.P.E.S. system can be found in Table 2, Section 2.4 and are listed in

Table 19 convenience.

Table 19. A.P.E.S. system Requirements Flow Down.

MO	Mission Objectives				
MO-2	Stabilize and isolate the A.P.E.S. platform from the induced vibrations of the Launch Vehicle.				
MO-3	Closed-loop control of the platform via real-time image processing.				

MSC	Mission Success Criteria	Source	Verification Method		Verification Source
MSC-2	The Flight Experiment is successfully activated and data is collected.	MO-2, MO-3	Inspection, Analysis		N/A
MSC-2.1	*Minimum Mission Success*: Platform is stabilized and isolated during the coast phase of flight	MO-2	Testing		N/A
MSC-2.2	*Minimum Mission Success*: Relative position and rotation data of the platform to the camera is collected during all phases of the experiment.	MO-2, MSC-2	Testing		N/A
MSC-2.3	*Minimum Mission Success*: The flight experiment terminates at apogee.	MO-4, MSC-2	Inspection		N/A
MSC-2.4	*Full Mission Success*: Platform is stabilized and isolated from environmental vibrations during the powered and un-powered portions of the flight.	MO-2, MSC-2	Testing		N/A
MSC-2.5	*Full Mission Success*: Platform does not come into contact with any other components of the A.P.E.S. System.	MO-3, MSC-2.4	Testing		N/A
MSC-4	*Minimum Mission Success:* The cost of the all the components, including the Launch Vehicle, Flight Experiment, Flight Avionics, and Motor, shall cost no more than $5,000.	USLI Handbook	Inspection, Analysis		N/A

FS	Flight Systems	Source	Verification Method	Status	Verification Source
LV-1	The Launch Vehicle shall carry a scientific or engineering payload.	USLI Handbook	Inspection	Completed	Section 4.4
LV-1.1	The maximum payload weight including any supporting avionics shall not exceed 15 lbs.	LV-1	Inspection	Completed	Table 21,

FS	Flight Systems	Source	Verification Method	Status	Verification Source
FS-1	The platform shall be stabilized and isolated during ascent.	MSC-2.4, MO-2	Testing	In Progress	
FS-1.1	The platform shall not deviate more than 0.1 inches from the center of experiment cylinder.	FS-1	Analysis, Testing	In Progress	
FS-1.2	The platform shall not come into contact with any components of the A.P.E.S. System.	FS-1, MSC-2.5	Testing	Designed	
FS-1.3	The platform shall not rotate more than 1 rad per second for than 1/10 of a second with respect to the camera.	FS-1	Analysis, Testing	In Progress	
FS-2	All elements of the A.P.E.S. Systems shall weigh no more than 15 lbs.	LV-1.1	Inspection	Completed	Table 21,
FS-2.1	The A.P.E.S. Flight Experiment shall not weigh more than 10 lbs.	FS-2	Inspection	Completed	Table 21
FS-2.2	The A.P.E.S. supporting electronics shall not weigh more than 5 lbs.	FS-2	Inspection	Completed	
FS-3	The A.P.E.S. experiment shall be terminated at apogee.	MSC-2.3	Testing	In Progress	
FS-3.1	The platform shall be secured during descent and landing.	FS-3	Testing	In Progress	

8.3. *Experiment Overview*

8.3.1. Hypothesis and Premise

The premise of the experiment is that –

> *If a platform can be levitated and stabilized in a dynamic magnetic field during the flight of a launch vehicle, then greater stability and lower structural mass may be achieved.*

The payload will utilize dynamic three-dimensional magnetic fields to create an Active Platform Electromagnetic Stabilization, or A.P.E.S., system for use during the ascent phase of the launch vehicle's trajectory. The launch vehicle ascent will provide a high vibrational intensity

environment in which to test the stabilization system. Two further premises are necessary for this A.P.E.S. system, namely:

1. *Under appropriate conditions, it is possible to control complex oscillating magnetic fields such that a system of ferromagnetic materials or permanent magnets may be levitated in non-rotational stability.*

2. *A design exists such that a platform of some size and low mass may be levitated using ferromagnetic materials or permanent magnets.*

Therefore, after completing a thorough analysis of the dynamics of materials being levitated and stabilized in magnetic fields, the Mile High Yellow Jackets will implement a design to apply this science to a platform within the Vespula launch vehicle.

8.3.2. Experimental Method and Relevance of Data

The parameters to be measured in the experiment are the coordinates of the position of a test sample – in the case of ground testing – and the coordinates of the platform for the ascent of the launch vehicle. To ensure full implementation of the scientific method, the experiments will be carried out such that the results are controlled by comparison – i.e. a series of tests of increasing complexity will be conducted such that the control theory of the A.P.E.S. system is constructed methodically. Analysis of optical and infrared data will provide Cartesian coordinates, which, in a known design, can be used to specify the position and displacements of the platform, defining all kinematics to a level of accuracy proportional to the sample and computational rates of the data acquisition system. This data provides an empirical basis for confirmation or rejection of an experimental hypothesis – a newly written control program can be considered as a hypothesis – and for the improvement of the system as a whole. Additionally, the data obtained throughout all ground and flight testing will be used to perform a sizing study that will identify feasible areas of application.

8.3.3. Ground Test Plan

Ground testing will serve two general purposes: (1) the development of data algorithms and control laws, and (2) the verification and validation of theory and control systems. By understanding and modeling the kinematics of a sample plate driven by dynamic magnetic fields, steady-state models can be formed allowing for stable non-rotating levitation with oscillation dampening. The testing process will ramp the complexity of the model, beginning with simple 1-dimensional tests, and increasing the number of solenoids and dimensions until a 3-dimensional multi-solenoid model has been created. Data collected from ground testing will directly inform the control of the flight A.P.E.S. system design. . See Appendix III for specific details on the Ground Testing Plan.

Figure 57: The A.P.E.S. system ground test platform

8.4. *Ground Testing*

Using the equations developed in the Modeling General Magnetic Fields, section XXX, the solenoid parameters NI were back solved for to 260 Ampere-Turns. The current was restricted to 80% of maximum allowable for the wire 0.86 Amperes and the solenoid was then constructed using a jig to wind 300 turns. Maximum field strength when run the solenoid was run at full current achieved over 1100 µT. Using the 3-axis AKM 8975 magnetic field sensor, the field

strength in the X-direction was tested at several currents and distances as per the Ground Test Plan. The results are illustrated in Figure 58.

Furthermore, in order to determine the field strength in the X-direction for any given position and current setting within the range tested, a Response Surface Equation (RSE) was created. The Response Surface is illustrated in Figure 59. The resulting RSE has the form of

$$\ln(B_x) = b_0 + \sum_{i=1}^{n} b_i X_i A_i + H.O.T. \tag{1.}$$

where b_0 is the intercept, b_i is the coefficient of the ith term, X is the position within the range tested and A_i is the current within the range specified. The resulting RSE is listed in Table 20.

Due to delays in manufacturing the solenoid driver boards and flight computer, no additional data is available to present.
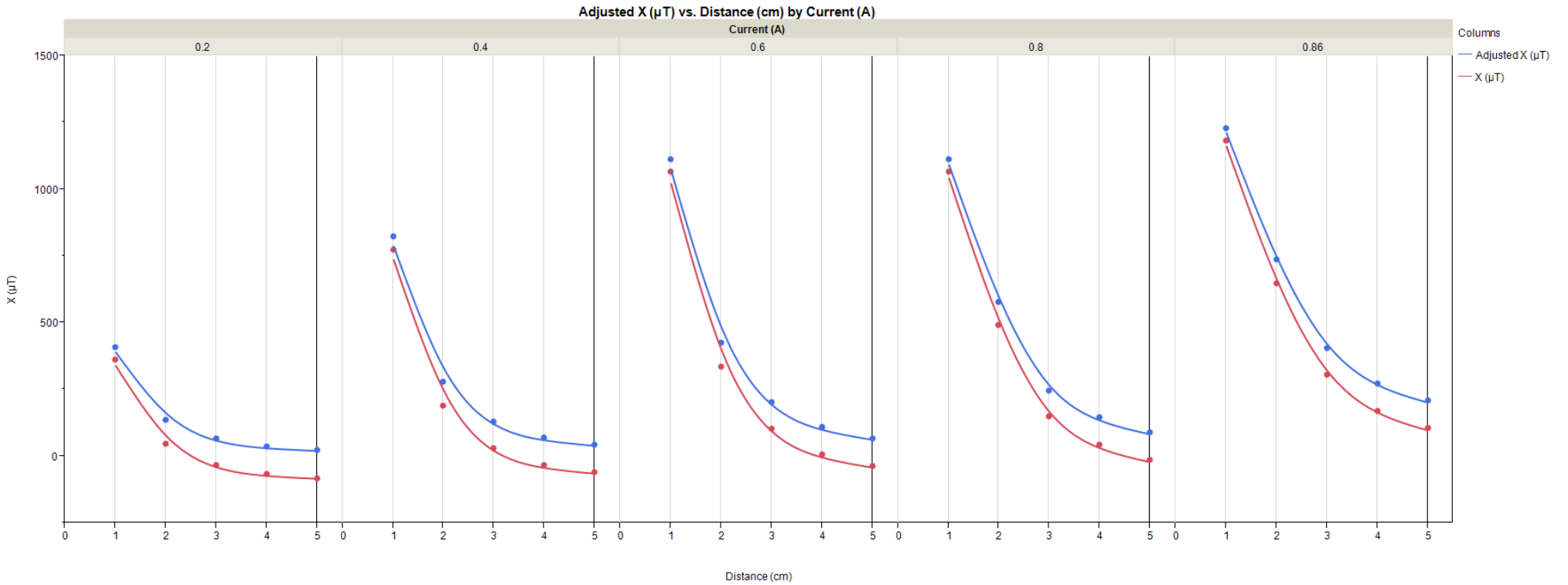
Figure 58. Field Strength in the X-Direction of the solenoid vs. radial distance at various current settings.
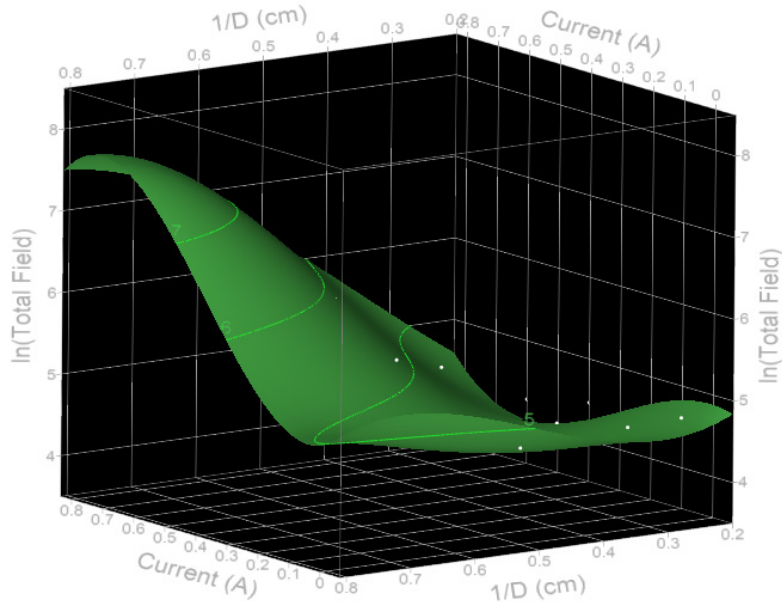
Figure 59. Response Surface of the field strength in the X-Direction.

Table 20. RSE coefficients and terms

Term	Estimate	Std Error	t Ratio	Prob>|t|
b_0	2.81755501	0.59373639	4.74546459	0.00021945
A	-1.4251419	1.04427097	-1.36472423	0.19122614
X	-5.37987105	4.39097585	-1.2252108	0.23822696
$X*X$	10.8426075	9.35256543	1.15931908	0.26333572
$X*X*X$	-6.36499083	5.58455774	-1.13974841	0.27116687
$A*X$	17.1758472	11.1812302	1.53613215	0.14404375
$A*X*X$	-57.4138468	33.6670109	-1.70534435	0.10746498
$A*X*X*X$	46.1097665	23.8093525	1.93662413	0.07065691
$A*A*X*X*X$	-170.759236	65.1181151	-2.62230004	0.0184835
$A*A*X*X$	218.596471	88.1941886	2.47858135	0.02471551
$A*A*X$	-53.8621328	24.275883	-2.21875072	0.04131437
$A*A*A*X*X*X$	142.367636	50.1506082	2.83880178	0.01185239
$A*A*A*X*X$	-190.6841	67.9226079	-2.80737307	0.01264749
$A*A*A*X$	51.1175767	18.696031	2.73414056	0.01470551

8.5. *A.P.E.S. Engineering Demonstration Unit Design*

8.5.1. Overview

__ illustrates the Flight Experiment Design. The platform that will be isolated from the vibrations of the launch vehicle contains several embedded neodymium magnets towards the center. This will aid in statically levitating the platform. In order to actively determine the position of the platform during ascent, the camera located at the top of the will stream video – with the help of the LEDs to provide adequate lighting - to the A.P.E.S.

Figure 60. Section view of the proposed flight model of the A.P.E.S. system

flight computer. The A.P.E.S. flight computer will then communicate via I2C to the appropriate solenoid drivers to vary the current to the six (6) vertical banks of solenoids to isolate the platform from the vibrations of the launch vehicle and maintain its position within the demonstration unit. An expanded view of the A.P.E.S. Engineering Demonstration Unit is illustrated in Figure 61.

Figure 61. Expanded view of the A.P.E.S. Engineering Demonstration Unit.

8.5.2. Flight Experiment Mass Summary

Table 21 lists the various components and weight summary for the A.P.E.S. engineering demonstration unit.

Table 21. Weight summary of the A.P.E.S. engineering demonstration unit.

Item	Unit Weight (lb)	Qty	Total Weight (lb)
Neodymium Magnets	0.0002	23	0.004
Balance Solenoids w/ Iron Cores	0.018	18	0.32
Main Support Solenoid w/ Iron Core	0.033	1	0.033
Plywood	0.009	1	0.009
Cardboard Tube	0.016	1	0.016
Fasteners	0.008	8	0.032
Adhesives	N/A		0.2
Total Weight			**0.66**

9. Flight Systems

9.1. *Flight Avionics*

9.1.1. Overview

To successfully complete the USLI mission, flight systems is further responsible for providing a fully functional flight computer system. Flight Avionics is the second subsystem of Flight Systems, responsible for data acquisition, experimental control, and telemetry.

9.1.2. Requirements and Products

The requirements for the Flight Avionics are derived from the Mission Objectives, Mission Success Criteria, and the needs of the A.P.E.S. engineering demonstration unit. These requirements are listed in Table 2, Section 2.4. The requirements flow down for the Flight Avionics are listed in Table 22 for convenience.

Table 22. Flight Avionics Requirements Flow Down.

MO	Mission Objectives

MO-2	Stabilize and isolate the A.P.E.S. platform from the induced vibrations of the Launch Vehicle.
MO-3	Closed-loop control of the platform via real-time image processing.
MO-4	Successful recovery of the launch vehicle resulting in no damage to the launch vehicle.

MSC	Mission Success Criteria	Source	Verification Method	Status
MSC-2	The Flight Experiment is successfully activated and data is collected.	MO-2, MO-3	Inspection, Analysis	Completed
MSC-2.1	*Minimum Mission Success*: Platform is stabilized and isolated during the coast phase of flight	MO-2	Testing	In Progress
MSC-2.2	*Minimum Mission Success*: Relative position and rotation data of the platform to the camera is collected during all phases of the experiment.	MO-2, MSC-2	Testing	In Progress
MSC-2.3	*Minimum Mission Success*: The flight experiment terminates at apogee.	MO-4, MSC-2	Inspection	In Progress
MSC-2.4	*Full Mission Success*: Platform is stabilized and isolated from environmental vibrations during the powered and un-powered portions of the flight.	MO-2, MSC-2	Testing	In Progress
MSC-2.5	*Full Mission Success*: Platform does not come into contact with any other components of the A.P.E.S. System.	MO-3, MSC-2.4	Testing	In Progress

FS	Flight Systems	Source	Verification Method	Status	Verification Source
FS-3	The A.P.E.S. experiment shall be terminated at apogee.	MSC-2.3	Testing	In Progress	
FS-3.1	The platform shall be secured during descent and landing.	FS-3	Testing	In Progress	

FA	Flight Avionics	Source	Verification Method	Status	Verification Source
FA-1	All Flight Avionics shall have a burn-in time of no less than 20 hours	MSC-2.2, MO-4	Inspection	In Progress	
FA-2	The Flight Computer shall collect Launch Vehicle position data, environment conditions (e.g. acceleration), and data from the A.P.E.S. experiment.	MSC-2.5, MSC-2.4, MSC-2,MO-2	Testing	Designed	
FA-3	The A.P.E.S. computer shall be able to perform real-time image processing and control the A.P.E.S. experiment.	MO-3	Testing	In Progress	
FA-3.1	The A.P.E.S. computer shall secure the platform at apogee for descent and landing	FS-3.1	Testing	In Progress	
FA-4	The Flight Avionics shall operate on independent power supplies	MSC-2.5, MSC-2.4, MSC-2,MO-2	Inspection	In Progress	
FA-4.1	The power supplies shall allow for successful payload operation during the Launch Vehicle flight with up to 3 hours of wait time.	USLI Handbook	Analysis, Testing	Completed	Figure 66
FA-5	The Flight Avionics shall downlink telemetry necessary to a Ground Station for the recovery of the Launch Vehicle	USLI Handbook	Analysis, Testing	In Progress	
FA-5.1	The GPS coordinates of all independent Launch Vehicle sections shall be transmitted to the Ground Station	MO-4	Inspection	In Progress	
FA-6	The Recovery Avionics and Recovery System shall be separate from the Flight Avionics.	USLI Handbook	Inspection	Completed	Figure 7, Section 9.2

9.1.3. A.P.E.S. Computer

9.1.3.1. Overview

Two major products of the Avionics subsystem are the flight computer and the experiment computer for A.P.E.S. The A.P.E.S. computer focuses entirely on the control of the A.P.E.S. system.

The A.P.E.S. computer will calculate the position of the platform and control the solenoids in order to change the magnetic field and stabilize the platform. Independent computing systems provides modularity for ease of implementation and debugging. The methodology for component selection shall include consideration of clock speed, I/O, and voltage requirements. Electromagnetic interference will be shielded by a Faraday cage. The system will incorporate redundancy to tolerate the loss of one or more sensors and/or communication lines.

9.1.3.2. Computer Vision Algorithm Study

During launch, the payload will be subjected to up to 11 g's of force through longitudinal axis of the launch vehicle. During flight, the platform will be subjected to strong perturbations and random forces in all dimensions of unpredictable magnitudes. This places strict time and accuracy performance constraints on the algorithm. In order to meet time requirements, image pre-processing will not be practical, and the required information will need to be extracted from the raw video data as it is received. The image transfer and encoding process currently takes up to 5ms, leaving even less time for processing.

In order to facilitate processing and localization, the OpenCV computer vision library version 2.3.1 has been installed on the A.P.E.S. computer, on top of a customized slim Linux distribution. Pre-optimized processing routines and state of the art algorithms will be used to meet the performance and precision requirements necessary to control the solenoids and maintain positional tolerances.

Preliminary tests have been carried out on three methods of payload detection – blob detection, color detection, and the more robust StarDetector algorithm based on Agrawal et. al '08. Average processing time for blob detection was around 15ms, whereas it was only 3.5ms for the simple color detection, and approximately 25ms for StarDetector -including the 1ms required for image capture. It is important to note that these tests were carried out on desktop computers with greater processing power than the ARM-A8 CORTEX processor on the A.P.E.S computer. However, from these tests, it was concluded that either the Circle or Simple Color Detection algorithm will yield the most optimal performance from the A.P.E.S. computer

The Table 23 summarizes the advantages and shortcomings of each of these methods.

Table 23. Summary of Image Processing Algorithms Tested.

Method	Advantage	Disadvantage
Blob Detection	Good tradeoff for precision and performance	Susceptible to noise, any foreign objects
Color Detection	Performance	Susceptible to changes in lighting, requires platform of homogenous color
Star Detector	Resilient to noise, computes size and response Laplacian	Processing Time, susceptible to features within object

9.1.3.3.   A.P.E.S. Detection, Characterization, and Control Process

Figure 62 illustrates the algorithm that will be used to detect, characterize and control the platform inside the A.P.E.S. engineering demonstration unit.

9.1.3.4.   Further Optimization

To improve performance further, try out some basic sparse detection methods such as skipping some number of pixels without degrading the detection performance, and setting the image's Region of Interest (ROI) and Color of Interest (COI).

Hardware and OS level optimization levels are also under investigation such as:

- Utilization of proprietary video drivers provided by TI that utilizes the NEON coprocessor on the OMAP3 for more efficient image encoding
- Utilization of a customized version of GStreamer that makes use of the hardware DSP on the OMAP.
- Utilization of vectorized image processing routines that may be run on the DSP for improved performance.

Figure 62. A.P.E.S. Detection, Characterization, and Control Process Flow Diagram.

9.1.4. A.P.E.S. Control Logic

9.1.4.1. Introduction to PID control

A proportional-integral-derivative (PID) controller is a common control loop feedback mechanism, as illustrated in Figure 63. The basis of the method is the measurement and minimization of an 'error' term, defined as the difference between a measured process variable and a setpoint, the desired state of the process. The PID controller attempts to minimize that error by appropriately adjusting the process control inputs. The "P" term corresponds to the present error, the "I" term the accumulation of past errors, and the "D" term is a prediction of future errors based on the current rate of change, or derivative, of the process. The weighted sum of these three actions is used to adjust the process.
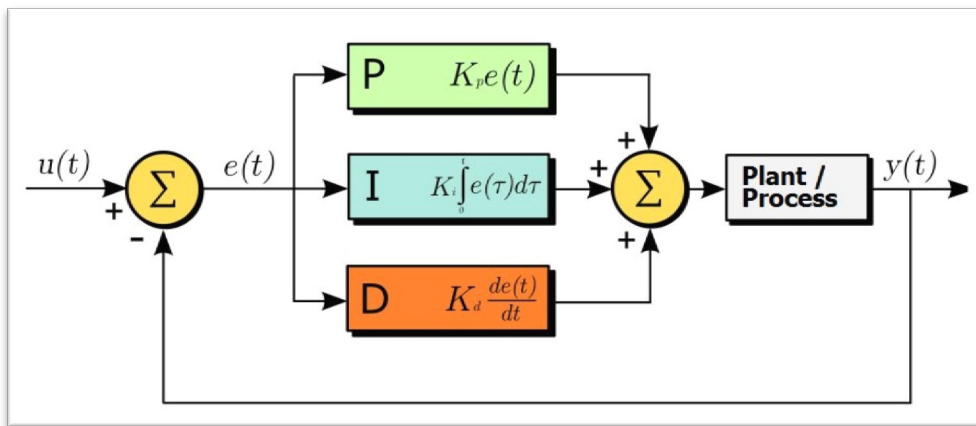
Figure 63. PID Controller Block Diagram

Various sensors are used to measure the state of the process and the information is fed back into the control loop. The rate at which the system shall adjust to changes is given by the "P" term. The degree to which the adjustment itself should be increased or decreased in order to converge with the desired state is given by the "I" term. Finally, the "D" term slows down the adjustment of the present state to the desired state to prevent the overcompensation that could be caused by the "I" term.

9.1.4.2. A.P.E.S. PID Control Design

In this application, a series of camera modules will be used to measure the output state of the controller, corresponding to the 3 dimensional Cartesian position of the A.P.E.S. platform. This position data will then be fed back into the PID controller. The error term in this implementation

corresponds to the distance the platform is from the desired setpoint: in the absolute center of the payload module. After calculating the necessary adjustments, the strength of the magnetic field required of each solenoid will be computed and the power to each adjusted accordingly via digital control.

9.1.4.3. Design Considerations

The speed of this loop is critical in ensuring the system achieves a marginally stable output. If the time between reading the output state and adjusting the solenoids is too long, the system state will have already changed between the periods of measurement and adjustment and the system will become unstable. The implementation will be verified to run in an acceptable timeframe to ensure stable control of the platform.

9.1.4.4. Tuning

The PID controller depends on appropriate coefficient values being chosen for each term. This process is called 'tuning'. The Zeiger-Nichols technique is a method that tunes the control loop while it is online by automating the trial and error systematically according to a given heuristic, and adjusting each term until a stable output is reached. In order to tune the control loop efficiently the Zeiger-Nichols technique will be utilized with the platform's average distance from the module center as the heuristic.

9.1.5. Flight Computer

The flight computer will run the ATMEGA 2560AU processor with the Arduino bootloader and other necessary components for ease of programming. The chip has sufficient I2C, serial, and analog inputs to read data from all sensors and log to an SD card based on Sparkfun's OpenLog break-out board. Additionally, the chip will run the Fastrax UP501 GPS module and send the data to an Xbee PRO for transmission to the ground station. An OpenLog board will provide logging capabilities. The chip will be programmed in the Arduino language, a subset of C++ with some additional libraries. Figure 64 provides a generalization of proposed flight computer software.
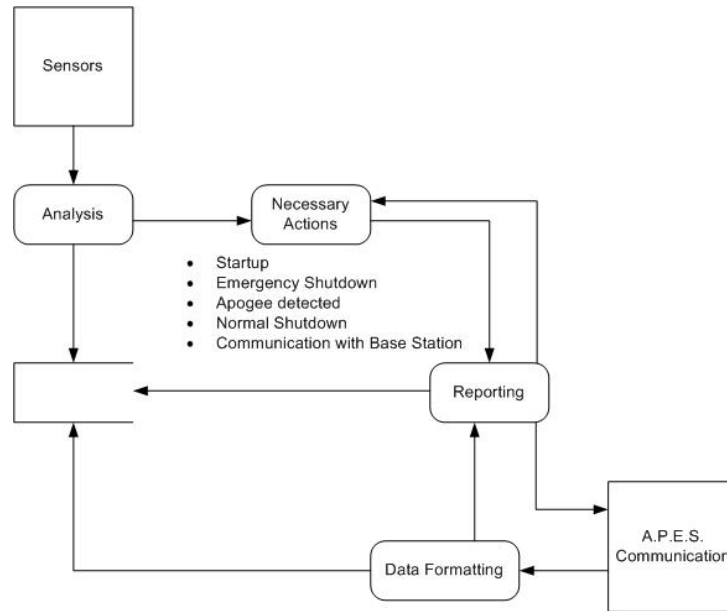
Figure 64: Generalization of flight computer software

The flight computer must accomplish several tasks and handle multiple responsibilities. The main goal of this system is to collect and monitor all the relevant data from the environment around it such as the strain on the launch vehicle, environmental factors such as temperature, stray magnetic flux from the A.P.E.S system, launch vehicle acceleration, and GPS position. During flight, the flight computer must also monitor the payload's control system and data through a serial bus and provide an emergency secondary disengage for the A.P.E.S. system in the case of a necessary emergency shutdown. During flight the avionics will log all data to a SD card. Solid state memory should allow recovery of flight data if a recoverable failure occurs. Post-recovery, the flight computer must switch to location and communication systems to transmit a GPS signal through the telemetry system to the ground station. Figure 65 and Table 24 provide the flight computer layout and major components listing respectively.
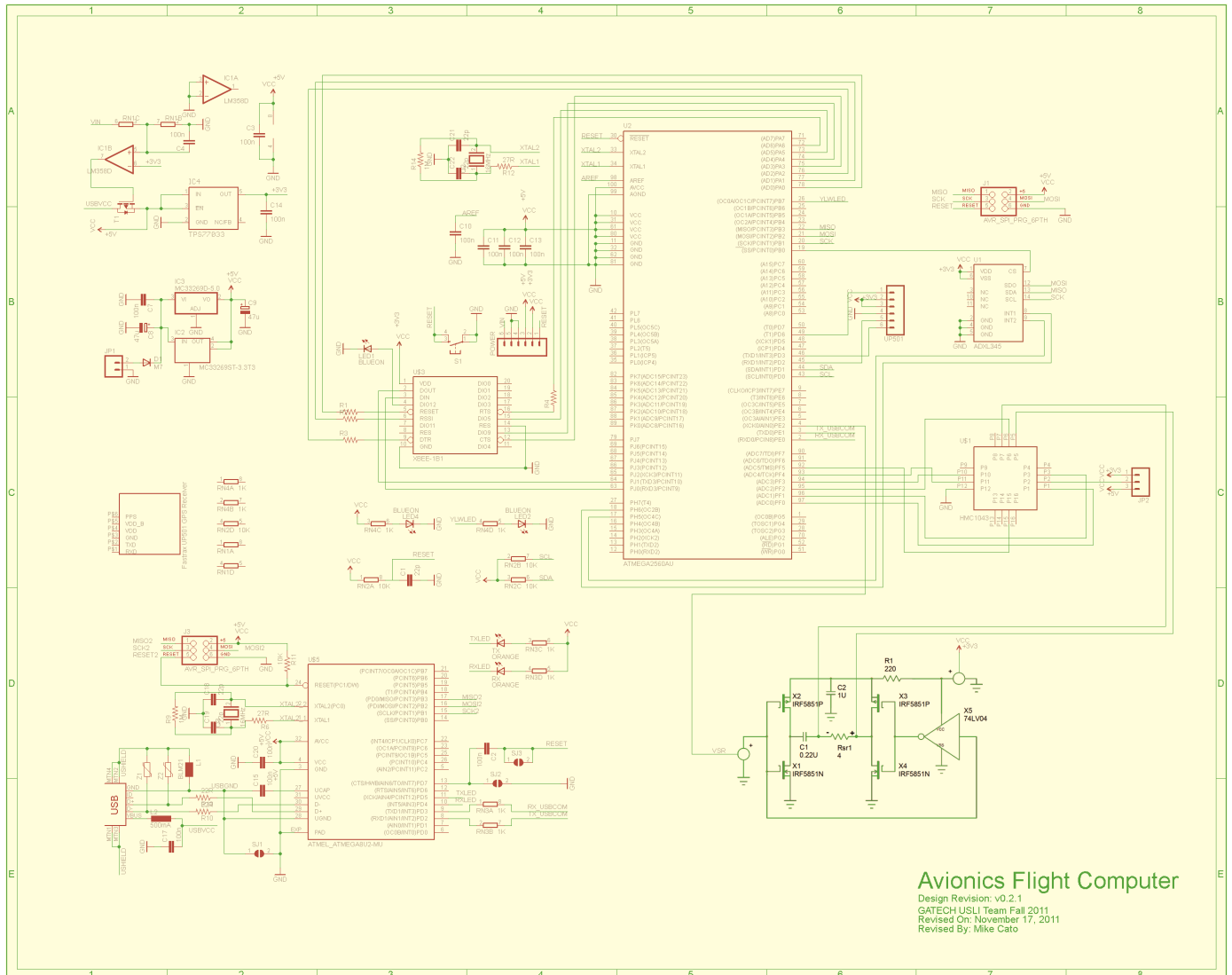
Figure 65: Custom flight computer layout.

Table 24: Major Flight Computer Components

Part Number	Component Picture	Description
1		The flight computer microprocessor, the ATmega 2560
2		The GPS receiver, the Fastrax UP501 GPS module
3		The Xbee PRO 900-XSC module for communication between launch vehicle and ground station
4		The OpenLog board will provide logging capability

9.2. *Power Systems*

9.2.1. Power Budget

The power budget for both the A.P.E.S. computer and the Flight Computer are illustrated in Figure 66. The duty cycle is representative of one (1) flight, or 140 seconds. For the A.P.E.S. computer and components, it is assumed that the hardware is active for only 40 seconds of the entire flight – from T-20s to T+20s.

Power Consumption			Modes								
			Standby			Typical			Max		
Subsystem	Component	Voltage	Amps	Watts	Duty Cycle	Amps	Watts	Duty Cycle	Amps	Watts	Duty Cycle
Avionics	adx1345	3.3	0.000	0.000	1.000	0.000	0.000	1.000	0.000	0.001	1.000
	hmc1043	3.3	0.012	0.040	0.000	0.012	0.040	1.000	0.012	0.040	1.000
	atmega8u2	5	0.000	0.002	1.000	0.014	0.070	1.000	0.021	0.105	1.000
	atmega2560	5	0.000	0.002	1.000	0.020	0.100	1.000	0.029	0.145	1.000
	UP501	3.3	0.005	0.017	1.000	0.023	0.077	1.000	0.035	0.117	1.000
	Xbee-XCS	3.3	0.000	0.000	1.000	0.330	1.089	1.000	0.330	1.089	1.000
	OpenLog	5	0.002	0.010	1.000	0.005	0.025	1.000	0.006	0.030	1.000
A.P.E.S.	Beagleboard	3.3	0.300	0.990	1.000	0.650	2.145	1.000	0.850	2.805	1.000
	MCP4275 DAC	5	0.000	0.000	0.000	0.000	0.001	1.000	0.000	0.002	1.000
	2x Webcam	5	0.000	0.000	0.000	0.300	1.500	1.000	0.600	3.000	1.000
Other	DRV103 + Solenoids	12	0.000	0.000	0.000	3.440	41.280	0.182	4.300	51.600	0.800
Max Power Draw (W)			1.06			46.33			58.93		
Duty Cycled Power Consumption (W)			1.02			12.55			48.61		
10% Contingency (W)			0.10			1.26			4.86		
Power Consumption with Contingency (W)			1.12			13.81			53.47		

(a)

SubTotals							
Standby		Typical		Maximum			
Amps	Watts	Amps	Watts	Amps	Watts		
0.020	0.070	0.404	1.401	0.434	1.526	Avionics	
0.300	0.990	0.950	3.646	1.450	5.807	A.P.E.S.	
0.000	0.000	3.440	41.280	4.300	51.600	Other	

(b)

Figure 66. (a) Power budget for the A.P.E.S. computer and the Flight Computer; (b) subtotals of the A.P.E.S. computer and the Flight Computer.

9.2.2. Power Supply

The avionics system, including computers and sensors, will be powered by a 9V battery. The supply will be attached to the Avionics Computer Board which is designed to have a voltage regulator circuit providing 3.3V and 5V rails. The supply will provide 1200mAh of power.
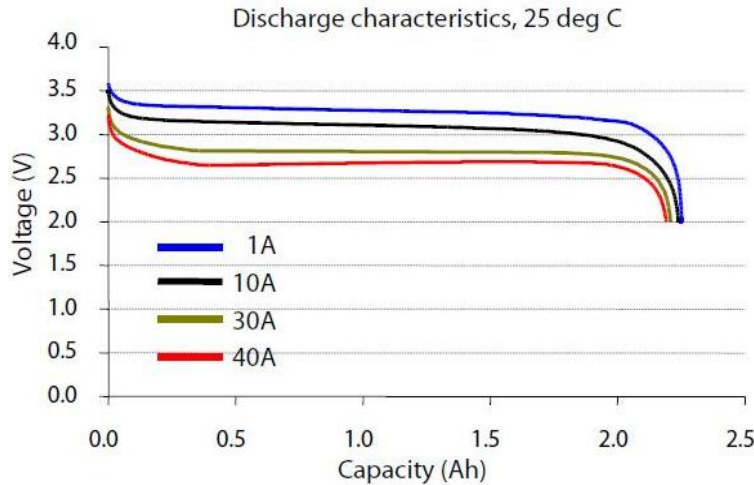
Figure 67: Discharge characteristics of the A123 battery

The avionics use a negligible amount of power in sleep mode providing a minimum of 5 hours of wait capability for the launch pad. Upon launch the system is activated and will have greater then needed power capacity to perform its duties until the launch vehicle is retrieved. Separately, the A.P.E.S. system will utilize a four-pack of A123 lithium iron phosphate (LiFePO) rechargeable batteries, one of which is shown in Figure 68. These batteries have a per-unit nominal capacity and voltage of 2.3 ampere-hours and 3.3V, respectively. Furthermore, the A123 batteries provide a maximum discharge rate of 70 amperes. Figure 67 illustrates the discharge characteristics of the A123 at four discharge rates. The ability of the A123 to provide a large current is critical to the A.P.E.S. system, which will rely on pulse-width modulation to change magnetic field intensity via manipulation of a root-mean-square current.

Figure 68: A single A123 LiFePO battery

9.3. *Telemetry and Recovery*

9.3.1. Ground station

The ground station for receipt of data shall consist of a laptop connected via USB to an Xbee Pro and Xbee Explorer with a rubber duck antenna. This will ensure simplicity, portability, and operability of the ground station.

9.3.2. Transmitter Design

In order to satisfy recovery requirements that the launch vehicle be found, a GPS module is included with the avionics in addition to radio communication equipment. The Fastrax UP501 provides a 10Hz update rate, rapid satellite acquisition, and low current draw. Position data is logged on-board and transmitted over the 900MHz radio band to our ground station. The telemetry system is designed to utilize two Xbee PRO 900-XSC modules for one-way communication from the launch vehicle to the ground station. Using a simple, loss-tolerant protocol with reliable delivery ensures the data is received if at all possible and that the information is correct. To extend the range beyond 1 mile, each module has a 900MHz monopole-monopole vertically polarized rubber duck antenna with 2 dBi gain and 10W of power. This antenna's performance is depicted graphically in Figure 69. Receipt of GPS data via radio to the ground station will satisfy the recovery requirement and bolster kinematics data of the launch vehicle trajectory.
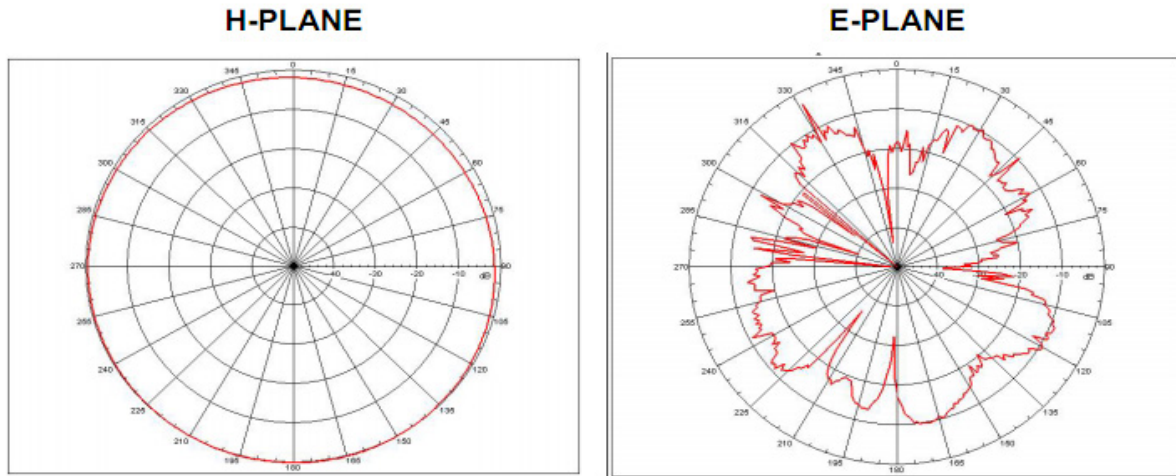
Figure 69: Antenna performance as a function of range

9.3.1. Effects of Excess RF Radiation on the Recovery Avionics

A simple testing procedure was implemented to ensure the safety of using the e-matches in proximity to the transmitter. An Xbee transmitter operating at 100mW, with an omnidirectional antenna was placed next to an e-match at several points of high transmission power along the antenna and in the near field. The transmitter then sent a variety of packets varying in length from a single byte to the entire ASCII alphabet. At no point during transmission did the e-match ignite. This result was expected given the low output power of the transmitter.

9.4. *Sensing Capabilities*

9.4.1. Flight Avionics Sensors

9.4.1.1. General Sensing

Sensing data will be provided to the flight computer through ten (10) different sensors chosen to give the most relevant data regarding experimental and launch vehicle performance. The sensing system must account for difficulties arising in communication interfaces, voltage requirements, and material sourcing. Components must survive periods of potentially strong magnetic flux density and sensors placed in launch vehicle modules which undergo separation must resist explosive impulses which may interfere or damage sensing components.

9.4.1.2.   Kinematics and Location

The accelerometer ADXL345 (shown in Figure 70) will provide acceleration data and, combined with the GPS module, provide rotation and position data for the launch vehicle trajectory. Three axis capabilities will implicitly define velocity, position, and rotational motion. The ADXL345 accelerometer can record up to ±16G. The ADXL345 is capable of entering a "standby" mode for periods of inactivity, an advantage for periods of inactivity during setup and preparation to launch.

Figure 70: ADXL345 accelerometer

9.4.1.3.   Magnetic Fields

The chosen magnetometer for detection of potentially harmful fields in the vicinity of the avionics is the HMC1043, and will determine the effectiveness of our shielding to contain the magnetic fields from the APES system. The sensor detects the magnetic field in three dimensions and "static" testing will allow for compensation for the contributions of the Earth's magnetic field. The sensor will be used to determine the flux within the avionics bay of the launch vehicle to help monitor the influence of the magnetic field to our other equipment. The HMC1043, in Figure 71 can sense up to ±6 gauss. A combination of distance and mu-metal shielding should diminish the A.P.E.S. fields significantly that such a small range should be appropriate.

Figure 71: HMC1043 Magnetometer

9.4.2. A.P.E.S. System Sensing

The A.P.E.S. computing system will require two types of sensors for feedback and control. Position of the levitating test platform inside of A.P.E.S. will be tracked and displacement data used for derivation of platform kinematics. The magnetic fields generated by the solenoids will also be monitored and compared to models and thresholds developed during ground testing. There are several serious issues to sensing in the A.P.E.S. experiment. First is the possibility of large magnetic flux – potentially as large as several hundred gauss. Strong magnetic flux will induce current in wiring often destroying sensitive digital electronics. High current such as the solenoids power cables may also risk induced current in electronics. To counteract these issues, mu-metal Faraday shielding and distancing from the computational elements will be utilized. However, sensors and detection equipment will be chosen to satisfy the expected parameters of the environment around the A.P.E.S. system.

Table 25: Possible A.P.E.S. distance sensors

Sensor	Cartesian Coordinate Axes	Viewing Angle >45 Degrees	Range <5cm	Resolution <1mm	Delay <20ms	Interf- erence	Flux Sensitive	Reliable under Shock and Vibrations	Small Form Factor <15mm
Ultrasonic Distance	1	No	No	No	No	No	No	No	No
IR Distance	1	No	Yes	Yes	Yes	No	Yes, w/Shield- ing	Yes	Yes
Laser Distance	2	Yes	Yes	Yes	No	No	Yes, w/Shield- ing	Yes	No
CMOS Camera	2	Yes	Yes	Yes	Yes	Yes	Yes, w/Shield- ing	Yes	Yes

9.4.2.1.   A.P.E.S. Distance Sensing

The full three-dimensional design would utilize two to three CMOS cameras. The OVM7690 Camera Cube CMOS camera meets all current design requirements and expected environmental conditions, as outlined in Table 25. The camera sensor is a small form factor (2x2x1mm) color image camera module, as illustrated in Figure 72, with integrated optical glass lens and on-chip image processing. A test pattern is used for initial software pixel-to-distance mapping and calibration for the camera output data and is mounted on the opposite side of the test structure as the camera. The test pattern must be an easily identifiable pattern – this will be made of fiber optic cables mounted on a panel attached to a specific color light emitting diode (LED). A second camera and test pattern are mounted perpendicular to the first, using a second specific color.

Figure 72: OVM7690 Camera Cube

Once the calibration is complete, the cameras output is read at 30-60 frames per second (FPS). The levitating platform is painted another specific color which is not the same as the colors already used for calibration patterns of the two cameras. Several white LEDs are used for flooding light to make the painted platform visible. A simple edge detection algorithm is used to find the displacement of the platform in each sample frame. Using the pixel to distance mapping from the initial calibration, the displacement between samples is calculated which in turn is used to update the Cartesian coordinate for the platform in three dimensions. The use of one camera for sensing on three axes was rejected because the small movements along the forward line of sight (depth perception) would not be interpreted with high enough resolution. Movement along the horizontal and vertical plane will be sufficient, so two axes can be used.

9.4.2.2.   A.P.E.S. Magnetic Field Sensing

While not critical to the flight mission of the A.P.E.S. system, sensing of magnetic fields during ground testing of the A.P.E.S. system will allow for better model generation as well as full confirmation of the theoretical basis of the project. Therefore, the MLX90363 magnetometer has been proposed for use in ground testing applications. The sensor is sensitive up to 0.7-1.0 Tesla, has a sample rate of 1 millisecond, and outputs magnetic field direction as a three coordinate vector. This sensor was chosen for its high magnetic flux sensitivity, decent resolution increments, and three axis direction vector output. The magnetometer controls on-chip digital signal processing.

9.5. *"De-Scope" Options*

9.5.1. Payload "De-Scope"

The de-scope option for the payload will utilize a single infrared distance detection along a single axis of linear motion, where a sample plate is levitated vertically at constant distance between the sensor and a solenoid during the ascent of the launch vehicle. The objective of the flight experiment would be to then maintain a constant position with a 2% settling time of less than 0.5 seconds for a unit impulse. This option provides an opportunity to develop many of the same control theories without the necessity to grapple complex 3-dimensional magnetic fields.

9.5.2. Flight Computer "De-Scope"

The de-scope option for the flight computer is to use a commercially available Arduino Mega board, rather than fabricate a custom board. This option provides full capability should timelines not permit the completion of design and construction of the custom board.

9.6. *Payload Integration*

9.6.1. Modularity and Motivation

The modular internal launch vehicle structure permits integrating the payload with minimal effort. A section of the internal launch vehicle structure is reserved for the altimeters, payload experiment, and flight computer. The ends of the modular section are fitted structurally with solid fiberglass to sustain the bursts of the recovery system. These solid fiberglass sections are fitted with shear pins to maintain stability during flight. The entire system stacks together for dual deployment. The volume designed for the payload is an area between the struts 8 inches long with an average diameter of 3.2 inches within the hexagonal inner side of the ribs. The A.P.E.S. device will be anchored to the top of this section via a "universal bracket" to one of the ribs, shown in

Below A.P.E.S. will be the flight system computer will in a shielded compartment. The computer will also be mounted to a rib using a universal bracket.
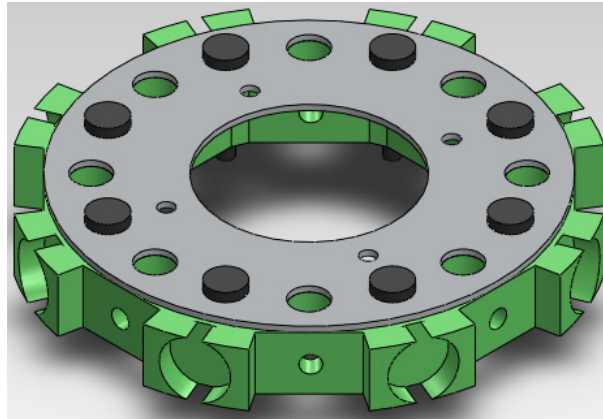
Figure 73: Universal mounting bracket bolted to rib

9.6.2. Universal Mounting Bracket

The unique and robust structure of the Vespula launch vehicle will allow greater reusability and modularity for integration of the flight and payload subsystems. In order to speed up integration time a generalized universal mounting system will be employed so that current and future subsystems can be quickly and effectively mounted to the major rib sections of the launch vehicle structure. When these and future internal components are designed and produced, minimal design consideration will be needed to account for attachment to the universal mounting bracket. This continues on the Georgia Tech Mile High Yellow Jackets tradition of simplifying and unifying the structural elements of the launch vehicle, simplifying design and improving construction time and structural robustness. The universal mounting bracket shall be built to accommodate structures such as the A.P.E.S. device with minimal fabrication and design requirements, and to fit within rib structures with few necessary design parameters on the ribs themselves, increasing the potential reusability of the universal mounting bracket should future teams alter the modular structure further. The use of the bracket also allows for the whole A.P.E.S. system to be removed more easily in case there any modifications are required. Furthermore this frees up the designs for the payload structure as it is fundamentally non-load bearing as the internal launch vehicle structure is taking care of that already.
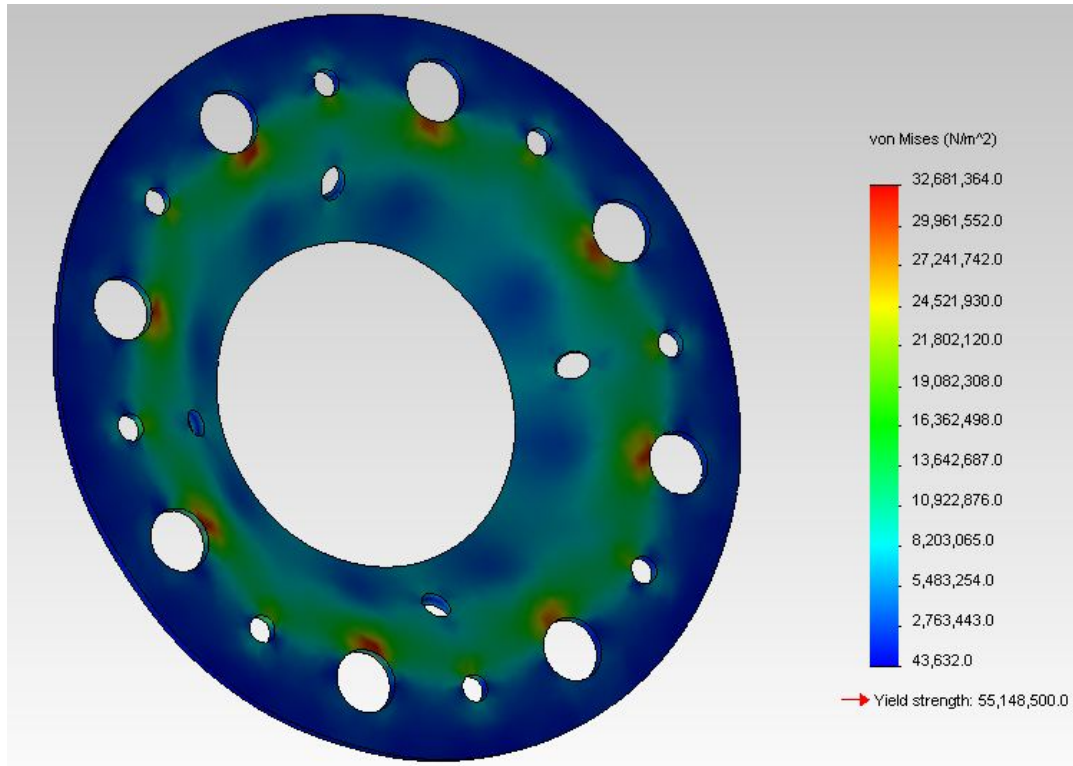
Figure 74: Basic finite-element-analysis of the universal mounting bracket

Finite-element-analysis carried out in the Solidworks Office environment details an axial load of 150 lb_f placed in the center of the mounting bracket. High stress regions appear due to the fallibilities of the Solidworks finite-element-analysis software and the difficulty of specifying distributed reaction loads. The results of the finite-element-analysis appear in Figure 74. While quarter inch (0.0625") aluminum was necessary to provide a factor of safety of 1.6 in the case of point application of resistive loads, it is more likely that the actual safety factor is closer to 1.8 or 2 meaning that 1/16" is more than sufficient for the loads experienced. Further study will be done to specific an exact safety factor and the design may be modified to ensure a minimum safety factor of 2.

The universal mounting bracket will mount into the launch vehicle structural ribs at approved attachment points using number 8 bolts. Initial designs allow for the A.P.E.S. structure to then bolt directly to the bracket also using number 8 bolts. Table 26 provides further characteristics of the universal mounting bracket.

Performance evaluation metrics will be developed further as elements of Flight Systems begin to be produced. However, several basic metrics exist already, namely, the reduction of all motion of the A.P.E.S. plate in a timely manner, i.e. a well-damped impulse response. The flight computer must survive for several hours on the launch pad. All data must be handled and recorded accurately by both the flight and experimental computers.

Table 26: Universal Mounting Bracket Specifications

Universal Mounting Bracket Parameter	*Design Value*
Thickness	0.0625 in.
Diameter	4.409 in.
Bolt Hole Diameter	0.164 in.
Rib Mount Bolt Radius from Center	1.809 in.
Number of Bolts to Rib	8 bolts maximum
A.P.E.S. System Mount Bolt Radius from Center	1.282 in.
Avionics System Mount Bolt Radius from Center	1.282 in.
Stringer through Holes Diameter	0.376 in.
Stringer Hole Radius from Center	1.809 in.
Mounting Bracket Material	6061-Aluminum

9.6.3. EMI Shielding

9.6.3.1. Overview

Due to the nature of the A.P.E.S. engineering demonstration unit, critical-to-flight components such as the Recovery Avionics (and associated wiring) and Flight Avionics must be properly shielded in order to ensure a safe and successful flight

9.6.3.2. Passive Shielding

The use of high magnetic permeability metal alloy such as Mu-Metal will aid in containing the magnetic field within the core of the A.P.E.S. Mu-Metal protects best against static or slowly varying electromagnetic fields by providing a low reluctance, or low magnetic resistance, path for the magnetic flux. A thin sheet of Mu-Metal will reduce the strength of the magnetic field by one – to – two orders of magnitude while maintaining a low weight fraction of the A.P.E.S. flight unit.

9.6.4. Solenoid Heating

Due to the power required to keep the platform stabilized, the solenoids will be operating close the maximum amperage limit for the gauge size of approximately 0.9 amps. These high power requirements will cause the wires in the solenoids to heat up and, if left unchecked, overheat and possibly melt the insulation in the wire leading to a failure of the solenoid and subsequently of the A.P.E.S. demonstration unit. Should heating prove a risk during ground testing, a computer fan will be mounted to the base of the A.P.E.S. device. This would allow for air to be pulled down through the central column containing all of the solenoids thereby cooling them down convectively. Using TK Solver, a flow rate of approximately 12.32 in^3/s is required in order to keep the solenoids within their temperature limits. Therefore, a typical COTS computer fan with a flow rate of at least 25 CFM, or 720 in^3/s, will provide sufficient convective cooling. For more details on the computation, please see Appendix IX.

9.6.5. A.P.E.S. Engineering Demonstration Integration

As illustrated by Figure 75, the A.P.E.S. flight unit can be easily integrated into the iMPS via the UMB. Prior to the installation of the stringers, the A.P.E.S. flight unit is secured on the UMB. Once secured, the UMB is then fastened to the rib. Once integration is complete, the stringers are then installed. Once the iMPS is fully constructed, the wiring harness is installed, connecting the solenoids to the LiFePo battery and the cameras to the A.P.E.S. computer.
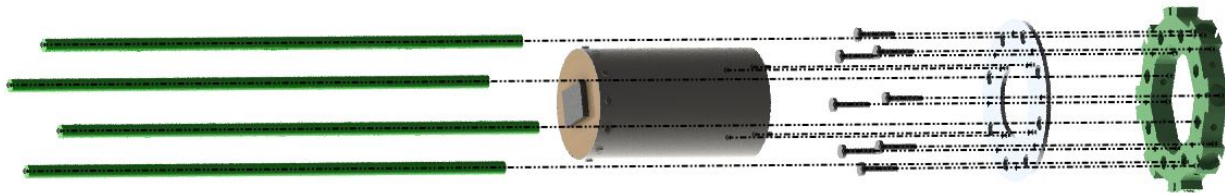
Figure 75. Payload Integration Expanded View.

10. General Safety

10.1. *Overview*

Ensuring the safety of our members during building, testing and implementation of the payload experiment is an ideal condition. Procedures have been created and implemented in all of our build environments to ensure safety requirements are met and exceeded. A key way the Yellow Jackets ensure team safety is to always work in teams of at least two when using equipment or during construction. This guarantees that should an incident occur with a device the other member could provide immediate assistance or quickly get addition help if required. The Invention Studio where the team does a majority of its work is equipped with safety glasses, fire extinguishers, first aid kits, and expert personnel in the use of each of the machines in the area. All the members of the payload and flight systems teams have been briefed on the proper procedures and proper handling of machines in the labs.

10.2. *Payload Hazards*

As already mentioned in Section 10.1, the same methodology to identify and assess risks for vehicle safety will be used to identify hazards for the payload. The entire payload and flight systems teams have been briefed on the possible hazards they may encounter while working with the payload and how to go about avoiding them. Hazards that relate specifically to the payload are listed in Table 27. Payload failure modes are outlined in Table 28.

Table 27: Hazards, Risks, and Mitigation

Hazard	Risk Assessment	Control & Mitigation
Electrocution	Serious Injury/death	Do not touch wires that are hot and not insulated. Wear rubber gloves when the device is in operation. Handle leads to the power supply with care. Use low voltage settings whenever possible.
Electromagnetic Fields	Interfere with electronic devices inside the body	Ground test equipment, keep people with electronic components in them away from the coil when the electromagnetic coil is in use.
Epoxy/glue	Toxic fumes, skin irritation, eye irritation	Work in well ventilated areas to prevent a buildup of fumes. Gloves face masks, and safety glasses will be worn at all times to prevent irritation.
Fire	Burns, serious injury and death	Keep a fire extinguisher in the lab. If an object becomes too hot or starts to burn, cut power and be prepared to use a fire extinguisher.
Soldering Iron	Burns, solder splashing into eyes	Wear safety glasses to prevent damage to eyes. Do not handle the soldering lead directly only touch handle. Do not directly hold an object being soldered.
Drills	Serious injury, cuts, punctures, and scrapes	Only operate tools under supervision of team mates. Only use tools in the appropriate manner. Wear safety glasses to prevent debris from entering the eyes
Dremel	Serious injury, cuts, and scrapes	Only operate tools under supervision of team mates. Only use tools in the appropriate manner. Wear safety glasses to prevent debris from entering the eyes
Hand Saws	Cuts, serious injury	Only use saws under supervision of team mates. Only use tools in the appropriate manner. Wear safety glasses to prevent debris from entering the eyes. Do not cut in the direction of yourself or others.

Hazard	Risk Assessment	Control & Mitigation
Exacto Knives	Cuts, serious injury, death	Only use knives under supervision of team mates. Only use tools in the appropriate manner. Do not cut in the direction of yourself or others.
Hammers	Bruises, broken bones, and serious injury	Be careful to avoid hitting your hand while using a hammer.
Power Supply	Electrocution, serious injury and death	Only operate power supply under supervision of team mates. Turn of power supply when interacting with circuitry.
Batteries Explode	Eye irritation, skin irritation, burns	Wear safety glasses and gloves. Make sure there are no shorts in the circuit. If a battery gets too hot stop using it an remove any connections to it.
Improper Dress during construction	Serious injury, broken bones	Wear closed toe shoes, clothing that is not baggy, and keep long hair tied back.
Exposed construction metal	Punctures, scrapes, cuts, or serious injury	Put all tools band materials away after use.
Neodymium Magnets	Pinching, bruising, and snapping through fingers.	Do not allow magnets to fly together from a distance, do not play with powerful magnets, keep free magnets away from powered solenoids.
RF Interference with the Recovery System	Pre-mature firing of the ejection charges potential causing significant damage to the Launch Vehicle, payload, and all supporting systems	RF Testing has verified that, at maximum power output, the on-board XBee transmitter will *not* unintentionally ignite our e-matches from excess RF radiation. Maximum output power is limited to 100 mW

Table 28: A.P.E.S. payload failure modes

Potential Failure	Effects of Failure	Failure Prevention
No power	Experiment cannot be performed	Check batteries, connections, and switches
Data doesn't record	No experimental data	Ensure power is connected to the payload computer and that all connections are firmly secured
Magnetic field interferes with flight computer	No experimental data	Shield the flight computer from any EMF interference
Accelerometers	Record erroneous acceleration values	Calibrate and test accelerometers
Solenoids	Experiment cannot be performed, wires melt	Check connections, ensure over heating will not occur during testing
Too much current goes into the solenoids	The wires in the solenoids get very hot	Make sure current is only pulsed into the solenoids
Improper dress during construction	Maiming, cuts, scrapes, serious injury.	Do not wear open toed shoes in the build lab. Keep long hair tied back. Do not wear baggy clothing.
Avionics	Chips or boards are manufactured incorrectly causing equipment failures and misfires	Test avionics operations, and perform a flight test.
Excessive solenoid heating	Solenoid failure resulting in a failed flight demonstration or damage to the launch vehicle and/or other components	

Table 29: Risk Identification and Mitigation Steps

Step Name	Step Definition
1. Hazard Identification	The first step is to correctly identify potential hazards that could cause serious injury or death. Hazard identification will be achieved through team safety sessions and brainstorming.
2. Risk and Hazard Assessment	Every hazard will undergo extensive analysis to determine how serious the issue is and the best way to approach the issue.
3. Risk Control and Elimination	After the hazards are identified and assessed a method is produced to avoid the issue.
4. Reviewing Assessments	As new information becomes available the assessments will be reviewed and revised as necessary.

The steps outlined above are being used to develop a set of standard operating procedures for launch vehicle construction, payload construction, ground testing, and on all launch day safety checklists.

Failure modes for the launch vehicle were developed to better ensure success of the entire project. Possible modes, resultant problem, and mitigation procedures are given for each failure mode. These modes will continue to evolve and expand in scope as the project progresses. The mitigation methods will be continuously incorporated into preflight checklists. The mitigation items detailed therein will be incorporated into the preflight checklist. Launch vehicle failure modes and mitigation are listed in Table 30.

Table 30: Launch vehicle failure modes and mitigation

Potential Failure	Effects of Failure	Failure Prevention
Fins	Launch vehicle flight path becomes unstable	Test fin failure modes at connection to launch vehicle to ensure sufficient strength
Structural ribs buckle on take off	Launch failure, launch vehicle destroyed, possible injury from shrapnel	Wear eye wear protection, test the internal structure to ensure a factor of safety against buckling
Thrust retention plate	Motor casing falls out	Test reliability of thrust retention plate

Potential Failure	Effects of Failure	Failure Prevention
Skin zippering	Internal components are exposed to flowing air currents, launch vehicle becomes unstable	Test skin adhesion reliability
Launch buttons	Launch vehicle becomes fixed to launch rail, or buttons shear off	Ensure buttons slide easily in launch rail, ensure rail is of the proper size
Drogue separation	Main shoot takes full brunt of launch vehicle inertia, launch vehicle becomes ballistic	Do a ground test of drogue separation as well as a flight test
Main shoot	Launch vehicle becomes ballistic, severe injury, irrecoverable launch vehicle	Do a ground test of main shoot deployment, as well as a flight test.
Land directly on fins	Fins break, and launch vehicle cannot be flow twice without fixing	Test fin failure modes at connection to launch vehicle to ensure sufficient strength
Ignition failure	Launch vehicle does not launch	Follow proper procedure when setting up launch vehicle ignition system
Motor failure	Motor explodes	Install motors properly according to manufacturer instructions.

11. Project Budget

11.1. *Funding Overview*

In order to fund the 2011-2012 Competition year, the Mile High Yellow Jackets have sought sponsorships from academic and industry sources. The current sponsors of the Mile High Yellow Jackets and their contributions can be found in Table 31. As of FRR, the Mile High Yellow Jackets have received $7,000 in funding. Additionally, the Team has also received a dedicated room in which the Team can construct and store their launch vehicle, payload, and other non-explosive components. All explosive components (i.e. black power) are properly stored in Fire Lockers in either the Ben T. Zinn Combustion Laboratory or the Center for Space Systems Flight Hardware Laboratory. Furthermore, the Georgia Tech Invention Studio supported all fabrication needs of the Team.

Table 31. Summary of sponsors for the Mile High Yellow Jackets.

Sponsor	Contribution	Date
Georgia Space Grant Consortium	$3,500	Sept. 2011
Georgia Tech School of Aerospace Engineering	$1,000	Oct. 2011
Georgia Tech Student Government Association	$1,000	Nov. 2011
SCITOR Corp.	$500	Nov. 2011
SpaceX	$1,000	Dec 2011
ATK Travel Stipend	$400	Apr 2011
ATK Motor Stipend	$200	Apr 2011
Coca-Cola (est.)	*($1,500)*	*Apr. 2011*
Total	$7,600	

11.2. *Projected Budget Update*

During initial planning, it was estimated that the total project cost for Project A.P.E.S. would be approximately $9,896.25 – or, including a 30% contingency, $12,565.12. Figure 76 illustrates the updated projected project costs and project reserves levels at each milestone based on the funding schedule in Table 31. It is important to note that the projected budget includes the Coca-Cola sponsorship funding.

	Projected Cost	Project Reserves
PDR	$924.53	35.5 %
CDR	$3,636.80	62.4 %
FRR	$7,513.39	78.2 %
Launch	$9,854.58	--
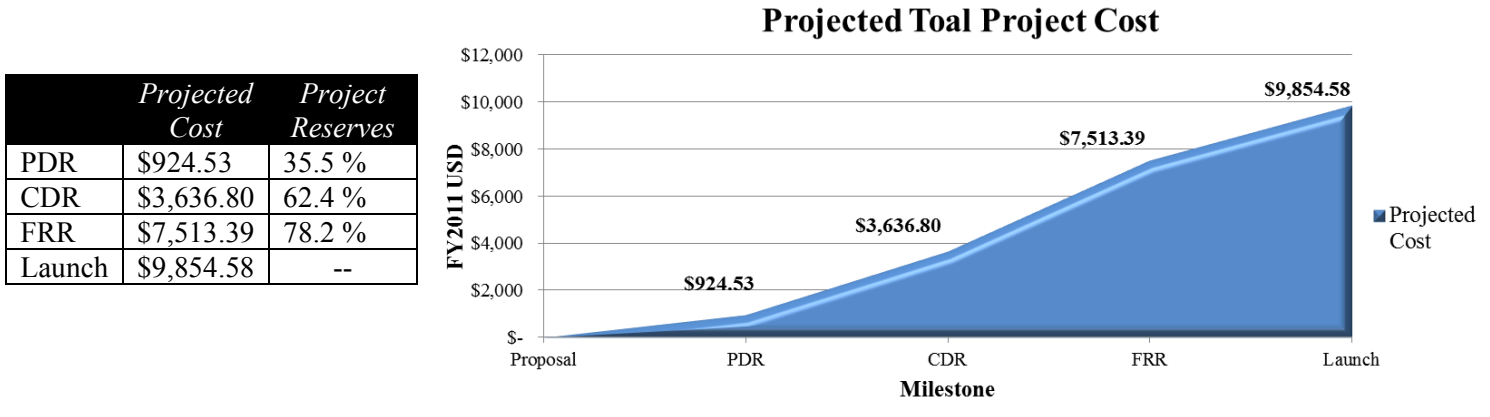
Figure 76. Projected total project cost.

11.3. *Actual Project Costs*

11.3.1. FRR Budget Summary

Figure 77 illustrates the budget breakdown as of the FRR Milestone. The summary is broken down into four (4) main categories: Launch Vehicle, Flight Systems, Operations, and Motors. The Launch Vehicle and Flight Systems categories are further broken down into two (2) sub-categories: Flight Hardware and Testing. Operational expenses include: non-system specific test equipment, Team supplies, non-system specific fabrication supplies, as well as any travel and outreach expenses. Any system-specific equipment bought for testing is charged against that specific system, whereas generic equipment. While motors are specific to the Launch Vehicle subsystem, they are critical component to the architecture and as such are tracked separately from the Launch Vehicle subsystem.

Figure 78 illustrates the actual total project costs - as of FRR - at each milestone. It is important to note that the total project cost is estimated at the competition launch milestone and includes a 25% contingency. Additionally, in regards to the (Actual) Total Project Cost levels, only funding that guaranteed or already acquired is considered. Resultantly, the Coca-Cola sponsorship will not be considered towards the funding levels of the Team.

2011-2012 Budget Breakdown	
LV - Testing	$ 1,333.08
FS - Testing	$ 775.14
LV - Flight Hardware	$ 860.05
FS- Flight Hardware	$ 604.88
Operations - Spent	$ 1,000.00
LV -Remaining	$ 181.87
FS -Remaining	$ 544.98
Motors	$ 1,000.00
Operations - Remaining	$ 700.00
Total	$ 7,000.00

2011-2012 Mile High Yellow Jackets Budget Summary
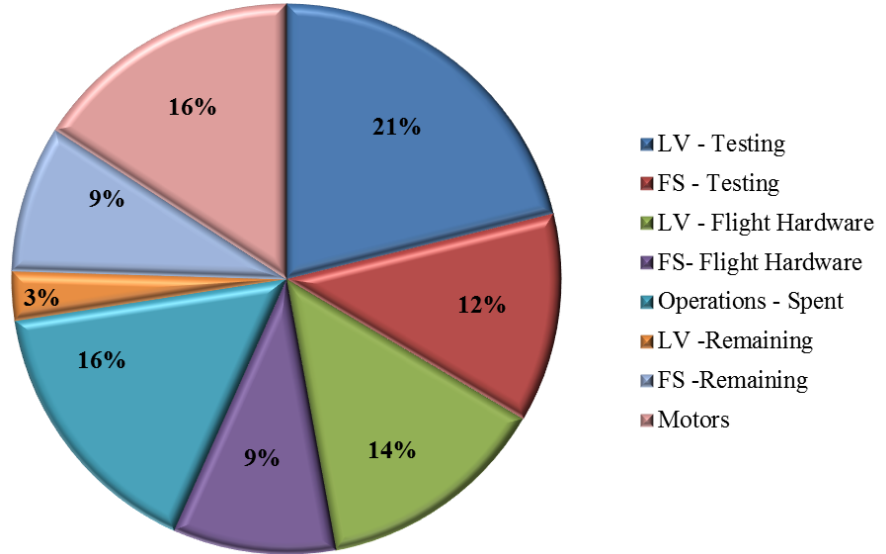
Figure 77. Project expenditures as of the CDR milestone.

	Actual Cost	Project Reserves
PDR	$ 985.61	61.2 %
CDR	$2,055.34	90.0 %
FRR	$5,423.58	28.7 %
Launch	$7,179.48	--

Actual Toal Project Cost
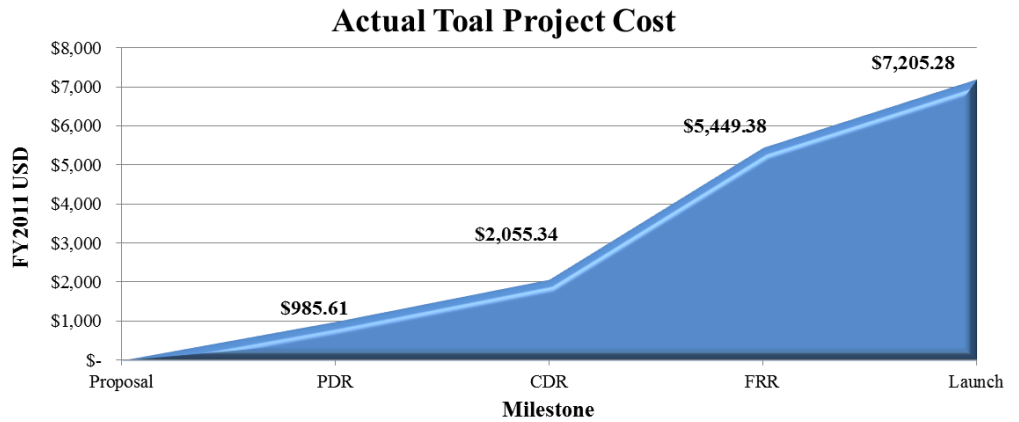
Figure 78. Actual total project costs and project reserves at each milestone.

11.3.2. Flight Hardware Expnditures

Figure 79 lists the overall expenditures for all Flight Hardware for the Launch Vehicle, Flight Avionics, and the Flight Experiment purchased up to the FRR milestone. Motor costs have been reduced to $160 through advanced purchase with Huff Performance. Figure 79 illustrates the total cost of the Flight Vehicle, Flight Avionics, and Flight Experiment at each milestone. It is estimated that the *Vespula* launch vehicle will cost under $2,500 at the time of the Competition Launch on April 21st, 2012. It is important to note that the expenditure summary incorporates 15% contingency at both FRR and Competition Launch milestones.

2011-2012 Overall Flight Vehicle Costs ($5,000 Limit)	
FS Flight Hardware	$ 604.88
LV Flight Hardware	$ 712.95
Motor	$ 160.00
Remaining	$ 3,522.17
Total	$ 5,000.00

Flight Vehicle & System Cost at FRR
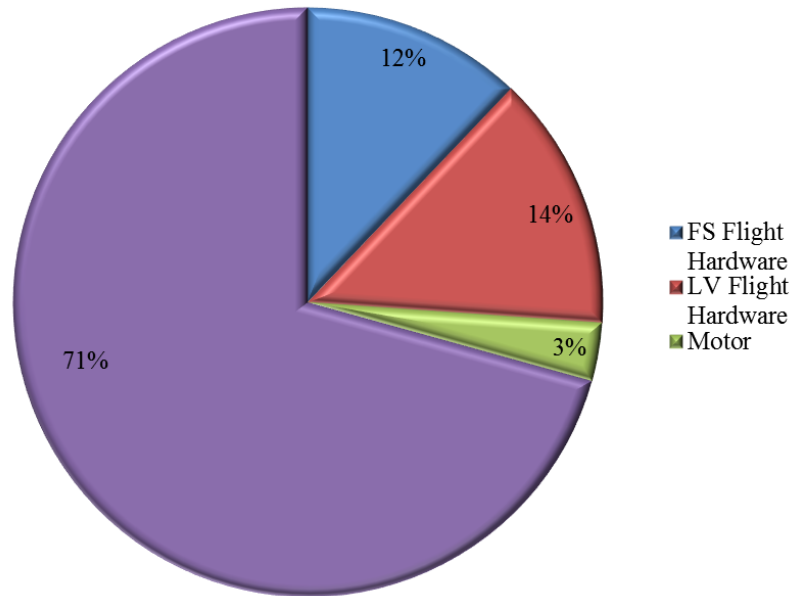
Figure 79. Summary of Flight Hardware expenditures up to the CDR milestone.

	Cumulative Costs	% Remaining
PDR	$ 174.10	96.5 %
CDR	$ 609.53	87.8 %
FRR	$ 1,477.83	70.44 %
Launch	$ 2,052.83	59.2 %

Total Flight Vehicle Expenditures
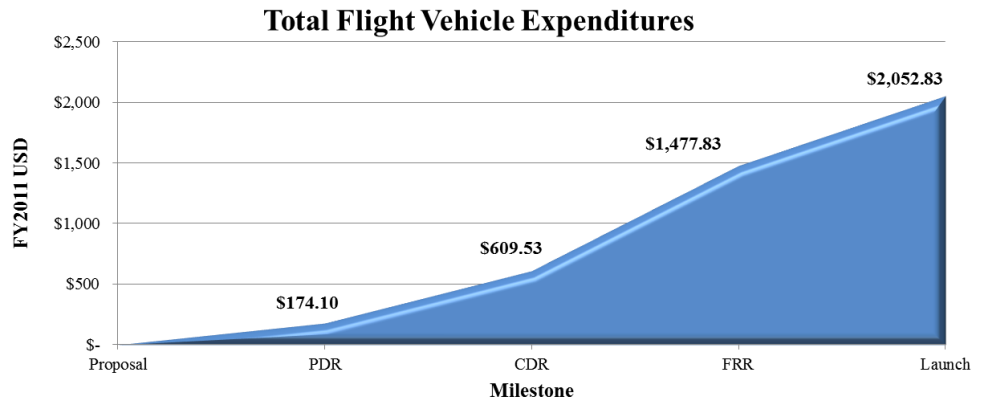
Figure 80. Total and Projected Flight Vehicle expenditures

Furthermore, Table 33 and Table 34 present the cost of the Project A.P.E.S. flight vehicle at the subsystem level. It is important to note that Table 33 and Table 34 assigns a cost to each component of the Flight Vehicle – regardless of whether it is legacy hardware or new hardware - while Figure 79 and Figure 80 only accounts for newly *purchased* hardware and discounts legacy hardware costs and donations to the Team. Table 32 summarizes and compares the two (2) costing methods presented. Additionally, it is worthwhile to note that the difference in Flight Vehicle cost between FRR and the Competition Launch, while large, is projected to be the worst case increase. This increase of approximately $500 when applied to the (Non-Discriminatory) Grassroots Method will yield a Flight Vehicle cost of just under $2,900 – well below the $5,000 limit.

Table 32. Comparison of Costing Methods

Method	Cost (FY2011 USD)
New Hardware Only (at FRR)	$1,477.83
New Hardware Only (at the Competition Launch)	$2,052.83
Legacy and New Hardware (Grassroots Method at FRR)	$2,397.60

Table 33. Flight Systems Bill of Materials with Cost Breakdown

Flight Avionics			
Item Description	Unit Price	Qty	Cost
Solenoid Driver Board	**$8.75**	**5**	**$43.75**
10 µF Capacitor	$0.43	1	$0.43
22 µF Capacitor	$0.91	1	$0.91
0.1 µF Capacitor	$0.26	1	$0.26
Flyback Schottky Diode	$0.45	1	$0.45
DRV103	$4.38	1	$4.38
Green LED	$0.38	2	$0.76
5.6 kΩ Resistor	$0.02	1	$0.02
205 kΩ Resistor	$0.04	1	$0.04
150 Ω Resistor	$0.02	1	$0.02
10 kΩ Resistor	$0.02	2	$0.04
D-to-A Converter	$1.19	1	$1.19
Trimpot	$0.25	1	$0.25
Flight Computer	**$255.10**	**1**	**$255.10**
Arduino Mega 2506	$58.95	1	$58.95
UP-501 GPS Receiver	$49.95	1	$49.95
OpenLog	$24.95	1	$24.95
ADXL321 Accelerometer	$17.31	1	$17.31
Xbee Pro 900 XSC RPSMA	$71.95	1	$71.95
L3G4200D Rate Gyro	$31.99		$31.99
A.P.E.S. Computer	**$192.18**	**1**	**$192.18**
BeagleBoard xM	$149.00	1	$149.00
Logitech C170 Webcam	$21.59	1	$21.59
HP HD-2200 Webcam	$21.59		$21.59
Ground Station	**$96.90**	**1**	**$96.90**
Xbee Pro 900 XSC RPSMA	$71.95	1	$71.95
XBee Explorer USB	$24.95	1	$24.95
Total Flight Avionics Cost			**$587.93**

Flight Experiment			
Item Description	Unit Price	Qty	Cost
A.P.E.S. Hardware	**$83.94**	**1**	**$290.31**
Neodymium Magnets	$33.12	1	$33.12
5/8" Iron Rod	$6.62	1	$6.62
30 AWG Magnet Wire	$25.89	1	$25.89
Cardboard Tube	$5.32	1	$53.19
Plywood	$7.99	1	$7.99
Fasteners	$5.00	1	$5.00
LiFePo Battery	$48.00	1	$48.00
LiFePo Battery Bracket	$110.50	1	$110.50
Total Flight Experiment Costs			**$290.31**

Table 34. Launch Vehicle Bill of Material with Cost Breakdown

Launch Vehicle			
Item Description	*Unit Price*	*Qty*	*Cost*
Booster Section	***$644.87***	***1***	***$644.87***
Thrust Plate	$1.76	1	$ 1.76
1/4-20 Threaded Rod	$2.62	4	$10.48
1/4-20 Nuts	$0.06	16	$1.03
1/4" Washers	$0.07	16	$1.06
Centering Ring	$0.45	1	$0.45
Fin	$51.67	3	$55.00
Motor Tube	$5.14	1	$5.14
Motor Case	$256.00	1	$256.00
Motor	$160.00	1	$160.00
Retention Ring	$ 7.02	1	$7.02
Epoxy	$15.67	1	$15.67
Rail Button	$1.54	2	$3.07
Primer	$5.49	1	$5.49
Paint	$5.99	3	$17.97
Clearcoat	$3.98	1	$3.98
Gasket	$0.25	3	$0.75
iMPS	***$225.57***	***1***	***$225.57***
G-10 Rib	$19.57	4	$78.26
G-10 Stringer	$5.45	12	$65.42
8-32 Bolts	$0.08	36	$3.05
Skin	$27.90	1	$27.90
Sealing Tape	$2.97	1	$2.97
Hook And Loop Fasteners	$17.97	1	$17.97
Nose Cone	***$30.00***	***1***	***$30.00***

Launch Vehicle			
Item Description	*Unit Price*	*Qty*	*Cost*
Recovery Section	***$648.95***	***1***	***$648.95***
60 Ft. – 1" Wide Nylon Webbing	$10.80	2	$21.60
Main Chute	$145.00	1	$145.00
Nomex Cloth	$12.00	2	$24.00
PVC Cup	$ 0.51	4	$2.04
Ematch	$1.33	4	$5.33
Black Powder (14 G)	$1.59	1	$1.59
D- Links	$7.36	3	$22.08
Steel Cable (8")	$3.33	2	$6.67
G-10 Tube (12")	$34.10	1	$34.10
Bulkhead	$2.54	2	$5.09
Ferrules	$1.92	2	$3.84
Arming Switch	$5.00	2	$10.00
Arming Switch Bracket	$68.00	1	$68.00
Stratologger	$80.00	2	$160.00
9V Battery	$2.50	2	$5.00
9V Battery Holder	$1.19	2	$2.38
G-10 Tube (6")	$17.05	1	$17.05
G-10 Coupler (5")	$20.63	1	$20.63
G-10 Tube (5")	$14.21	1	$14.21
Drogue Chute	$66.00	1	$66.00
U-Bolt	$8.81	1	$8.81
JB Weld	$5.27	1	$5.27
Shear Pins	$0.03	8	$ 0.27
Total Launch Vehicle Cost			$1,519.39

11.3.3. Actual Costs vs. Projected Costs

Figure 81 compares the actual vs. projected total project costs. With the exception of the PDR milestone, all other milestones have achieved a lower total project cost or are expected to achieve a lower project cost. It is important to note that the total project cost at FRR is inflated due to (1) costs associated with furnishing a recently acquired workspace, (2) costs associated with starting-up an engineering team, such as generic test equipment, tools, and supplies, and (3) costs associated with travel to launch sites – including: Manchester, TN, Palm Bay, FL, Lilly, GA, and Huntsville, AL.

The Mile High Yellow Jackets have been able to achieve these reduced project costs through:

- Internal design reviews at regular intervals
- Creation and review of Manufacturing and Fabrication Orders (MFO's) prior to ordering materials
- Communication, proper analysis, and constructive criticism by peers all throughout the design, manufacturing, fabrication, and testing processes.

	% Difference
PDR	6.2 %
CDR	-43.5 %
FRR	-27.8 %
Launch	-27.2 %
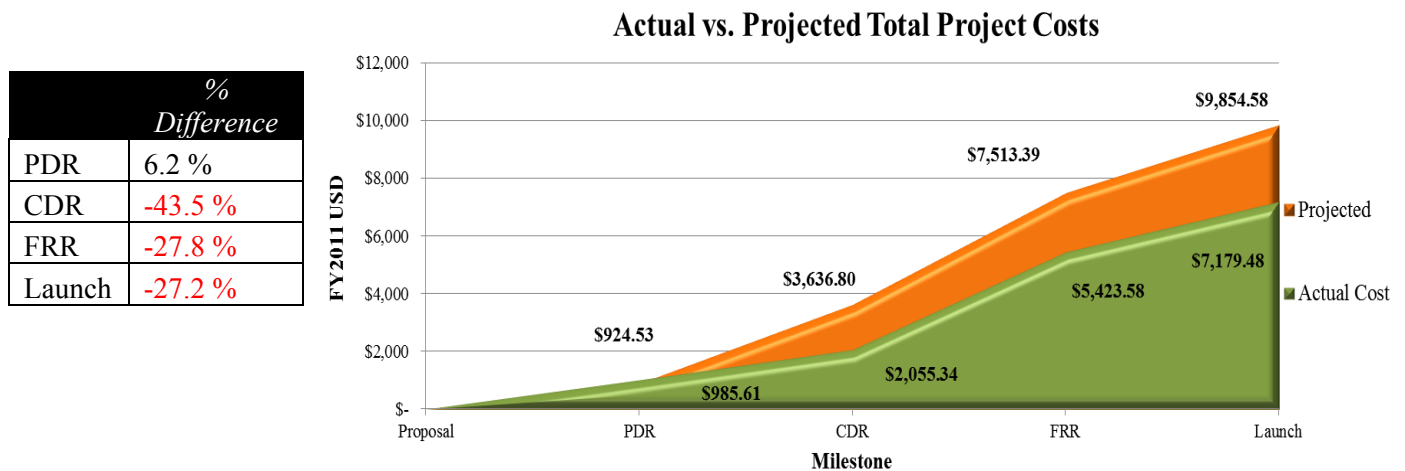
Figure 81. Actual vs. Projected Costs for the 2011-2012 competition year.

12. Project Schedule

12.1.   *Schedule Overview*

The Mile High Yellow Jacket's project is driven by the design milestone's set forth by the USLI Program Office. The design milestones are listed in Table 35. The project Gantt Chart for Project A.P.E.S. – located in Appendix I– contains only high-level activities due to the unique launch vehicle and payload designs. A more detailed Critical Path chart is located in Section 12.2.

Table 35. Design milestones set by the USLI Program Office.

Milestone	Date
Proposal	26 SEP
Team Selection	17 OCT
Web Presence Established	4 NOV
PDR Documentation	28 NOV
PDR VTC	6 DEC
CDR Documentation	23 JAN
CDR VTC	2 FEB
FRR Documentation	26 MAR
FRR VTC	5 APR
"Rocket Week"	18-21 APR
PLAR Documentation	7 MAY

12.2.   *Critical Path Chart: CDR to PLAR*

The updated Critical Path chart illustrated by Figure 82 demonstrates the highly integrated nature of Project A.P.E.S. The critical path chart identifies:

- High Risk Tasks
- Low-Moderate Risk Tasks
- Earned Value Management (EVM) Goal Tasks
- Looping Tasks
- Critical and Alternate Paths
- Major Inputs to Tasks

Since CDR, the Critical Path chart includes the following changes:

Launch Vehicle Critical Path:

- "*Fabrication of Launch Vehicle Sections*" has been changed from a 'Low-Moderate Risk Task' to an EVM Goal Task since this is a major project milestone that has been successfully completed.
- The current location (indicated by a **Blue** border) on the Launch Vehicle Critical Path is at the "*Full-Scale Launch Vehicle Test Flight*"
- The "*Alternate Payload Integration Path*" is indicated as the route to be taken to successfully integrate the Flight Experiment after the launch vehicle testing.
  - o It should be noted that the data-recording Flight Computer has been successfully flown during the March 10th Launch.

Flight Systems Critical Path:

- The "*Ground Testing & Control Logic Development*" has been changed to be a Low-Moderate Risk Task.
  - o This has been changed due to the delay in manufacturing the necessary solenoid driver boards necessary to continue ground testing.
- The current location (indicated by a **Blue** border) on the Flight Systems Critical Path is at the "*Ground Testing & Control Logic Development / Verification of Field Equations & Control Logic / Fabrication of Flight Experiment Components*"

Flight Avionics Critical Path:

- The "*Image Processing Development & testing*" task has been changed from a 'Low-Moderate Risk Task' to an EVM Goal Task since this is a major project milestone that has been successfully completed.
- The "*A.P.E.S. Computer Functionality Testing*" task has been changed from a 'Low-Moderate Risk Task' to an EVM Goal Task since this is a major project milestone that has been successfully completed.
- An alternate route has been identified in the event the "*Custom Flight Computer Fabrication & Testing*" task becomes a high Schedule and Project risk.
  - o The alternate route has been identified to be the "*Customize Rapid Prototyping Micro-controller Platform*" task.
- The current location (indicated by a **Blue** border) on the Flight Avionics Critical Path is at the "*Customize Rapid Prototyping Micro-controller Platform / A.P.E.S. Computer Functionality Testing*"
- The alternate routing going from the "Custom Flight Computer Fabrication" to the "*Full System Integration & Testing*" task via the "*Customize Rapid Prototyping Micro-controller Platform*".
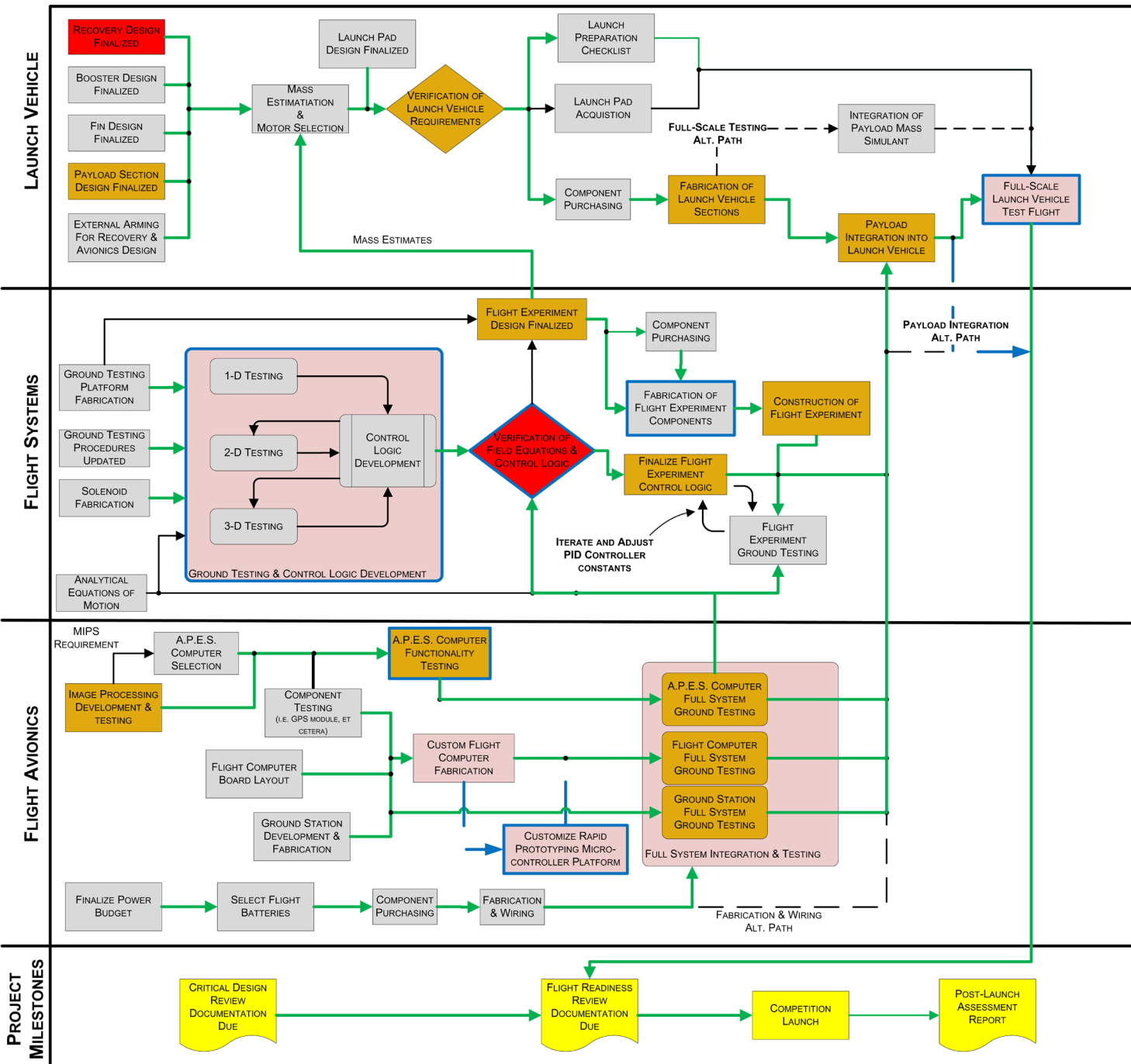
Figure 82. Critical Path Chart from CDR to PLAR

12.3. *Schedule Risk*

12.3.1. High Risk Tasks

From the Critical Path chart, two (2) items have been identified as "High Risk Items." These items were identified at CDR and have been closely monitored. These items are:

- Verification of Field Equations & Control Logic
- Recovery System Design

These items remain listed as High Risk Tasks since they have not demonstrated full functionality through testing since CDR. The Flight Control Logic has not been fully verified due to various manufacturing equipment malfunctions that are beyond the control of the Team. The Recovery System experienced a partially-successful flight on March 10th, however, the main chute failed to deploy. The failure has been attributed to the main parachute being packed to tightly into the recovery compartment. The mitigation of this failure included reanalyzing the mass of the Launch Vehicle and determining that a 10-foot diameter main parachute can be used while still meeting the landing kinetic energy requirements in Table 16.

Table 36 lists the mitigations for these two (2) items.

Table 36. Identification and Mitigations for High-Risk Tasks.

High-Risk Task	Potential Impact on Project A.P.E.S.	Mitigation
Verification of Field Equations & Control Logic	1) Unsuccessful flight experiment demonstration 2) Flight Experiment does not function properly during flight 3) Flight Experiment encounters a flight anomaly that results in excessive draw and damage to the Flight Avionics, Power Supply, and/or Launch Vehicle	1) Develop multiple paths to achieve the end goal of developing thee robust control logic that is required for the successful demonstration of the Flight Experiment. 2) Ensure Flight Systems personnel have direct and free access to experienced personnel on and off of the team. 3) Ensure personnel have direct and free access to the simulation and analysis tools necessary for the development (and subsequent verification) of the control logic. 4) Ensure direct and free access to the proper equipment necessary in developing and implementing the Control Logic for the A.P.E.S. experiment.
Recovery System Design & Fabrication	1) Excessive kinetic energy at landing resulting in dis-qualification from the USLI competition at CDR 2) Excessive kinetic energy during landing resulting in damage to the rocket. 3) Failure to deploy the drogue and/or main parachute resulting in a high energy impact with the ground damaging or destroying the Launch Vehicle.	1) Ensure Recovery System Lead has direct and free access to experienced personnel on and off the team. 2) Provide real-time feedback of the design decisions to ensure all recovery-related requirements are meet with at least a 5% margin wherever possible. 3) Ensure proper manufacturing techniques are utilized during the fabrication of the recovery system.

12.3.2.   Low-to-Moderate Risk Tasks

The "low-to-moderate risk tasks" are considered to be those risks that pose a risk to either the project schedule and/or project budget but little to no risk of not meeting the Mission Success Criteria in Table 1. The risks and mitigations are provided in Table 37.

Table 37. Low to Moderate Risk items and mitigations.

Risk	Risk Level	Potential Impact on Project A.P.E.S.	Mitigation
Full-Scale Launch Vehicle Test Flight	Moderate	1) Schedule Impact 2) Budgetary Impact 3) Not qualifying for Competition Launch	1) Ensure Launch Procedures are established practiced prior to any launch opportunity. 2) Ensure proper construction of the Launch Vehicle. 3) Have a sufficient number of launch opportunities that are in different geographical areas as to minimize the effects of weather on the number of launch opportunities.
Ground Testing & Control Logic Development	Moderate	1) Schedule Impact 2) No Experimental Flight Data is recorded prior to the Competition Launch.	1) Ensure personnel have direct and free access to experienced personnel on and off of the team.
Custom Flight Computer Fabrication	Moderate	1) Budgetary Impact 2) Impact to Mission Objectives	1) Ensure proper manufacturing techniques are observed during fabrication. 2) Ensure Manufacturing and Fabrication Orders (MFO's) are sufficiently detailed for the task. 3) Ensure that an alternate path has been identified and implemented in a timely manner that meets the requirements of the Flight Computer and schedule.

13. Educational Outreach

13.1. Overview

The goal of Georgia Tech's outreach program is to promote interest in the Science, Technology, Engineering, and Mathematics (STEM) fields. The Mile High Yellow Jackets' intend to conduct various outreach programs targeting middle school students and educators. The Mile High Yellow Jackets have an outreach request form on their webpage – as shown in Figure 83 - for educators to request

Figure 83. Online Outreach Contact Form through which educators may contact the Mile High Yellow Jackets.

presentations or hands-on activities for their classroom.

13.2. FIRST LEGO League

FIRST LEGO League is an engineering competition designed for middle school children where they build an autonomous LEGO MINDSTORMS robot. An example robot is illustrated in Figure 84. Every year there is a new competition centered on a theme exploring a real-world problem. The Mile High Yellow Jackets will have a booth at the Georgia State FIRST Lego League Tournament where we will teach the fundamental concepts behind our payload and showcase our past rockets. In addition team members will aid in judging the tournament. This

Figure 84. Example of a First LEGO League autonomous robot.

outreach event is anticipated to reach over 700 middle school students and educators. The lesson plan for First LEGO League can be found in Appendix XII

The Mile High Yellow Jacket's table included their small-scale test vehicle from the 2008-2009 competition cycle. Images from the First LEGO League event are shown in Figure 85.

Figure 85. Images from the First LEGO League Outreach Event.

13.3.   *Civil Air Patrol Model Rocketry Program*

The Civil Air Patrol (CAP), the Official Auxiliary to the U.S. Air Force, is a volunteer organization whose primary missions are Emergency Services, Cadet Programs, and Aerospace Education. In the Aerospace Education program, Cadets have the opportunity to earn a Model Rocketry Badge by furthering their knowledge in the history and physics of rocketry as well as building five (5) separate rockets ranging from non-solid fuel rockets to scale models of historic rockets as well as rockets that must meet specific altitude and payload requirements. The Mile High Yellow Jackets will be working with a local Atlanta-based squadron, the DeKalb County Cadet Squadron (DCCS). The earning of the Model Rocketry Badge will be split into two different

Figure 86. A Civil Air Patrol Model rocket constructed by a cadet during the TITAN phase of the Model Rocketry Program.

events scheduled for April 5th and April 12th. The Mile High Yellow Jackets Educational Outreach Chair is working with the DCCS liaison in order to ensure that all program criteria are met. This outreach event is anticipated to reach approximately 20 to 30 Cadets in the 6th to 9th

grade range. Specific details regarding the main concepts that are to be learned by the Cadets participating in the Model Rocketry Program can be found in the lesson plan in Appendix XIII

13.4.   *National Air and Space Rocket Discovery Station*

The Mile High Yellow Jackets have created a Rocket Discovery Station which focuses on the differences between rockets and planes and Newton's Third Law. This Discovery Station is being integrated into the Discovery Station Program at the Smithsonian National Air and Space Museum, Udvar Hazy Center. The Rocket Discovery Station made its debut at the Women in Aviation and Space Day on Saturday, March 24th. The station was on the floor for two hours and had a visitor count of 137 people and Discovery Stations have an average visitor of 10,000 people per year. A key feature of the station is that it can easily be be done in a classroom or at home because it does not require any special supplies or equipment. The lesson plan for the station is on our website and in Appendix XIV.

Figure 87. Images of the National Air & Space Rocket Discovery Station.

13.5.   *Visit to the Capital*

In late February four members of the Mile High Yellow Jackets went to Congress to talk to Georgia Representatives on behalf of the Georgia Space Grant Consortium(GSGC). Their testimonials described the invaluable opportunities that GSGC has given them, including participating in the University Student Launch Initiative, Georgia Tech Microgravity University Team, and sending a crew to the Mars Desert Research Station. Figure 88 is a photograph of the Georgia Tech delegation and the head of the Georgia Space Grant Consortium, Dr. Stephen Ruffin.

Figure 88. Four members of the Mile High Yellow Jackets accompany Georgia Space Grant Consortium representatives to Capitol Hill to speak with various Congressmen,

Reference

Niskanen, Sampo. OpenRocket vehicle Technical Documentation. 18 July 2011. Web.

Apke, Ted. "Black Powder Usage." (2009). Print. <http://www.info-central.org/?article=303>.

PerfecFlite. StratoLogger SL100 Users Manual. Andover, NH: Print. <www.perfectflite.com>.

Roensch, S. (2010). "Finite Element Analysis: Introduction." 2011, from **http://www.finiteelement.com/feawhite1.html**.

"G-10 Fiberglass Epoxy Laminate Sheet." MATWEB.com. http://www.matweb.com/search/datasheet_print.aspx?matguid=8337b2d050d44da1b8a9a5e61b0d5f85

"Shape Effects on Drag." NASA Web. 19 Nov. 2011. <http://www.grc.nasa.gov/WWW/k-12/airplane/shaped.html>.

Cavcar, Mustafa. "Compressibility Effects on Airfoil Aerodynamics." (2005). Print.

"Apogee Paramagnetic Oxygen Gas Experimental Electromagnetic Separator: Preliminary Design Review." Comp. Georgia Tech University Student Launch Initiative. Atlanta: 2009. Print.

Cheng, David. Field and Wave Electromagnetics. 1st ed. Reading, MA: Addison-Wesley Publishing Company, 1985. Print.

Millspaugh, Ben, Ph.D. "Civil Air Patrol: Model Rocketry." Leadership Development and Membership Services Directorate, National Headquarter, Civil Air Patrol, Maxwell AFB, AL. Print.

Appendix I: Project A.P.E.S. Gantt Chart
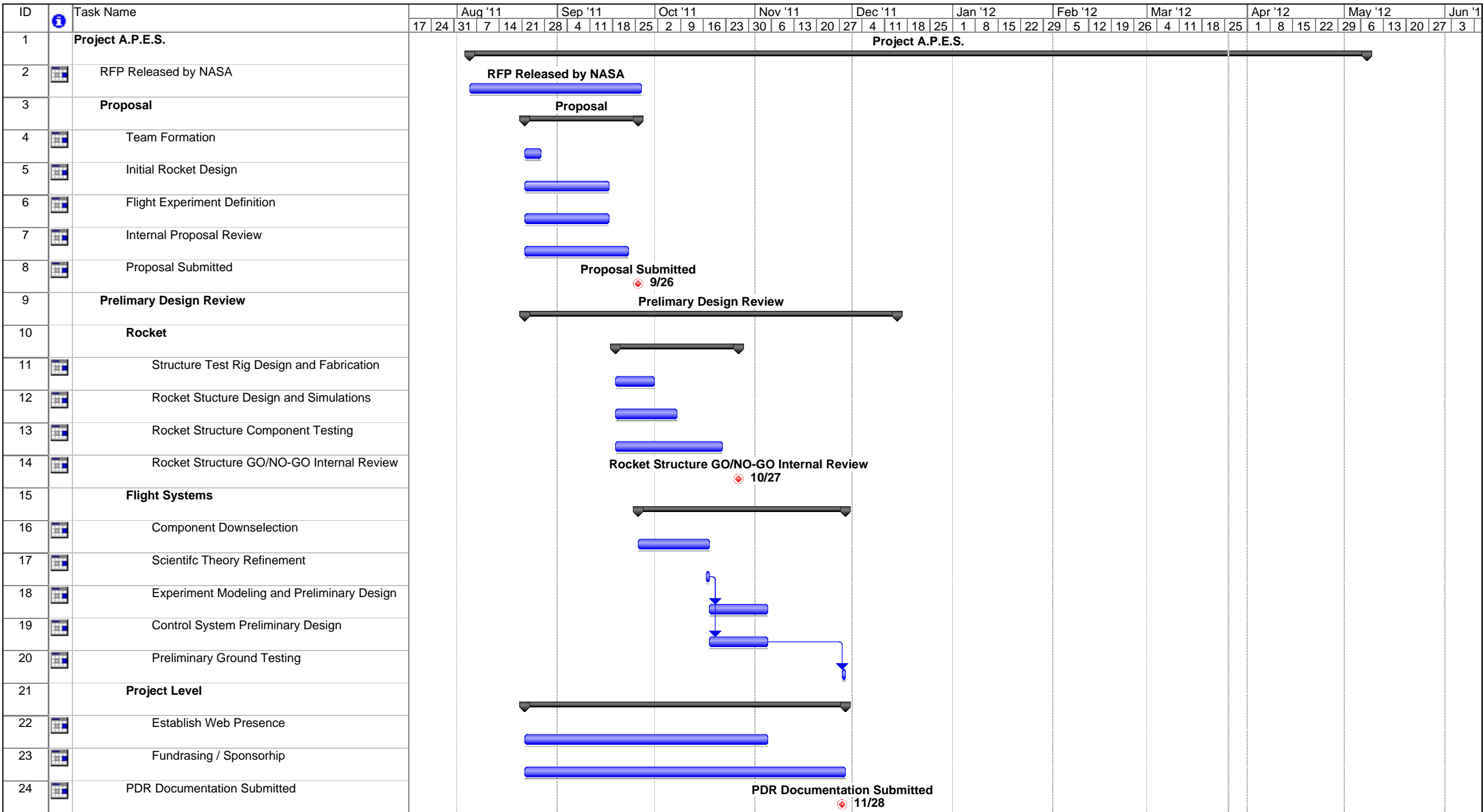
ID		Task Name	Aug '11	Sep '11	Oct '11	Nov '11	Dec '11	Jan '12	Feb '12	Mar '12	Apr '12	May '12	Jun '1

(Timeline columns: 17 | 24 | 31 | 7 | 14 | 21 | 28 | 4 | 11 | 18 | 25 | 2 | 9 | 16 | 23 | 30 | 6 | 13 | 20 | 27 | 4 | 11 | 18 | 25 | 1 | 8 | 15 | 22 | 29 | 5 | 12 | 19 | 26 | 4 | 11 | 18 | 25 | 1 | 8 | 15 | 22 | 29 | 6 | 13 | 20 | 27 | 3)

ID	Task Name
1	**Project A.P.E.S.**
2	RFP Released by NASA
3	**Proposal**
4	Team Formation
5	Initial Rocket Design
6	Flight Experiment Definition
7	Internal Proposal Review
8	Proposal Submitted
9	**Prelimary Design Review**
10	**Rocket**
11	Structure Test Rig Design and Fabrication
12	Rocket Stucture Design and Simulations
13	Rocket Structure Component Testing
14	Rocket Structure GO/NO-GO Internal Review
15	**Flight Systems**
16	Component Downselection
17	Scientifc Theory Refinement
18	Experiment Modeling and Preliminary Design
19	Control System Preliminary Design
20	Preliminary Ground Testing
21	**Project Level**
22	Establish Web Presence
23	Fundrasing / Sponsorhip
24	PDR Documentation Submitted

Milestones/labels on chart:
- **Project A.P.E.S.**
- **RFP Released by NASA**
- **Proposal**
- **Proposal Submitted** ◉ 9/26
- **Prelimary Design Review**
- **Rocket Structure GO/NO-GO Internal Review** ◉ 10/27
- **PDR Documentation Submitted** ◉ 11/28

Project: 2011-2012 USLI Gnatt Chart.r
Date: Mon 3/26/12

Task	▬▬▬	Progress	▬▬▬
Split	....	Milestone	◆
Summary	▬▬▬	Project Summary	▭▭▭
External Tasks	▬▬▬	External Milestone	◇
Deadline	⇩		

Page 1

ID	Task Name
25	PDR Telecon
26	**Critical Design Review**
27	**Rocket**
28	Full-Scale Structure Build
29	Recovery System Ground Test
30	Competition Rocket Build
31	Initital Test Flight
32	**Flight Systems**
33	Flight Systems Integration
34	Control System Detailed Design
35	Detailed Experiment Modeling
36	Experiment Refinement
37	**Project Level**
38	Website Updates
39	Outreach Events
40	CDR Documentation Submitted
41	CDR Telecon
42	**Flight Readiness Review**
43	**Rocket**
44	Final Test Preparation
45	Final Test Flight
46	Competition Launch Preparation
47	**Flight Systems**
48	Experiment Refinement

Chart annotations:
- Critical Design Review
- Project Level
- CDR Documentation Submitted 1/23
- Flight Readiness Review

49		Control System Refinement											
50		**Project Level**											
51		Website Updates											
52		Outreach Events											
53		FRR Documentation Submitted								FRR Documentation Submitted 3/26			
54		FRR Telecon											
55		Competition Launch									Competition Launch 4/22		
56		Post-Launch Assument Review Submitted									Post-Launch Assument Review Submitt 5/7		
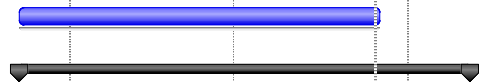
Project: 2011-2012 USLI Gnatt Chart.r
Date: Mon 3/26/12

Task		Progress
Split		Milestone

Summary		External Tasks
Project Summary		External Milestone

Deadline

Page 3

Appendix II: Launch Checklist

1. **Avionics Ground Testing**
   a. Test avionics ensuring a successful GPS lock and communication with the ground station.

2. **Prepare payload bay**
   a. Ensure batteries and switches are wired to the altimeters correctly
   b. Ensure batteries, power supply, switch, data recorder and pressure sensors are wired correctly
   c. Install fresh batteries into battery holders and secure with tape
   d. Test the altimeters

Altimeter	In Circuit	Out of Circuit
Altimeter 1		
Altimeter 2		

   e. Insert altimeter and payload into the payload bay
   f. Connect appropriate wires
   g. Verify payload powers on correctly and is working properly. If it is not, check all wires and connections
   h. Turn off payload power
   i. Arm altimeters with output shorted to verify jumper settings. This is to check battery voltage and continuity
   j. Disarm altimeter, un-short outputs

3. **Assemble charges**
   a. Test e-match resistance and make sure it is within spec
   b. Remove protective cover from e-matches
   c. Measure amount of black powder determined in testing
   d. Put e-matches on tape with sticky side up

E-match	Resistance
E-match 1	
E-match 2	
E-match 3	
E-match 4	

   e. Pour black powder over e-matches

   f. Seal tape

   g. Retest e-matches

4. **Check Altimeters**
   a. Ensure altimeter is disarmed
   b. Connect charges to altimeter bay
   c. Turn on altimeter and verify continuity
   d. Disarm altimeter

OFF   **ON**

5. **Pack Parachutes**
   a. Connect drogue shock cord (long side) to booster section and altimeter bay (short side)
   b. Fold excess shock cord so it does not tangle
   c. Add Nomex cloth to ensure only the Kevlar shock chord is exposed to ejection charge
   d. Insert altimeter bay into drogue section and secure with shear pins
   e. Pack main chute
   f. Attach main shock cord to payload bay (long side to nose cone)
   g. Fold excess shock cord so it does not tangle
   h. Add Nomex cloth under main chute and shock cord ensuring that only the Kevlar part of the shock cord will be exposed to the ejection charge
   i. Connect shock cord to nose cone, install nose cone and secure with shear pins

6. **Assemble motor**
   a. Follow manufacturer's instructions
   b. Do not get grease on propellant or delay
   c. Do not install igniter until at pad
   d. Install motor in launch vehicle
   e. Secure positive motor retention

7. **Final Prep**
   a. Turn on payload via a switch and start stopwatches

b. Inspect launch vehicle. Check CG to make sure it is in safe range; add nose weight if necessary

c. Bring launch vehicle to the range safety officer (RSO) table for inspection

d. Bring launch vehicle to pad, install on pad, verify that it can move freely (use a standoff if necessary)

e. Install igniter in launch vehicle

f. Touch igniter clips together to make sure they will not fire igniter when connected

g. Make sure clips are not shorted to each other or blast deflector

h. Arm altimeters via switches and wait for continuity check for both

i. Return to front line

8. **Launch.**
   a. Stop the stopwatches and record time from arming payload and launch
   b. Watch flight so launch vehicle does not get lost

9. **Post Launch**
   a. Recover launch vehicle, document landing
   b. Disarm altimeter(s) if there are unfired charges
   c. Disassemble launch vehicle, clean motor case, other parts, inspect for damage
   d. Record altimeter data
   e. Download payload data

Troubleshooting

Test	Problem	Control & Mitigation
Power on payload	Payload does not power on	Check batteries have sufficient charge, check wires are connected correctly
Check E-match resistance	E-match resistance does not match required specifications	Replace e-match before use
Power on altimeters	Altimeters do not power on	Check batteries have sufficient charge, check wires are connected correctly
Check for altimeter continuity after installing e-matches	No continuity	Check wires are connected correctly
Launch Rocket	Engine does not fire	Disconnect power, ensure igniter clips are not touching, ensure power is reaching clips ,ensure motor is assembled correctly

Appendix III: Ground Test Plan

Ground Test Plan

Goals

The A.P.E.S. ground test data will provide the basis for empirical modeling of the force interactions for various configurations of the experiment at various voltages. All actions will be incremented to allow for a detailed model for extrapolation and interpolation of the data for future flight control systems. Goals are detailed in Table 38: Ground Test goals.

Table 38: Ground Test goals

Ground Test Goal	Ground Test Goal Definition
1	DC Steady State Solenoid Testing
2	Map Magnetic Fields
3	Detect force equilibrium
4	Develop model for control of voltage

Test Sequence 1

The static magnetic field of a solenoid will be mapped at various distances and currents utilizing the 3-axis AKM 8975 magnetic sensor. From this, a Response Surface Equation (RSE) will be developed in order to map the total field strength at a given distance and current. The ranges for the distance and current tested are listed in Table 39.

Table 39. Range of test values used during Test Sequence 1.

Parameter	Value
Distance Range	1 cm to 5 cm
Current Range	0 A to 0.86 A

Test Sequence 2

Equilibrium testing with no internal magnetism. A single vertically-oriented solenoid will be utilized to lift the test article to equilibrium points within a cylinder, from 1 cm to 7 cm in steps of 1 cm. Hall-effect sensors will be used to map fields at each equilibrium point identically to the static field mapping. The optical detection sensors will detect distance from below the

cylinder. The optical detection sensors sensor will be lowered to the minimum read distance using Maker Beam. The minimum read distance shall be confirmed by data sheets and calibration.

Test Sequence 3

Equilibrium de-scope testing with internal magnetism. One (1) neodymium magnet shall be placed in the center of the test article and covered with reflective material. A single vertically-oriented solenoid will be utilized to lift the test article to equilibrium points within a cylinder, from 1 cm to 7 cm in steps of 1 cm. Hall-effect sensors will be used to map fields at each equilibrium point identically to the static field mapping. The test setup should allow for both pulling of the test article as well as pushing of the test article.

Test Sequence 4

Similar testing will be completed using a horizontal sheet with the sample placed on top. Solenoids will be used to pull and hold the sample in the middle of the platform at equilibrium. These tests will be completed with the permanent magnet sample. The Camera Cube will allow for object detection. Fields will be mapped at equilibrium.

Test Sequence 5

A permanently magnetic test article will be levitated from rest in 3-dimensions to equilibrium at central points in the test stand. Incrementing of the equilibrium point will allow for greater control of the test article. Object detection will be accomplished with the Camera Cube. Fields will be mapped at equilibrium.

Test Sequence 6

The flight model will be tested and disturbances will be introduced.

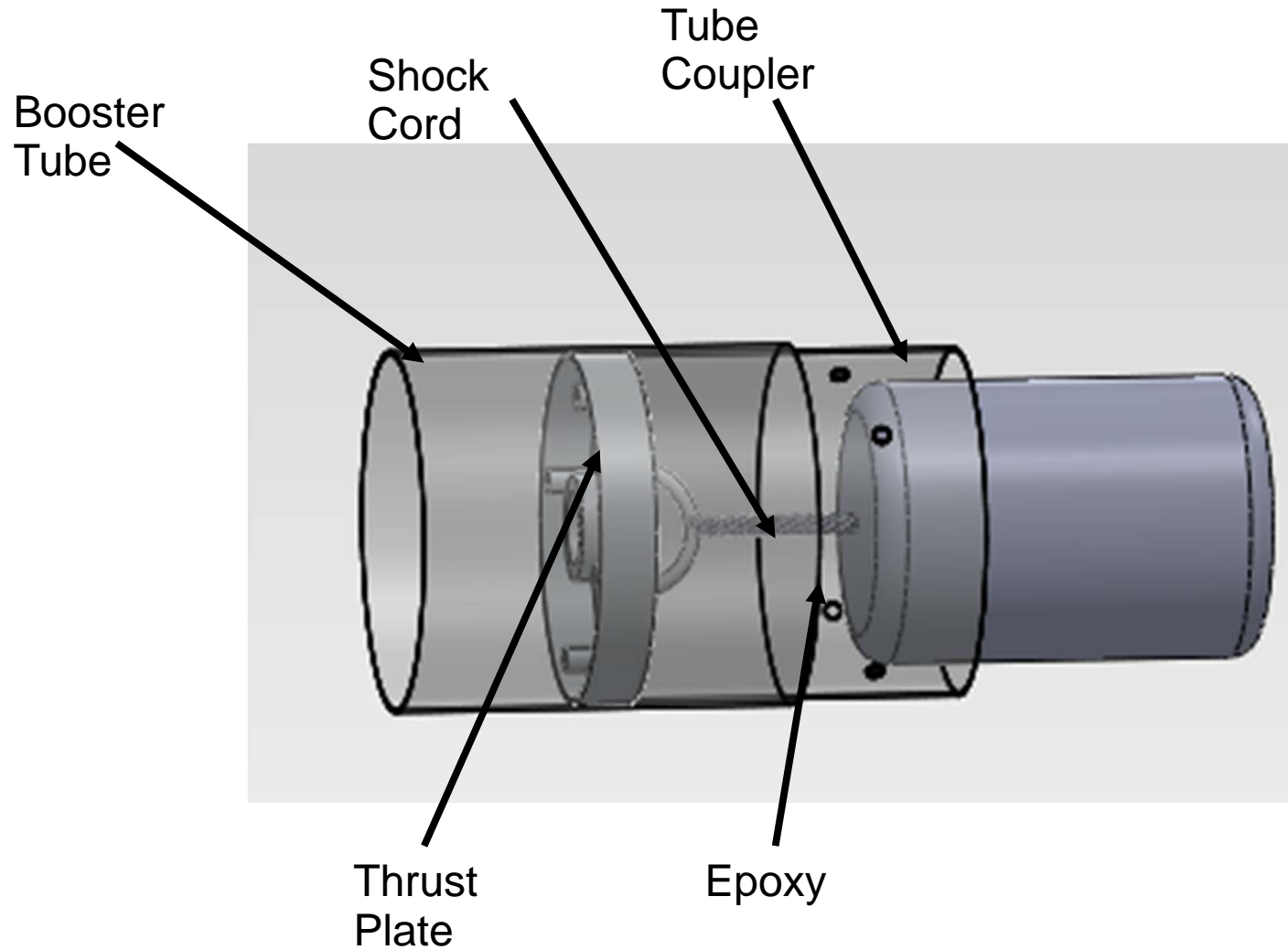**Appendix IV: Recovery Manufacturing and Fabrication Order**
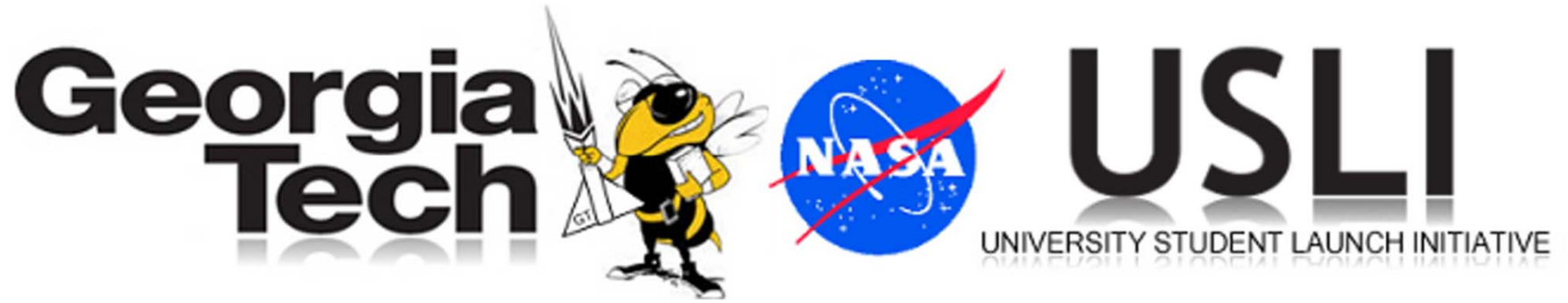
RECOVERY MFO

Drogue Assembly – Thrust Plate

1) Bolt in U-Bolt into Thrust plate
2) Epoxy Thrust Plate and Tube Coupler into Booster Tube.


Tube Coupler

Shock Cord

Booster Tube

Thrust Plate

Epoxy

Drogue Assembly - Bulkhead

3) Epoxy Garolite bulkhead to aft-most iMPS rib
4) Epoxy PVC Cups (2x) to parachute bulkhead.
5) Cut steel cable to length and pass through holes in bulkhead. Use Arbor press to press ferrules onto cable. Seal with JB weld.

PVC Cup

Steel Cable

Bulkhead
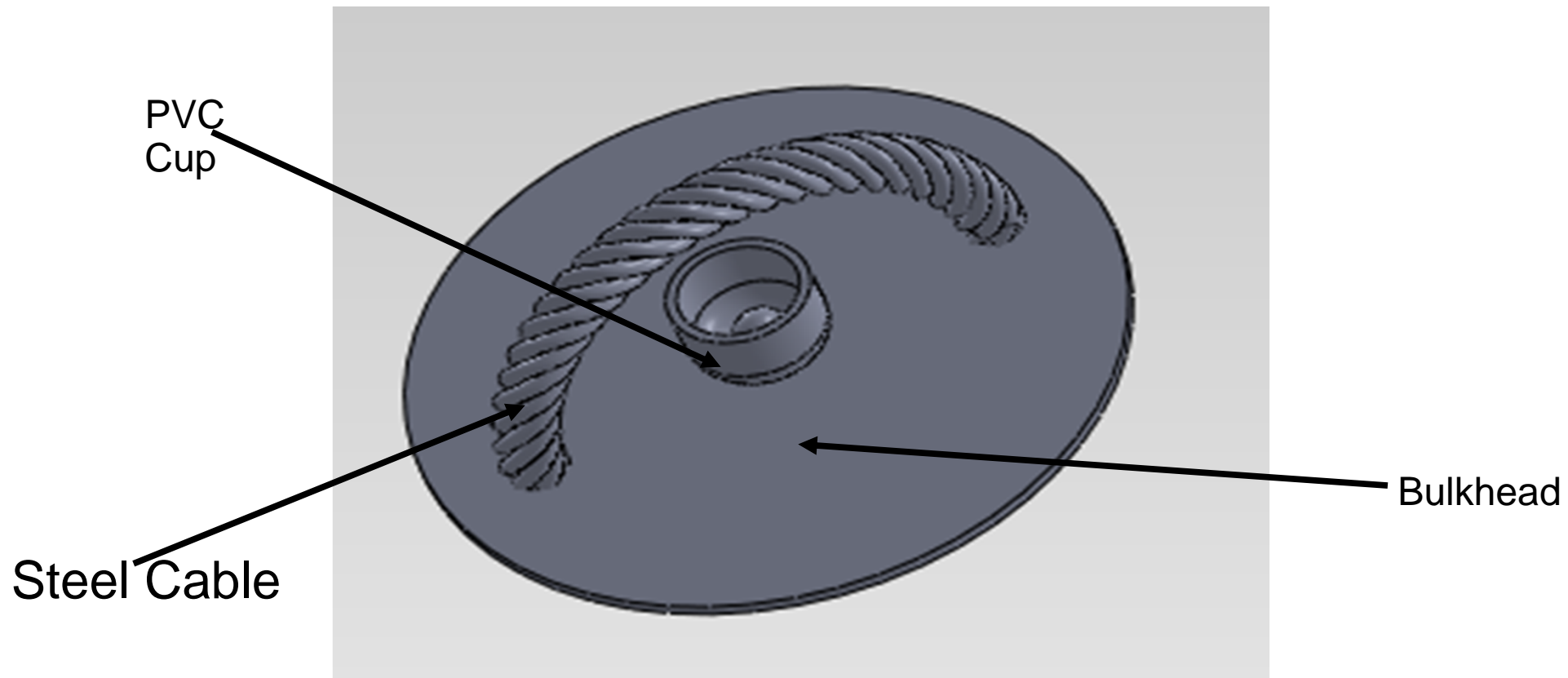
6) Epoxy the Parachute Tube to the Bulkhead/Ejection Charge/Steel Cable assembly.

Bulkhead /Ejection Charge/ Steel Cable
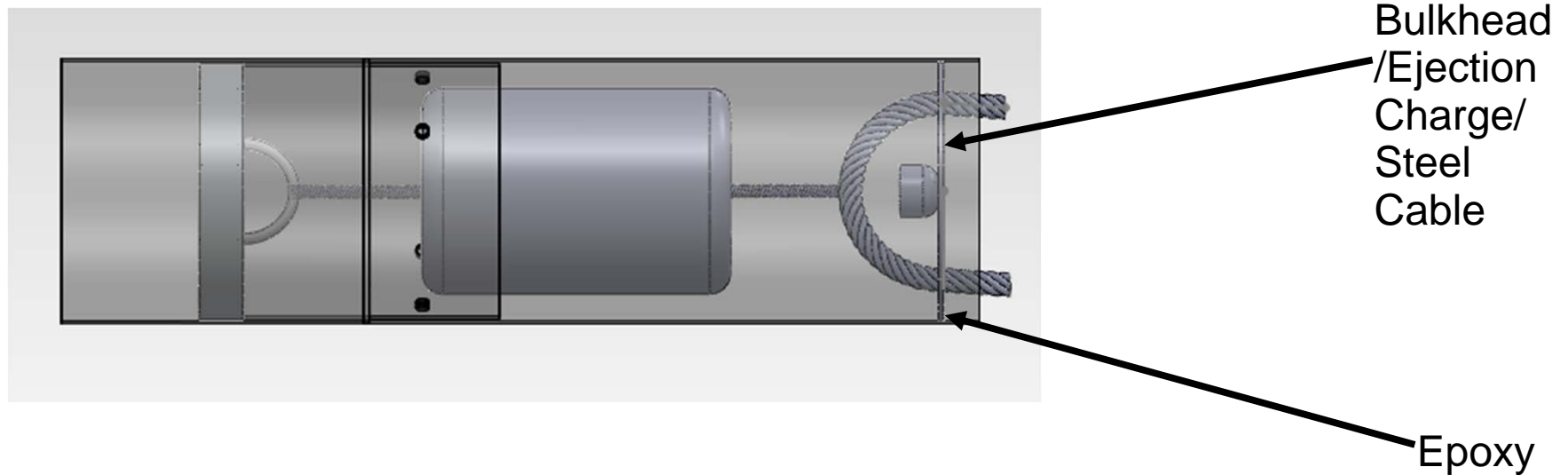
Epoxy

Drogue Assembly – Install Shear Pins

7) Match drill 4x shear pin holes with 1/16" drill bit.

Parachute Tube

Parachute

Shear Pins

8) Epoxy Garolite bulkhead to forward-most iMPS rib
9) Epoxy PVC Cups (2x) to parachute bulkhead.
10) Cut steel cable to length and pass through holes in bulkhead. Use Arbor press to press ferrules onto cable. Seal with JB weld.
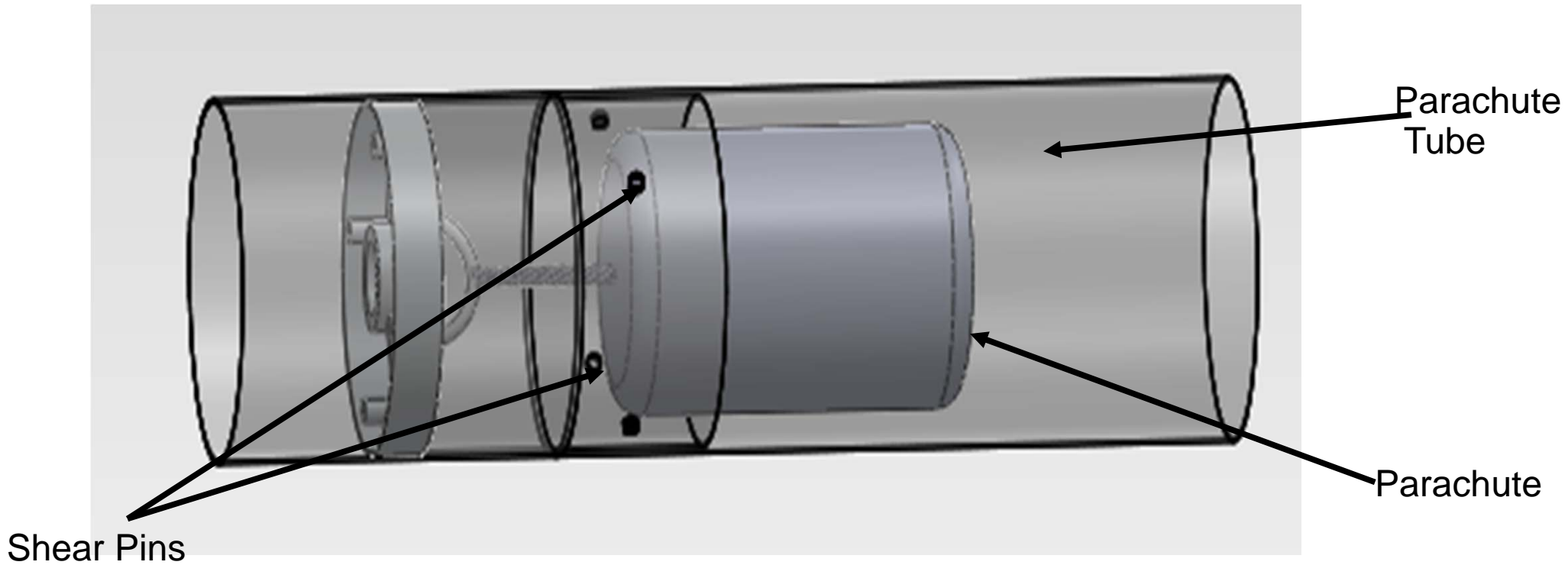

PVC
Cup

Steel Cable

Bulkhead

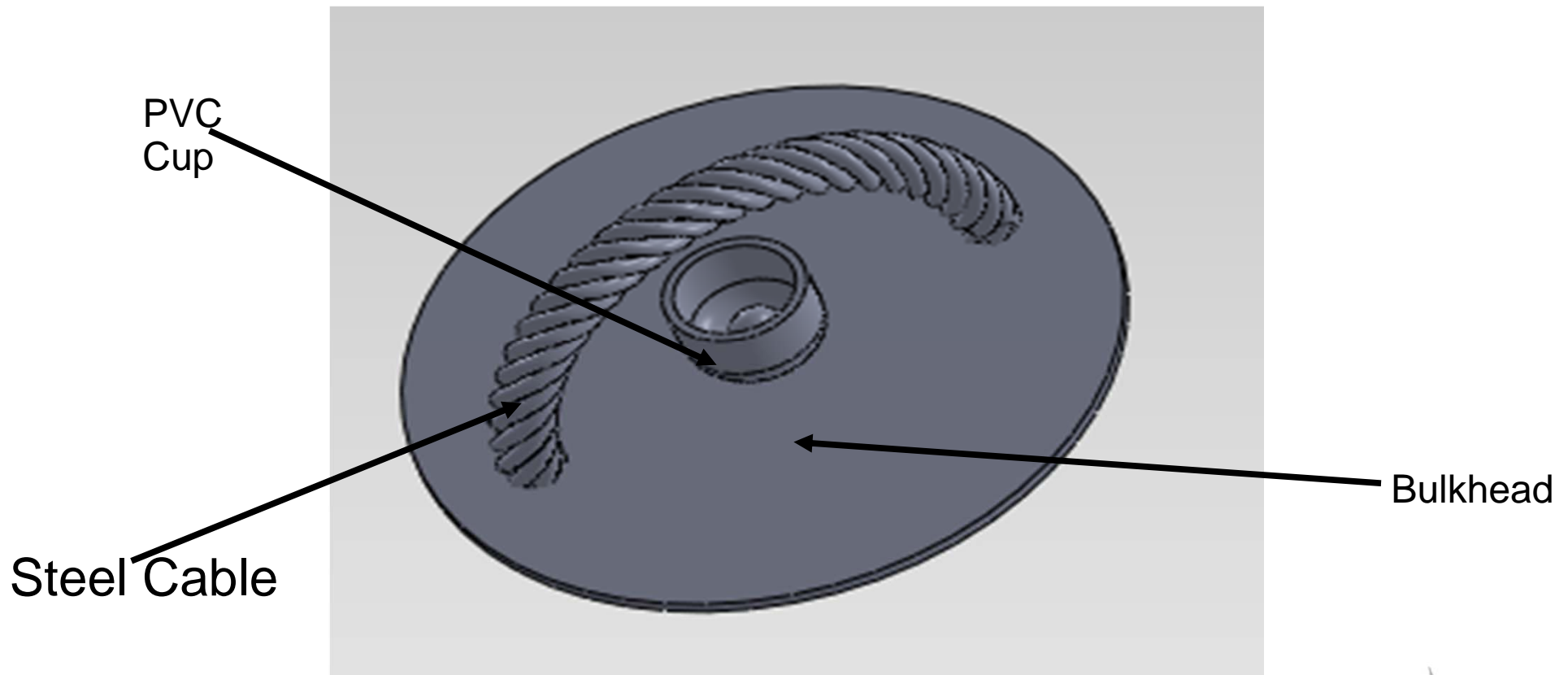11) Epoxy the Parachute Tube to the Bulkhead/Ejection Charge/Steel Cable assembly.

Main bulkhead

Bulkhead
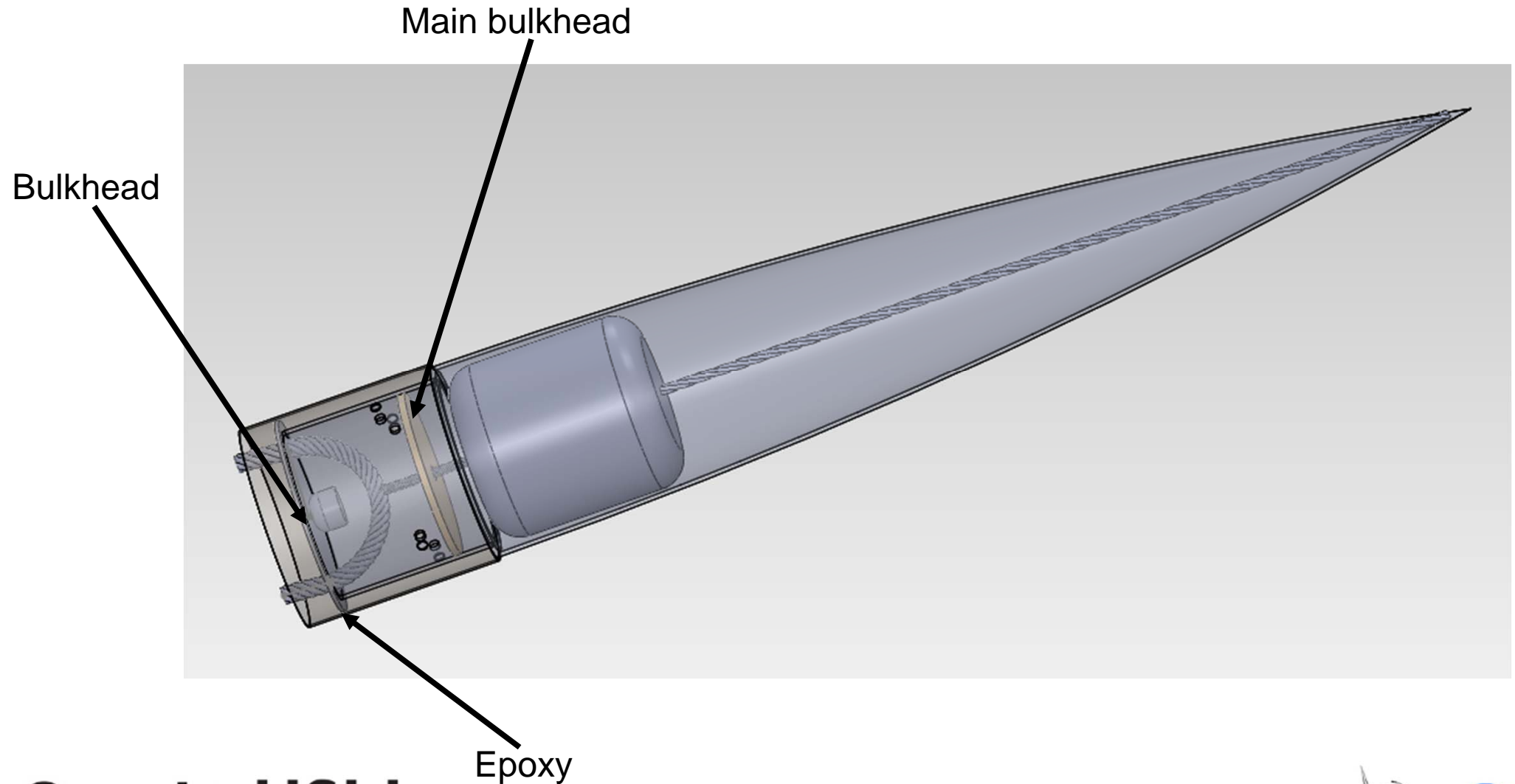
Epoxy

12) Match drill 4x shear pin holes with1/16" drill bit.

Nose Cone

Nose Tube
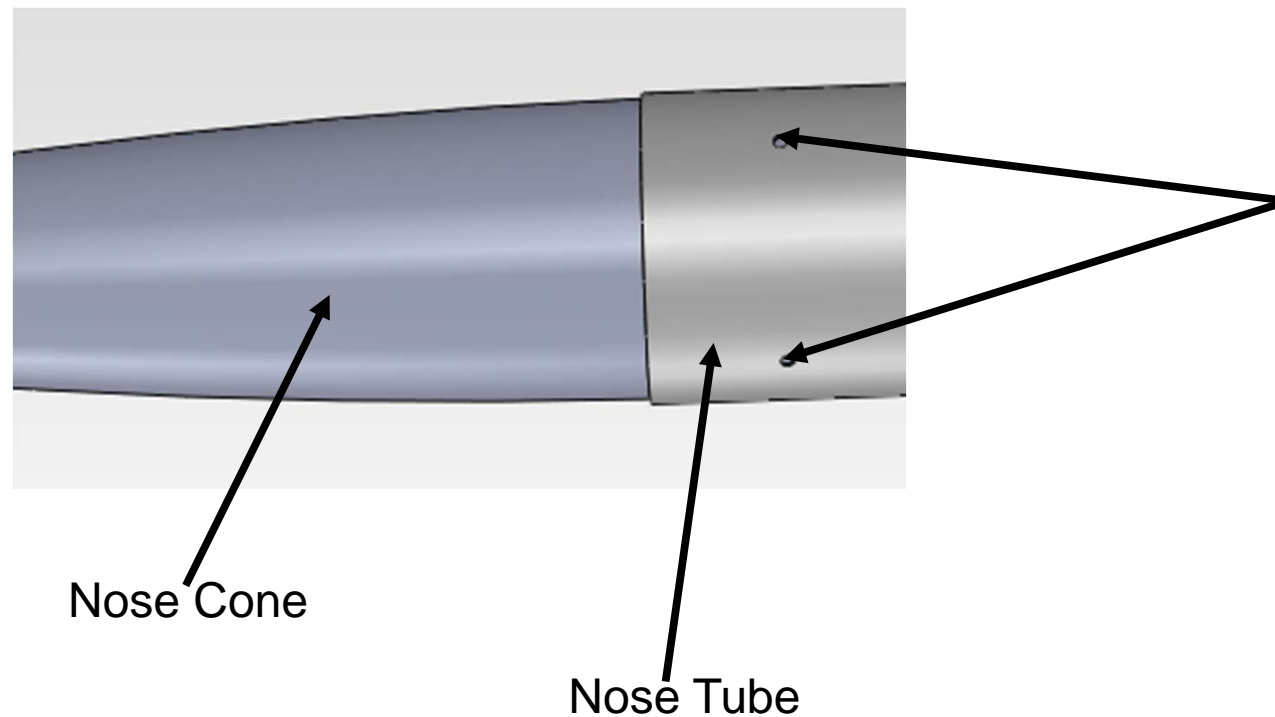
Appendix V: Booster Section Manufacturing and Fabrication Order

Booster MFO

Booster Assembly – Thrust Plate

1) Use nuts (8x) threaded for ¼-20 to fasten threaded rods (4x) to thrust plate

¼ -20 nuts (8x)

2) Slide motor tube into centering ring and slide motor tube/centerning ring assy onto threaded rods.
3) Epoxy motor tube to thrust plate

Centering Ring with Motor tube
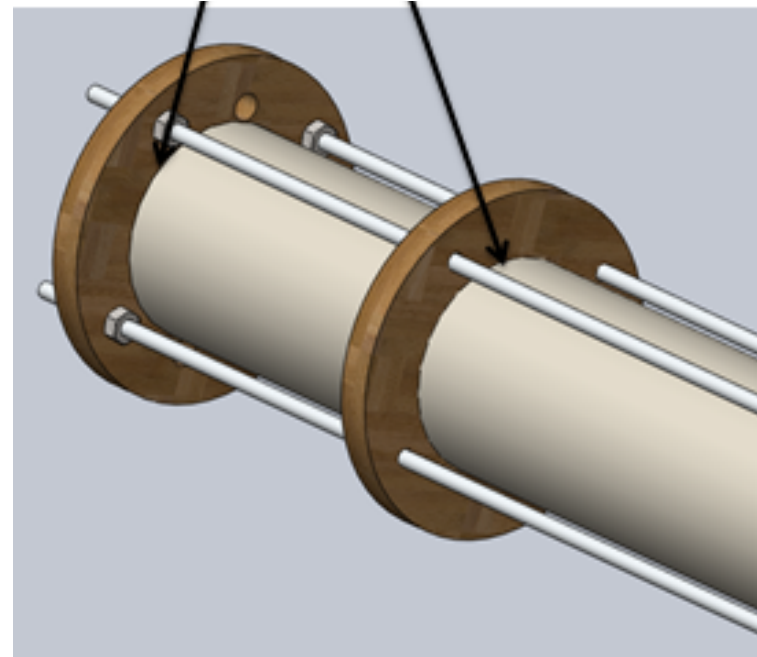
Booster Assembly – Fins

5) Using motor case as a guide, set position of Retention ring, then fasten Retention ring to threaded rods using ¼-20 nuts (8x)

6) Insert fins into retention ring fin tabs and set centering ring against the forward part of fin
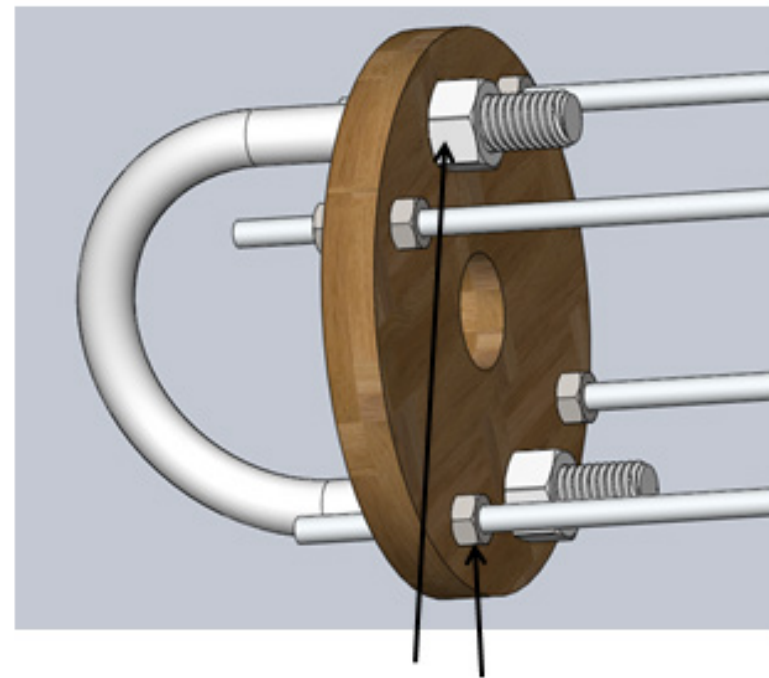
7) Epoxy centering ring to motor tube

8) Epoxy fins to motor tube and centering ring, using bubble levels to ensure correct position of fins relative to motor tube

9) Epoxy tabs for skin fasteners to fins, centering ring, and thrust plate at locations shown (20x)

10) Cover entire assembly with Primer, automotive paint, and clear coat
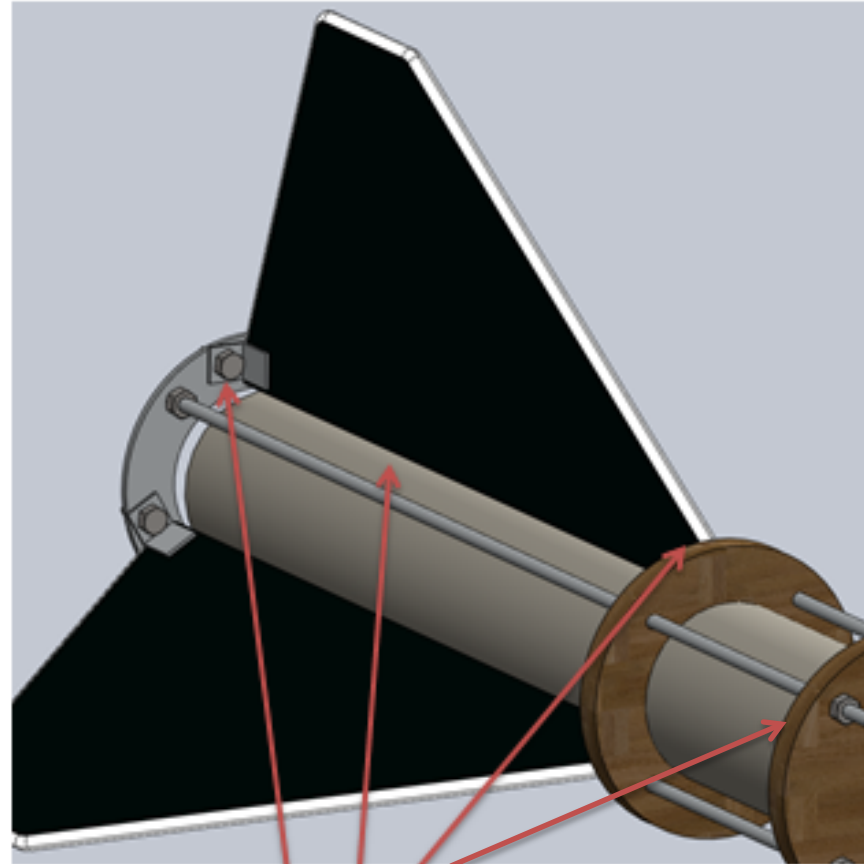
Mounting points for skin tabs

Appendix VI: iMPS Manufacturing and Fabrication Order

iMPS – Manufacturing and Fabrication Order

Rib Fabrication

- Material: 5/8" thick G-10 Fiberglass plate (12"x12")
1) Use precision mill to drill stringer mounting holes and 5 cutter starting holes using V drill bit
2) Cut out rib (4x) from material on water jet using supplied dxf file.

8x Stringer mounting holes
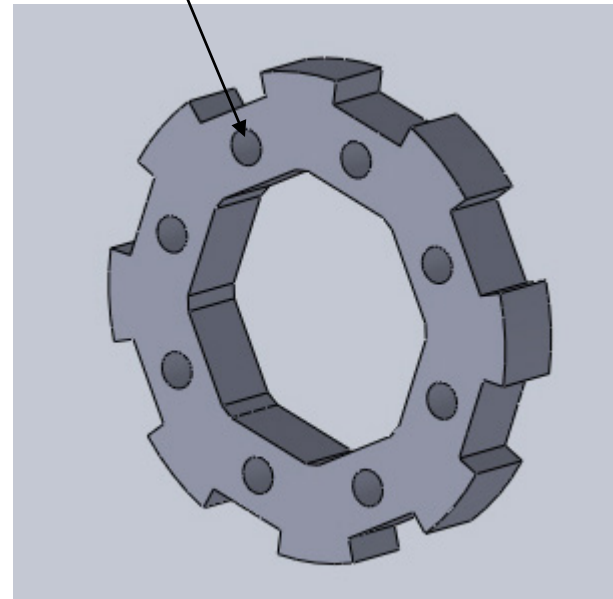
Stringer Fabrication

3) Cut stringers (12x) from 3/8" diameter G-10 rod stock to length (14")
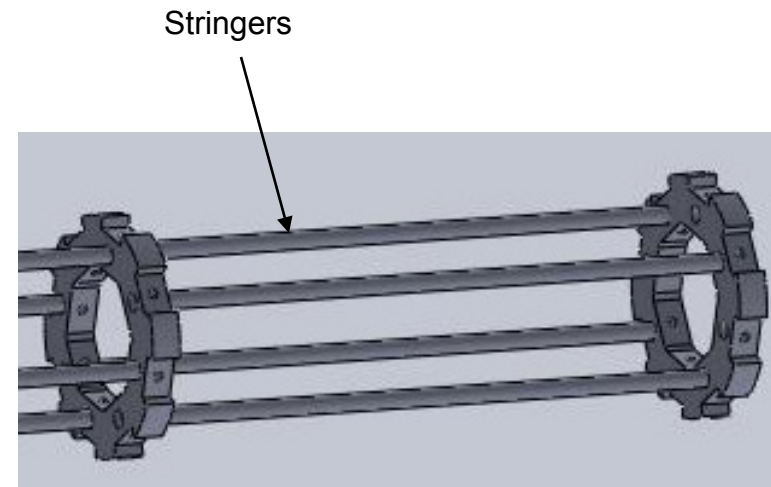
Stringers

Assembly

4) Slip stringers into corresponding stringer mounting holes. Use level to ensure level construction of structure

5) Match drill through rib and stringer with #18 drill bit

6) Install 8-32 fasteners (24x)

7) Glue hook and loop fasteners to ribs for skin attachment (32x)

8-32 bolts
8-32 nuts
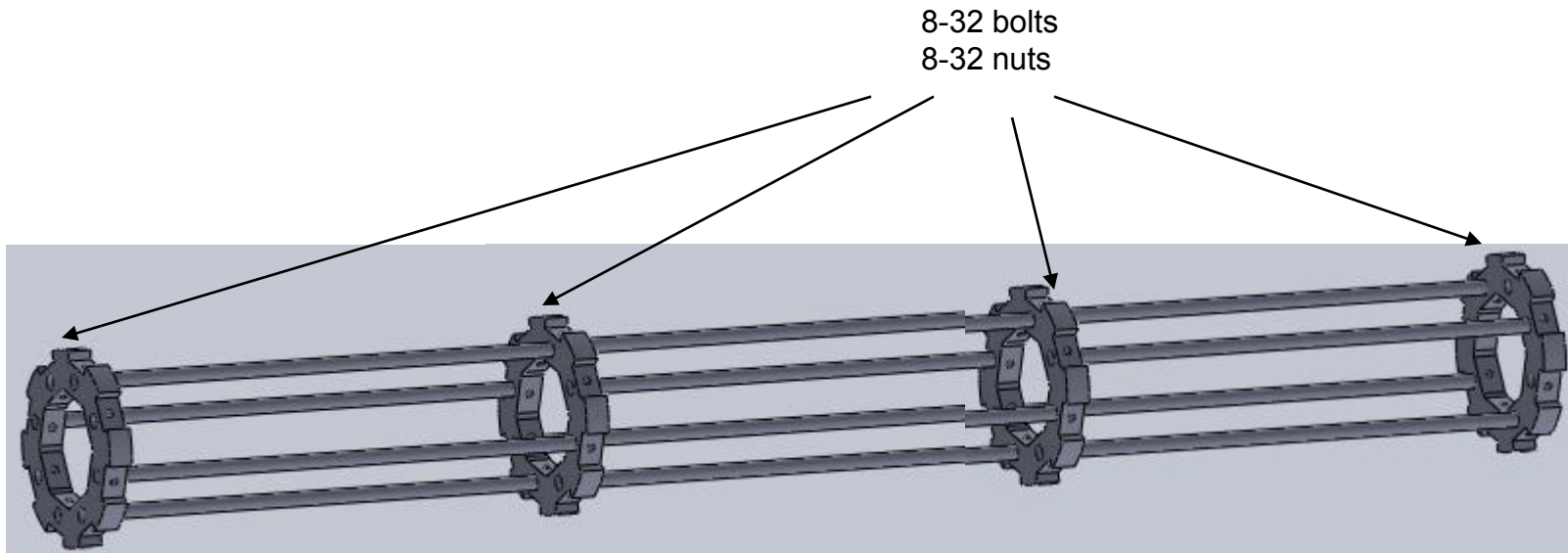
Appendix VII: Recovery System "How-To" Guide

Recovery How-To's

Akshaya Srivastava

March 19, 2012

Chapter 1

Drogue Chute Packing

Step 1.1: Lay out Parachute on a flat surface and line up the ends. put some talcum powder on the inside of the parachute to prevent sticking.

Step 1.2: Fold the parachute in half, taking care to not tangle the shroud lines

Step 1.3: Fold the parachute in half again, taking care to not tangle the shroud lines
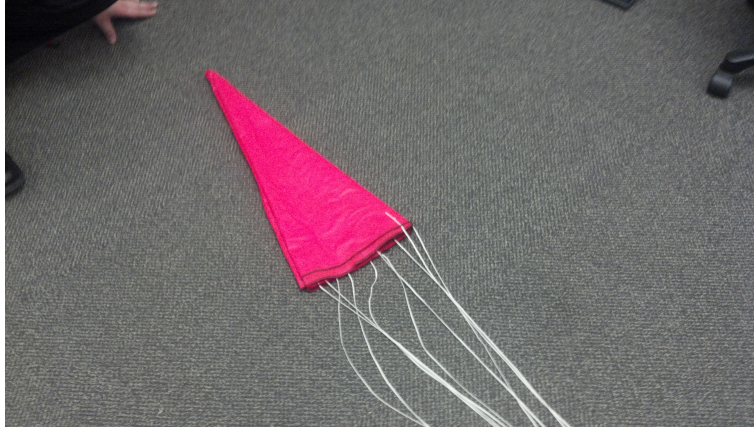
Step 1.4: Fold the parachute in half again, taking care to not tangle the shroud lines

Step 1.5: Place shroud lines onto the folded parachute, with the shroud line folded as shown

Step 1.6: Roll up the parachute from the tip, keeping the roll as tight as possible
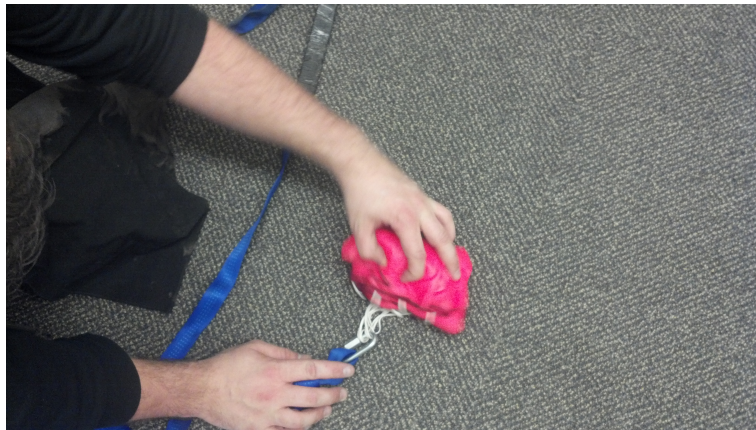
Step 1.7: Finished Folded Parchute

Step 1.8: Place the folded parachute onto a NOMEX cloth

Step 1.9: Fold NOMEX cloth around the parachute

Chapter 2

Main Chute Packing

Step 2.1: Lay out Parachute on a flat surface and line up the ends. put some talcum powder on the inside of the parachute to prevent sticking.

Step 2.2: Fold the parachute in half, taking care to not tangle the shroud lines

Step 2.3: Fold the parachute in half again, taking care to not tangle the shroud lines

Step 2.4: Fold the parachute in half again, taking care to not tangle the shroud lines

Step 2.5: Place shroud lines onto the folded parachute, with the shroud line folded as shown

Step 2.6: Roll up the parachute from the tip, keeping the roll as tight as possible

Step 2.7: Finished Folded Parchute

Chapter 3

Ejection Charges
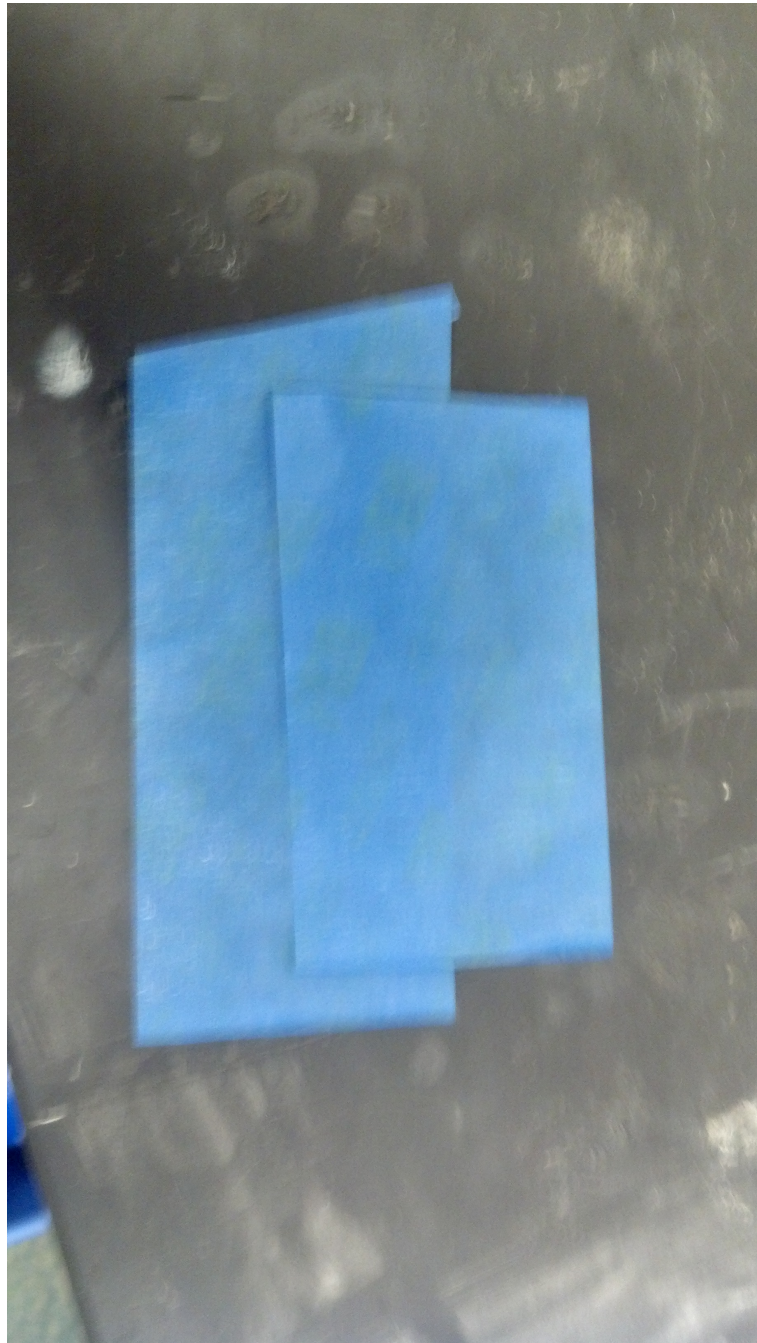
Step 3.1: Lay out two overlapping pieces of tape, sticky side up.
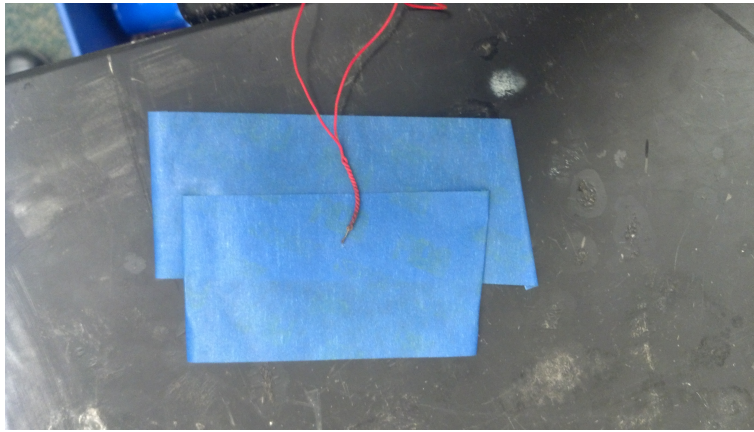
Step 3.2: Place e-match on tape, being careful not to break the pyrogen

Step 3.3: Pour pre-measured black powder on top of ejection charge
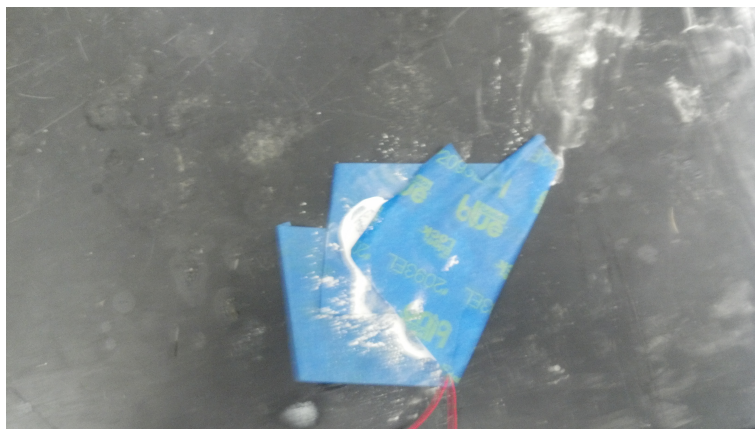
Step 3.4: Fold one half of tape over the e-match.
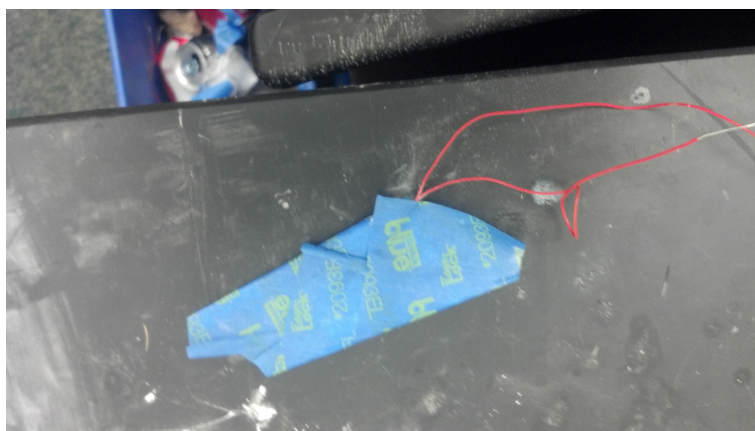
Step 3.5: Fold other half over the e-match, taking care not the break the pyrogen.

Step 3.6: fold top half over the to the bottom of the charge; again, be careful not to break the pyrogen. An extra piece of tape may be used to keep it in place.

Step 3.7: Finish by writing how much black powder that particular charge contains.

Chapter 4

Knots Used

Step 4.1: Double Fisherman's Knot
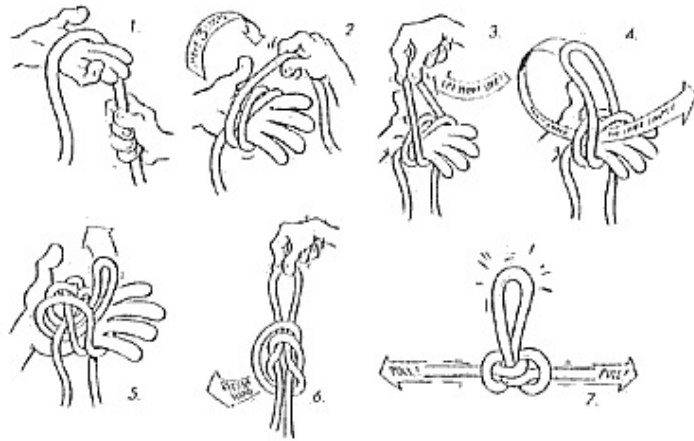
Step 4.2: Butterfly Knot
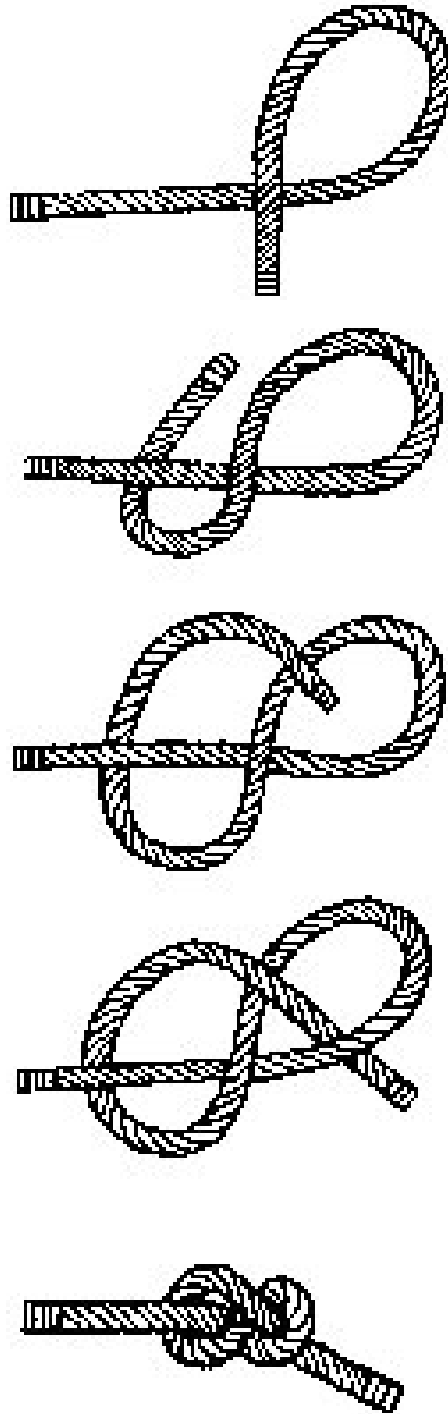
Step 4.3: Figure 8 Knot
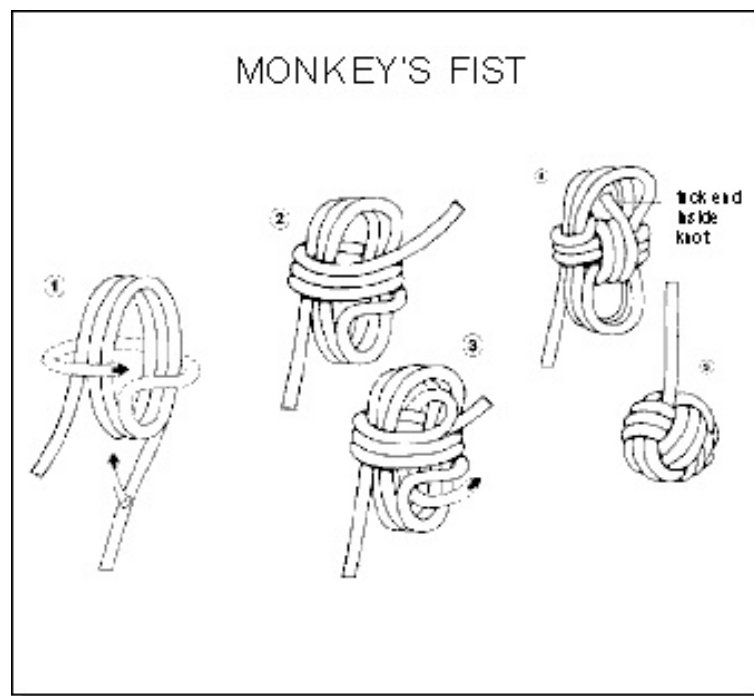
Step 4.4: Monkey's Paw Knot

Appendix VIII: Mathematical and Physical Modeling of Magnetic Fields

In order to accomplish the objective of stabilizing a platform with magnetic fields during the ascent of a launch vehicle, a control system must be developed with inputs of voltages and currents supplied to solenoids and optical sensing feedback for kinematics data. To create the control system, equations and experimentation to model the fields and resultant forces on an object in the field will be derived and conducted, respectively, from the scientific principles governing electromagnetism. Typically, electromagnetic equations are focused on defining axial interactions, while the A.P.E.S. experiment requires a comprehensive understanding of three-dimensional magnetic fields. The following sections will define the governing equations and concepts that are the foundation for the experimental testing and will serve as the basis for a data-centered control system.

Modeling General Magnetic Fields

If two magnets or electromagnets are at a large enough distance from each other, or small enough compared to the distances involved, then they can be modeled as being magnetic dipoles. A magnetic dipole can be thought of as a small current loop; this still creates a non-vanishing magnetic field at distances much larger than the radius of the loop. The magnetic dipole moment of a single current loop is defined as

$$\mathbf{m} = I\mathbf{S} \tag{1}$$

where the $\mathbf{S}$ vector, and hence $\mathbf{m}$ as well, is oriented perpendicular to the planar area of the loop so that curling the fingers of one's right hand in the direction of the current gives the direction of $\mathbf{S}$ as the direction of the thumb. The magnetic potential due to a magnetic dipole of moment $\mathbf{m}$ is

$$\mathbf{A}(\mathbf{r}) = \frac{\mu}{4\pi} \frac{\mathbf{m} \times \mathbf{r}}{r^3} \tag{2}$$

where $\mathbf{r}$ is the vector from the dipole to the field point where the potential is being calculated, r is the magnitude of vector $\mathbf{r}$, and μ is the permeability of the medium at the field point. The magnetic flux density $\mathbf{B}$ and the magnetic field $\mathbf{H}$ due to the dipole are, respectively,

$$\mathbf{B(r)} = \nabla \times \mathbf{A} = \frac{\mu}{4\pi r^3}(3(\mathbf{m} \cdot \hat{\mathbf{r}})\hat{\mathbf{r}} - \mathbf{m}) \tag{3}$$

$$\mathbf{H(r)} = \frac{\mathbf{B}}{\mu} = \frac{1}{4\pi r^3}(3(\mathbf{m} \cdot \hat{\mathbf{r}})\hat{\mathbf{r}} - \mathbf{m}) \tag{4}$$

Where $\hat{\mathbf{r}}$ is the unit vector in the direction of $\mathbf{r}$, and the distance r is much greater than the radius of the loop.

There are two ways to approximate model the vector potential field, the magnetic field, and the magnetic induction field as produced by a solenoid using these equations. The first method is to model the solenoid as a single dipole of moment $\mathbf{m} = N I \mathbf{S}$ at the center of the solenoid, where N is the number of turns in the solenoid, as a solenoid has N current loops each of moment $I\mathbf{S}$. However, this does not take into account the fact that each loop of the solenoid is not at the same location. Therefore, a more precise way of modeling the solenoid – albeit still an approximation – would be to place one dipole of moment $I\mathbf{S}$ at the center of each loop that makes up the solenoid, or perhaps one moment per k loops of moment $kI\mathbf{S}$, where we have a choice of k. However, computational difficulty is greatly increased due to the necessity of finite-element solver techniques as the mathematics progresses. The magnetic $\mathbf{H}$ field produced by each model are shown below, where N is taken to be 11 loops (distributed over 2 cm of length for the second model) and $\frac{1}{4\pi}I\mathbf{S}$ is taken to be $\mathbf{k}$ A $\cdot$ cm^2. One dipole of moment 11$\mathbf{k}$ A $\cdot$ cm^2 is placed at the origin in the typical cartesian plane in Figure 89, and 11 dipoles of moment $\mathbf{k}$ A $\cdot$ cm^2 are distributed from -1 to 1 along the y-axis in Figure 90, for the sake of simplicity.
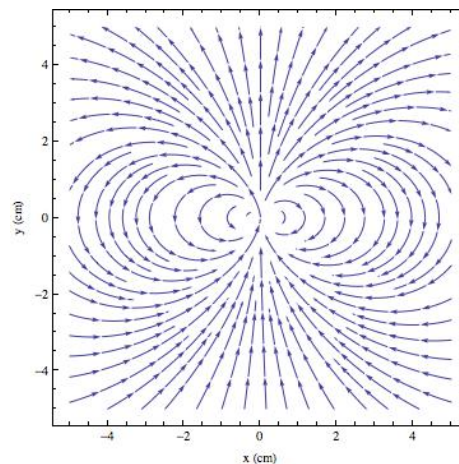
Figure 89: field generated by a single dipole
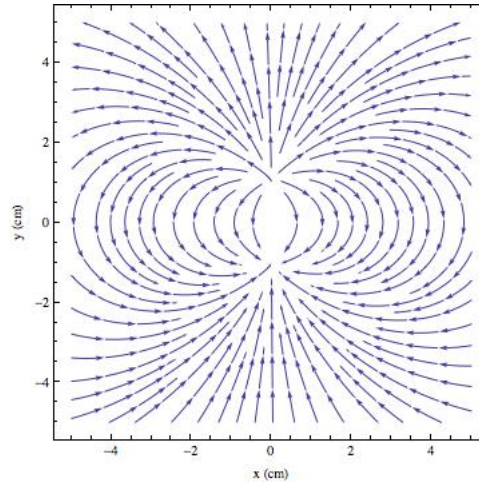
Figure 90: field generated by multiple dipoles

Generation of Magnetic Forces in Materials

All materials are composed of atoms, with a positively charged nucleus and negatively charged electrons. The movement and rotation of these charges form microscopic magnetic dipoles, which have magnetic dipole moments. The magnetization vector, **M,** of a material at a point is defined as the volume "density" of magnetic dipole moment, i.e.

$$\mathbf{M} = \lim_{\Delta v \to 0} \frac{\sum \mathbf{m}_k}{\Delta v} \tag{5}$$

where each $\mathbf{m}_k$ is the magnetic moment of the kth atom in the volume Δv, and the sum is over all the atoms. The force on a magnetic material can be determined by summing the forces on the dipoles in the material due to the field that it is placed in. The magnetization of a material depends on the field it is placed in, and the flux density depends on the field, as follows:

$$\mathbf{M} = \chi_m \mathbf{H} \tag{6}$$

$$\mathbf{B} = \mu_0(\mathbf{H} + \mathbf{M}) = \mu_0 \mathbf{H}(1 + \chi_m) = \mu_0 \mu_r \mathbf{H} = \mu \mathbf{H} \tag{7}$$

where χ_m is the material's magnetic susceptibility, μ_r is its relative permeability, and μ is the absolute permeability. The parameters χ_m and μ_r are not always constant, especially in the case of ferromagnetic materials. However, assuming a linear relationship between **M** and **H** –

approximately true in the case of magnetically soft ferrite – or a constant **M** in the case of a permanent neodymium magnet, using the **H** field of a dipole or multiple dipoles as the field of the solenoids, the force on the platform due to the fields interacting with the microscopic dipoles in the material can be calculated.

Forces on Materials in Magnetic Fields

The force on an object is the sum of the forces on all of the magnetic dipoles that make up the object. By definition, the magnetic dipole moment of an infinitesimal volume of the object dV is $\mathbf{m} = \mathbf{M}\,dV$. The force due to the field of a magnetic dipole of moment $\mathbf{m}_s$ on a magnetic dipole of moment $\mathbf{m}$ that is in a material of permeability μ is:

$$\mathbf{F}(\mathbf{r}, \mathbf{m}_s, \mathbf{m}) = \frac{3\mu}{4\pi r^4}\left[(\mathbf{m}_s \cdot \hat{\mathbf{r}})\mathbf{m} + (\mathbf{m} \cdot \hat{\mathbf{r}})\hat{\mathbf{m}}_s + (\mathbf{m}_s \cdot \mathbf{m})\hat{\mathbf{r}} - 5(\mathbf{m}_s \cdot \hat{\mathbf{r}})(\mathbf{m} \cdot \hat{\mathbf{r}})\hat{\mathbf{r}}\right] \qquad (8)$$

Where **r** is the vector from $\mathbf{m}_s$ to **m**, and $\hat{\mathbf{r}}$ is again the unit vector in the direction of **r**. First the case of a ferrite platform is considered, with approximate constant χ_m and μ. In this case, the force on the platform is calculated to be:

$$\mathbf{F}(\mathbf{r}, \mathbf{m}_s) = \iiint \frac{3\mu\chi_m}{16\pi^2 r^7}\left[(\mathbf{m}_s \cdot \hat{\mathbf{r}})\mathbf{m}_s - (\mathbf{m}_s \cdot \mathbf{m}_s)\hat{\mathbf{r}} - 4(\mathbf{m}_s \cdot \hat{\mathbf{r}})^2\hat{\mathbf{r}}\right] dV \qquad (9)$$

Where $\mathbf{m}_s$ is now used as $\mathbf{m}_s = NI\mathbf{S}$ for the solenoid and the integral is evaluated over the volume of the platform. If it is assumed that the object is small such that the quantity integrated does not vary significantly over the volume, the force on the platform of volume V, due to the solenoid of moment $\mathbf{m}_s = NI\mathbf{S}$, is:

$$\mathbf{F}(\mathbf{r}, \mathbf{m}_s, \mathbf{m}) = \frac{3VN^2I^2S^2\mu\chi_m}{16\pi^2 r^7}\left[(\hat{\mathbf{n}} \cdot \hat{\mathbf{r}})\hat{\mathbf{n}} - \hat{\mathbf{r}} - 4(\hat{\mathbf{n}} \cdot \hat{\mathbf{r}})^2\hat{\mathbf{r}}\right] \qquad (10)$$

Where $\hat{\mathbf{n}}$ is the unit vector in the direction of **S** – the unit normal to the loop area of the solenoid – and **r** is the position vector from the solenoid center to the center of mass of the platform. While approximate, it is clear that the force will vary as the square of current and inversely by the seventh power of the distance between the solenoid and the platform assuming a

magnetically-soft ferrite material. To check the validity of this equation, and assuming that both $\hat{\mathbf{n}}$ and $\mathbf{r}$ are in the positive $\mathbf{k}$ direction in a Cartesian plane, such that the platform is above the dipole, it is found that:

$$\mathbf{F} = \frac{-3VN^2I^2S^2\mu\chi_m}{4\pi^2r^7}\mathbf{k} \tag{11}$$

Or that the platform is pulled towards the dipole, which matches the basic experience of magnetic materials attracted to magnets due to induction.

The equations given above are derived in Appendix 3. However, the validity of these equations is primarily for the case of a single solenoid acting on a platform with constant permeability. Forces originating from more than one solenoid do not add in the conventional sense, as the induction of a ferrite material is highly non-linear. These equations must be re-derived from equation (8), as the fields and magnetization of the platform change in the n-solenoid problem.

Much easier is the case of a permanent neodymium magnet with constant magnetization $\mathbf{M}$ throughout. In this case, the force on the platform is the sum o0f the force on each $\mathbf{M}\,dV$ segment,

$$\mathbf{F}(\mathbf{r},\mathbf{m}_s,\mathbf{M}) = \iiint \frac{3\mu_0}{4\pi r^4}[(\mathbf{m}_s \cdot \hat{\mathbf{r}})\mathbf{M} + (\mathbf{M} \cdot \hat{\mathbf{r}})\hat{\mathbf{m}}_s + (\mathbf{m}_s \cdot \mathbf{M})\hat{\mathbf{r}}$$
$$- 5(\mathbf{m}_s \cdot \hat{\mathbf{r}})(\mathbf{M} \cdot \hat{\mathbf{r}})\hat{\mathbf{r}}]\,dV \tag{12}$$

Here, the constant involves μ_0 rather than just μ, since the $\mathbf{M}$ vector is constant and is largely independent of $\mathbf{H}$. Again, the exact value of the expression is highly dependent on the shape of the volume integrated upon. However, if the volume V is small, the force can be taken due to the solenoid field $NI\mathbf{S}$ as:

$$\mathbf{F}(\mathbf{r},\mathbf{m}_s,\mathbf{m}) = \frac{3VNIS\mu_0}{4\pi r^4}[(\hat{\mathbf{n}} \cdot \hat{\mathbf{r}})\mathbf{M} + (\mathbf{M} \cdot \hat{\mathbf{r}})\hat{\mathbf{n}} + (\hat{\mathbf{n}} \cdot \mathbf{M})\hat{\mathbf{r}} - 5(\hat{\mathbf{n}} \cdot \hat{\mathbf{r}})(\mathbf{M} \cdot \hat{\mathbf{r}})\hat{\mathbf{r}}] \tag{13}$$

Where $\hat{\mathbf{n}}$ is defined as before. Equation (11) is also an approximate solution, but here it is evident that the force on a permanent magnet varies only directly on the current in the solenoid and inversely by the fourth power of the distance, rather than by the square of current and

inversely by the seventh power of distance in the case of forces from induction in a ferrite platform. The force will also depend on the orientation of **M**. Unlike for the case of a material with constant permeability, the forces on a permanent magnet due to multiple solenoids *do* add in the conventional sense, greatly simplifying computational analysis.

Appendix IX: TK Solver Report for Required Solenoid Cooling Flow Rate

Solenoid cooling problem

Variables Sheet

Input	Name	Output	Unit	Comment
36.9	Q		BTU/hr	
180	t1		F	
90	t3		F	
.2	r2		in	
.09375	r1		in	
19.3	Kw		BTU/(hr*in*F)	
.472441	L		in	
	h	0.694365	BTU/(hr*in^2*F)	
	A	0.593687	in^2	
.4	d		in	
	Deff	0.039370	in	
	Nud	21.508420		
.001271	Ka		BTU/(hr*in*F)	
	ReD	1780.852569		
.712	Pr			
	V	3.285601	in/s	Final air velocity required
.06545	roh		lb/ft^3	
0.000000	mu		lb*s/ft^2	

Rules Sheet

Rules

$$Q = \frac{t1 - t3}{\dfrac{\ln\left[\dfrac{r2}{r1}\right]}{2 \cdot \pi \cdot Kw \cdot L} + \dfrac{1}{h \cdot A}}$$

$$A = \pi \cdot d \cdot L$$

$$Deff = \frac{L}{12}$$

$$Nud = \frac{h}{\dfrac{Ka}{Deff}}$$

$$Nud = 0.3 + \frac{0.62 \cdot ReD^{(.5)} \cdot Pr^{\left[\frac{1}{3}\right]}}{\left[1 + \left[\frac{.4}{Pr}\right]^{\left[\frac{2}{3}\right]}\right]^{\left[\frac{1}{4}\right]}} \cdot \left[1 + \left[\frac{ReD}{282000}\right]^{\left[\frac{5}{8}\right]}\right]^{\left[\frac{4}{5}\right]}$$

$$ReD = \frac{Deff \cdot V \cdot roh}{mu}$$

Units Sheet

From	To	Multiply By	Add Offset	Comment
ft/s	in/s	12	0	
inches	in	1	0	

Appendix X: Recovery Testing Document

Appendix XI: Recovery MATLAB code

```matlab
%% Author: Akshaya Srivastava
% Date: 12/19/2011
% Purpose: USLI Recovery System Design and Analysis

clc
clear
close all

%% Main Parachute Sizing and Ejection Optimization Code
% Code will find optimal height and main parachute size for deployment
% given a certain speed. The Drogue Chute Area is asssumed constant based
% on a worst case scenario. Ejection charges will also be calculated based
% on user choosing what height the main chute should deploy at based on
% 3D plots created by code. Equations have been derived in notebook (an
% image of the design process is available upon request). Limitations and
% contraints have been extracted from the USLI Handbook. All units are in
% SI for calculations. Conversion code is implemented as required, for ease
% of checking whether requirements in the USLI Handbook are met. All
% Parachutes are assumed to be one inch thick. Drift is considered and
% program won't end until the drift conditions have been satisfied. Drift
% Conditions include 1) a maximum total drift of 2500 ft [USLI HANDBOOK]
% and 2) a maximum drift between drogue and main chute deployments
% of 1800 ft.

%% Assumptions made
% 1) Cd of Drogue = 1.2 (can be updated with testing)
% 2) Cd of Main = 1.4 (can be updated with testing)
% 3) STP Conditions at Landing
% 4) Need to Pressurize all the Volume (needs to be updated with
%    actual model)
% 5) Thickness of all parachutes is assumed to be 1-inch to account for
%    harness, shroud lines, and other hardware.
% 6) Drogue Descent Speed was assumed to be 50 fps
% 7) Once a chute is deployed, the time the rocket to takes to reach
%    terminal velocity/descent rate is negligible
% 8) Drogue Drift shouldn't exceed 1800 ft.
% 9) The main chute will reach the ground after deployment in 30 seconds


% Constants with direct effect on flight profiles
mass_si = 18.1653; %kg
ke_max_possible_si = 376.8; %J - Found in PDR and USLI HANDBOOK
v_max_possible_si = sqrt((2*ke_max_possible_si)/mass_si); %m/s
drift_total = 2501; %ft-limit used for loop
wind_eng = 0:5:20; %mph - provided by USLI Handbook
wind_si = wind_eng *.44704; %m/s - Converting to SI
delta_t = 2500/22; %s - 2500 ft at 15 mph (=22 ft/s) [USLI HANDBOOK]

% Constants with indirect effect on flight profiles
C_d_main = 1.4; %dimensionless assumed quantity for now...
C_d_drogue = 1.2; %dimensionless assumed quantity for now...
```

```matlab
rho_si = 1.225; %for now take air density at landing(2000ft=95% of sea lvl)
g_si = 9.81;%m/s^2
R_air_si = 287.04; %J/(kg*K) - molecular gas constant of air
R_air = 53.3533; %(ft*lbf)/(lb*R) - molecular gas constant of air
V_drogue = ((1/3)*pi()*(4.7)^2)*(25.5); %in^3-volume of drogue chamber
V_main = 12*(pi()*(5)^2); %in^3-volume of main chamber accounting for stuff
R_combust = 22.16*12; %in*lbf)/(lb*R) - gas combustion constant (FFFF BP)
T_combust = 3307; %R - gas combustion temperature (FFFF BP)

%% Defining Drogue Data
% All Drogue Data is computed here
v_drogue_si = 15.24;%15.24m/s=50ft/s
temp_drogue = -.0036*5280+59.007 + 459.67;%R-at a mile high
temp_drogue_si = (temp_drogue-32-459.57)*(5/9) + 273.15; %K-for press. calc
rho_drogue = rho_si * .8549;%SI units at a mile high
drogue_area = g_si*(mass_si^2* sqrt((wind_si(length(wind_si))^2+...
    v_drogue_si^2)))/(C_d_drogue*(.5*mass_si*v_drogue_si^2)*15.24...
    *(rho_drogue));%m^2-Worst case scenario (ke is calculated)

% Converting Drogue Chute Area and Diameter
drogue_area = drogue_area * 10.7639104 %ft^2 (Shown)
drogue_dia = sqrt((4*drogue_area)/pi()) %ft (Shown)

pressure_drogue_si = R_air_si*rho_drogue*temp_drogue_si; %Pascals
pressure_drogue = pressure_drogue_si * .000145037738; % lbf/in^2

eject_drogue = (((V_drogue-drogue_area)*(23.7-pressure_drogue))/...
    (R_combust*T_combust))*454 %grams (Shown)

%% Calculating Main Chute Data
% Defining loops to iterate and make graphs. One graph of velocity vs
% optimal height per wind speed. The area of the parachute will also be
% displayed per wind speed and velocity.

v_val = 1:.2:v_max_possible_si; %m/s-Values of velocity to iterate through

chute_area = zeros(length(wind_si),length(v_val)); %m^2- used to store the
                                                   %values of chute sizing

optimal_h = zeros(length(wind_si),length(v_val)); %m-used to store
                                                  %minimum height

drift = zeros(length(wind_si),length(v_val)); %m-used to store drift values

for u = 1:length(wind_si)
    for v = 1:length(v_val)
        chute_area(u,v) = g_si*(mass_si^2* sqrt((wind_si(u))^2+...
            (v_val(v))^2))/(C_d_main*ke_max_possible_si*rho_si*v_val(v));
                                                   %m^2-done
                                                   %with assumed
                                                   %values
```

```
            optimal_h(u,v) = (v_val(v))*delta_t; %m-Minimum depoloyment height
            drift(u,v) = sqrt((wind_si(u))^2+(v_val(v))^2)*delta_t; %m-drift

            %placing an upper bound on drift for plots [USLI HANDBOOK]
            if (drift(u,v)*3.2808399 > 2500)
                drift(u,v) = NaN;
            end
        end
    end
end

%% Creating 3D plots to show results
chute_area = chute_area - drogue_area; %m^2 - finding main chute area
chute_dia = real(sqrt(4*chute_area/pi)); %m - getting main chute diameter



v_mat = [v_val;v_val;v_val;v_val;v_val]; %terminal velocity mesh for plots
u_mat = []; %wind velocity mesh for plots
for i = 1:length(v_val)
    u_mat = [u_mat transpose(wind_si)]; %filling in wind velocity mesh
end

% 3D plot and labels - English Units
figure
surf(v_mat.*3.2808399,chute_dia.*3.2808399,optimal_h.*3.2808399)
xlabel('Descent Rate (ft/s)')
ylabel('Diameter of Main Parachute (ft)')
zlabel('Minimum Deployment Height (ft)')
title('Descent Rate - Size - Height (English)')

% 3D Plot to show drift with respect to wind velocity and terminal velocity
% English units
figure
surf(v_mat.*3.2808399,u_mat.*3.2808399,drift.*3.2808399)
xlabel('Descent Rate (ft/s)')
ylabel('Wind Velocity (ft/s)')
zlabel('Drift (ft)')
title('Wind - Descent Rate - Drift (English)')

%Loop to keep drift in bounds.
while (drift_total>2500)
    drogue_drift = 2001;
    while (drogue_drift > 1800)
    prompt = ['Based on figures displayed, Choose a height to' ...
        ' deploy the main chute (ft): '];%prompt for user input
    h_chosen = input(prompt); %ft-Asks user to choose a height.
    h_chosen_si = h_chosen*3.2808399; %m-Used only in calculations
    drogue_drift = wind_si(4)*((1609-h_chosen)/50)*3.2808399;
                                        %ft-keeping drift
                                        %within bounds

    %% Calculation of Ejection Charge for Main Chute
```

```matlab
    temp_main = 59.007-.0036*h_chosen + 459.67;%R-at altitude chosen;
    temp_main_si = (temp_main-32-459.57)*(5/9) + 273.15; %K-for pressure
    rho_main = rho_si *((h_chosen^2)*.00000002914 - h_chosen * ...
        .0029+99.995)/100;%SI-done by percent change density at altitude

    pressure_main_si = R_air_si*rho_main*temp_main_si; %Pascals
    pressure_main = pressure_main_si * .000145037738; % lbf/in^2

    %% Displaying Specific Data for Chosen Height
    delta_t_chosen = 30; %sec-chosen and can be modified (Shown)

    chute_area_chosen = ((2*mass_si*g_si*delta_t_chosen^2)/(rho_main*...
        C_d_main*(h_chosen/3.2808399)^2))*10.7639104 %ft^2 (Shown)

    v_chosen = h_chosen/delta_t_chosen %ft/sec (Shown)
    drift_chosen = sqrt(15^2+v_chosen^2)*delta_t_chosen %ft-Shown
    chute_chosen_diameter = sqrt(4*chute_area_chosen/pi()) %ft-Shown
    drift_total = drogue_drift+drift_chosen;%ft-shows drift at 15ft/s winds
    %condition to go back into loop
    if (drift_total > 2500)
        drogue_drift = 2001;
    else
        drift_total
    end

    eject_main = (((V_main-chute_area_chosen)*(24.7-pressure_main))/...
        (R_combust*T_combust))*454 %grams (Shown)
    end

    % Extra plot to show drift at various windspeeds
    figure
plot(wind_eng,sqrt(wind_si.^2+(v_chosen/3.2808399)^2)*delta_t_chosen*3.280839
9)
    xlabel('Wind Velocity (ft/s)')
    ylabel('Drift (ft)')
    title('Wind - Drift (English)')

end
```

Appendix XII: FIRST LEGO League Lesson Plan

Electricity and Magnetism

January 28th , 2012

Main Concepts

- ✓ How electricity works.
- ✓ The difference between conductors and insulators.
- ✓ How electricity is related to magnetism.

Activities

ACTIVITY ONE: Electric Bug

To make a bug: Materials:

- ➢ 1 D battery   ➢ compass
- ➢ 1 light blub
- ➢ poster putty
- ➢ colored paper
- ➢ wire
- ➢ pipe cleaners

Hook: Do you think you can get the bug to light up?

- ❖ Make the bug light up. Right now the light bulb is lit. *How do you think the light is on?* It's not connected to the wall. *Is it magic?*
- ❖ Inside the bug is a battery and when the bulb is on the circuit is complete and electricity is flowing. *Do any of you know what electricity? Can you explain it?*
- ❖ Everything is composed of atoms and in atoms there are these things called electrons. Sometimes electrons jump from one atom to another. When there are a lot of atoms doing this we call it an electric current. In some materials the electrons can jump a lot and in other materials they can't jump at all. When the electrons can jump around the material is called a conductor and when the electrons can't jump the material is called an insulator.
- ❖ I have a bunch of different materials here. *Which ones do you think are conductors? Which ones do you think are insulators?*
- ❖ Try to make the bulb light with the different materials. Once you have tried all the materials put the conductors on one side and the insulators on the other.
- ❖ Okay, so these are conductors and these are insulators. *What is different about them?*

❖ The conductors are all metal and the insulators are not metal. So in metals the electrons can jump around a lot.

End: This is how electricity works. This is how the lights in your house turn on when you flip the switch.

Appendix XIII: Civil Air Patrol (CAP) Model Rocketry Program
Lesson Plan

Model Rocketry Program

March 2012

Main Concepts

The CAP Model Rocketry Program is broken up into three (3) stages.

Stage One – REDSTONE

- ✓ Identify historical facts about the development of rockets
- ✓ Describe the major contributions of the four great rocket pioneers.
- ✓ Recall facts about the rocket pioneers' lives and accomplishments.
- ✓ Design, build and launch two non-solid fuel hands-on rocket options

Stage Two – TITAN

- ✓ Explain Newton's three Laws of Motion. -Describe the aerodynamics of a rocket.
- ✓ Design, build and launch two of the hands-on rocket options.
- ✓ Demonstrate knowledge of the NAR safety code.

Stage Two – SATURN

- ✓ Describe altitude tracking.
- ✓ Explain baseline distance.
- ✓ Describe the ingredients of a model rocket engine.
- ✓ Define Newton seconds. -Define total impulse.
- ✓ Demonstrate knowledge of the NAR safety code.
- ✓ Design, build and launch one rocket in the Saturn stage.

Activities

ACTIVITY ONE: Electric Bug

Materials:

- Civil Air Patrol Model Rocketry Handbook
- Appropriate supplies for all rocket builds

Appendix XIV: National Air & Space Rocket Discovery Station Lesson Plan

Lift Off!

March 2012

Main Concepts

- ★ Role of oxidizer in combustion
- ★ Differences and similarities between airplanes and rockets
- ★ Newton's 3rd Law

Teaching Objects

- ★ Balloons
- ★ String
- ★ Scissors
- ★ Tape
- ★ Engine poster
- ★ Rocket poster
- ★ optional: Balloon pump

Constructing the Rocket Demonstration

Put the string through the straw and tie each end to an object so that the string is taught. Tape the inflated balloon to the straw. When you are ready, let go of the balloon.

Hook: Do you know what a rocket is?

Ask: What is a rocket?

Explain: A rocket is an object that can be propelled by the combustion of its contents.

Ask: Can you name any rockets?

Explain: (in chronological order)

- ★ <u>Redstone</u>: used for the sub-orbital launches in the Mercury program
- ★ <u>Atlas D</u>: used for the orbital launches in Mercury Program
- ★ <u>Titan II</u>: used for all the Gemini Program launches
- ★ <u>Saturn V</u>: used for the Apollo Program Launches
- ★ <u>Space Shuttle</u>: has two solid rocket booster (they are white) and are reusable

Ask: Have you ever seen a rocket launch? On tv or in person? What did you see and notice? Did you see flames coming out the back?

Explain: Rockets uses fire to make them go forward.

Ask: What do you know about fire? What are the three things every fire needs?

Explain: Every fire needs a fuel, oxygen, and a spark. When people talk about engines they call oxygen an oxidizer.

Ask: We know that rocket engines make a fire but how exactly do you think rocket engines work?

Explain: Rockets have a tank for fuel and a tank for an oxidizer, or oxygen. When they want to make the rocket go forward they combine the fuel and the oxidizer and light it on fire. They then push it out the back and that's why you see a flame when rockets launch.

Ask: How are rockets and planes alike?

Explain: They both use a fuel and an oxidizer, or oxygen, and they can both fly.

Ask: How are rockets and planes different?

Explain: A plane has wings and a rocket doesn't, ect. The main difference between rockets and planes is that planes use the oxygen in the air as their oxidizer while rockets carry their oxidizer with them. This means that planes can only fly where there is enough oxygen in the air while rockets can fly anywhere. This is why rockets work in space and why planes are sometimes called air breathers.

Ask: So rockets use a fuel and an oxidizer to create thrust, which is any force that pushes the rocket forward. But how does pushing the fire out the back of the rocket make it move forward?

Explain: Newton was a physicist who lived over 280 years ago and he discovered three laws which all objects obey. His third law says that every action has an equal and opposite _____ (wait for them to say reaction). This means that by pushing the flame out the back of the engine a reaction force which pushes the rocket forward is created. When you are swimming and push backwards against the water you go forwards right? Its the same thing with the rocket. By pushing the flame out the back of the engine a reaction force is created which pushes the rocket forward.

Ask: Would you guys like to see a rocket in action?

Explain: So this is a balloon attached to a string. When the air is pushed out the back of the balloon a reaction force is created which pushes the balloon forward.

Ask: Are you guys ready to see Newton's third law in action? Can you guys count down from five?

Explain: Five, four, three, two, one. ***Let go of the balloon.*** This is how rockets work.